

**RECEIVED**  
LAWRENCE  
RADIATION LABORATORY

UCRL-20032

C. 2

JAN 6 1971

**LIBRARY AND  
DOCUMENTS SECTION**

TWO REGGEON EXCHANGE CONTRIBUTIONS TO  
HADRON SCATTERING AMPLITUDES AT HIGH ENERGY

Chris Quigg  
(Ph. D. Thesis)

October 1970

AEC Contract No. W-7405-eng-48

**TWO-WEEK LOAN COPY**

*This is a Library Circulating Copy  
which may be borrowed for two weeks.  
For a personal retention copy, call  
Tech. Info. Division, Ext. 5545*

**LAWRENCE RADIATION LABORATORY**  
**UNIVERSITY of CALIFORNIA BERKELEY**

UCRL-20032

C. 2

## DISCLAIMER

This document was prepared as an account of work sponsored by the United States Government. While this document is believed to contain correct information, neither the United States Government nor any agency thereof, nor the Regents of the University of California, nor any of their employees, makes any warranty, express or implied, or assumes any legal responsibility for the accuracy, completeness, or usefulness of any information, apparatus, product, or process disclosed, or represents that its use would not infringe privately owned rights. Reference herein to any specific commercial product, process, or service by its trade name, trademark, manufacturer, or otherwise, does not necessarily constitute or imply its endorsement, recommendation, or favoring by the United States Government or any agency thereof, or the Regents of the University of California. The views and opinions of authors expressed herein do not necessarily state or reflect those of the United States Government or any agency thereof or the Regents of the University of California.

TWO REGGEON EXCHANGE CONTRIBUTIONS TO HADRON  
SCATTERING AMPLITUDES AT HIGH ENERGY

Contents

Abstract . . . . .	vii
I. Introduction . . . . .	1
II. Some Necessary Results from S-Matrix Theory . . . . .	4
1. The Scattering Amplitude: Analytic Structure . . . . .	4
2. Dispersion Relations . . . . .	5
3. The Mandelstam Representation . . . . .	6
4. Signed Amplitudes and the Mandelstam Representation . . . . .	8
5. The Froissart-Gribov Projection . . . . .	10
6. Singularities in $s$ of the Partial Wave Amplitudes . . . . .	13
7. Sommerfeld-Watson Transforms . . . . .	15
8. Mellin Transforms . . . . .	21
Figure Captions . . . . .	23
Figures . . . . .	24
III. The Amati-Fubini-Stanghellini Branch Cut . . . . .	32
1. Generation of the AFS Cut by Two-Body Unitarity . . . . .	32
2. The Rothe Cancellation . . . . .	34
3. Diagrams with Cuts . . . . .	36
Figure Captions . . . . .	38
Figures . . . . .	39
IV. The Double Cross Diagram . . . . .	45
1. Sudakov Variables: A Simple Example . . . . .	45
2. The Two Reggeon Branch Point . . . . .	47
3. Polkinghorne's Modification . . . . .	52

4.	Application to Physical Processes . . . . .	52
5.	Objections to the Graphical Approach . . . . .	54
	Figure Captions . . . . .	57
	Figures . . . . .	58
V.	A Phenomenological Model of Regge Cuts . . . . .	64
	Figure Captions . . . . .	73
	Figures . . . . .	74
VI.	Regge Cuts and Exchange Degeneracy . . . . .	80
1.	Regge Cuts and Duality . . . . .	80
2.	Systematics of Exchange Degeneracy Breaking . . . . .	83
3.	Regge Cuts and the Breaking of Exchange Degeneracy . . . . .	91
4.	Reggeon-Reggeon Cuts and Line-Reversal Violations . . . . .	97
5.	Exotic Quantum Number Exchange . . . . .	101
	Figure Captions . . . . .	114
	Figures . . . . .	117
VII.	Summary and Conclusion . . . . .	138
	Acknowledgments . . . . .	140
	Appendices . . . . .	142
A.	Definitions and Conventions . . . . .	142
1.	Kinematical Quantities . . . . .	142
2.	Single Particle States . . . . .	144
3.	Scattering Amplitudes . . . . .	147
4.	Crossing Relations for Helicity Amplitudes . . . . .	152
5.	Perturbation Theory Conventions . . . . .	154
	Figure Captions . . . . .	157
	Figures . . . . .	158

B. Properties of Rotation Matrices . . . . .	162
1. Definition and Properties . . . . .	162
2. Expansions in Terms of Other Functions . . . . .	164
3. Computational Details . . . . .	167
C. Reggeization of S-Channel Helicity Amplitudes . . . . .	170
References . . . . .	180

## I. INTRODUCTION

The recent fashion of describing two body to two body hadronic processes in terms of branch cuts (together with the usual Regge poles) in the crossed channel complex angular momentum plane seems to hold great promise for the accommodation of high-energy scattering data. At present Regge cut models are much too flexible to have real predictive power, but there is some reason to hope (see Chapter VI) that understanding will be gained through a study of the interplay between Regge cut corrections and duality-breaking schemes. In this thesis I will discuss the formulation of a model amplitude for the Regge box graph, which represents the physical picture of beam particle and target particle interacting twice, and the use of such an amplitude in two cases of experimental interest. The first obtains when normal quantum numbers are exchanged in the t-channel but simple Regge pole descriptions fail to represent the data adequately. [Normal quantum numbers are those which occur in the simple quark model. For bosons these occur in the SU(3) product  $3 \otimes \bar{3}$ , whereas for fermions they are contained in  $3 \otimes 3 \otimes \bar{3}$ . All other quantum numbers are "exotic." ] In such instances it has become common practice to invoke the virtues of the absorptive peripheral model (Jackson, 1965) by considering amplitudes in which elastic scattering either precedes or follows the quantum number exchange. The second case is that in which both Reggeons represent quantum number exchange, so the amplitude may represent the exchange of exotic quantum numbers in the t-channel. In the latter circumstance the box graph presents an alternative to the exchange of a single exotic trajectory.

The rejection of the idea of meromorphy in the  $j$  plane and the concomitant consideration of Regge cuts are motivated both by theoretical notions and by phenomenological necessity. All dynamical models of scattering amplitudes extant require the existence of branch cuts in the angular momentum plane. None of these models is sufficiently mature to permit the calculation of the discontinuity across the cut in interesting cases, but the existence and location of the branch points can be stated with some certainty. The graphical approach employed here suffers from this ambiguity, but by appeal to the successes of the peripheral model with absorption it is possible to formulate a definite if arbitrary model. Phenomenologically, the fact that Regge poles don't work has been widely documented in the past year, even by adherents to the aesthetics of meromorphy (Barger, 1969). I hasten to add that the difficulties with Regge poles are quantitative and in no way minimize the remarkable fecundity of the Regge pole hypothesis (Regge, 1959, 1960; Chew and Frautschi, 1961, 1962), which is expounded by Barger and Cline (1969). The case for Regge cuts has been reviewed by Chiu (1969), Fox (1970), Jackson (1970), and Sonderegger (1969). While it is important to remember that Regge cuts are not a phenomenological panacea (see Fox, 1970), it seems evident that complicated  $j$ -plane structure is unavoidable.

The plan of the succeeding chapters is as follows. In Chapter II, I list some of the terminology and classical results of S-matrix theory, to establish a frame of reference for later discussions. The history of the Amati-Fubini-Stanghellini branch cut takes up most of

Chapter III. Chapter IV contains a brief discussion of a particular Feynman diagram which produces a prototype Regge cut. It is there that I make contact with the recent work of Gribov on a Reggeon calculus. I formulate a phenomenological amplitude for two-Reggeon exchange in Chapter V. In Chapter VI I discuss some aspects of the relevance of Regge cuts to the questions of exchange degeneracy and the existence of exotic trajectories. Chapter VII is a summary of the work. Conventions and such are collected in the appendices.

## II. SOME NECESSARY RESULTS FROM S-MATRIX THEORY

I record here results from analytic S-matrix theory which will be useful in the succeeding development. All of this material is classical, but it will be valuable to have the concepts fresh in mind later. The reader is referred to Eden, et al. (1966) and Collins and Squires (1968) for more complete expositions.

To make this rather dull, technical chapter somewhat readable I have relegated many definitions and conventions to Appendix A. The intent of the present chapter is merely to remind the reader of terminology to be used later; therefore I ignore the complications of spin here.

### 1. The Scattering Amplitude: Analytic Structure

In this thesis I am concerned almost exclusively with the four line connected part of the S-matrix, i.e. the two body to two body scattering amplitude. The kinematical quantities for two body scattering are given in Chapter A.1. The S-matrix and scattering amplitude for a general process are written down in Chapter A.3. Here I write the two-to-two amplitude as  $A(s,t,u)$  or, suppressing the redundant variable, as  $A(s,t)$ .

In each channel there will occur the singularities required by unitarity. Thus there are simple poles corresponding to bound states, and branch points corresponding to production thresholds (Eden, 1952). Traditionally the branch cuts in the relevant energy plane are drawn along the positive real axis as shown in Fig. II-1. (The minor complications of complex thresholds which occur for unstable particle scattering are ignored here.) With this choice the physical s-channel amplitude is the boundary value

$$A(s,t) = \lim_{\epsilon \rightarrow 0^+} A(s+i\epsilon, t), \quad (\text{II.1.1})$$

and is Hermitian analytic. [That is,  $A$  and its Hermitian conjugate  $A^\dagger$  are boundary values of the same analytic function. See Eden, et al. (1966), Section 4.6.]\*

## 2. Dispersion Relations

Assume that the singularities shown in Fig. II-1 represent all the singularities of  $A(s,t)$  on the physical sheet. Take  $\rho$  as the contour of Fig. II-2, inside of which  $A(s,t)$  is regular. We define the discontinuity functions at fixed  $s$ ,

$$D_t(s,t) \equiv (1/2i)[A(s,t_+) - A(s,t_-)], \quad (\text{II.2.1})$$

$$D_u(s,u) \equiv (1/2i)[A(s,t(u_+)) - A(s,t(u_-))],$$

where  $t_{\pm} = \lim_{\epsilon \rightarrow 0^+} (t \pm i\epsilon)$ , the discontinuity being taken across all cuts in  $t$  (or in  $u$ ) at fixed  $s$ . By Hermitian analyticity

$$A(s,t^*) = A^*(s,t), \quad (\text{II.2.2})$$

so

$$D_t(s,t) = (1/2i) \text{Disc}_t[A(s,t)], \quad t > t_0; \quad (\text{II.2.3})$$

$$D_u(s,u) = (1/2i) \text{Disc}_u[A(s,t(u))], \quad u > u_0.$$

Then, suppressing for brevity any bound state poles, we can apply Cauchy's theorem and obtain the result

---

\* I denote complex conjugation by a star (\*) and Hermitian conjugation by a dagger (†).

$$A(s,t) = (1/2\pi i) \int_C dt' \frac{A(s,t')}{t' - t}. \quad (\text{II.2.4})$$

Let us assume that  $A(s,t) \rightarrow 0$  as  $|t| \rightarrow \infty$ . Then the contribution to the integral from the semicircles at infinity will vanish. This gives

$$\begin{aligned} A(s,t) &= \text{Pole terms} + (1/\pi) \int_{t_0}^{\infty} \frac{dt' D_t(s,t')}{t' - t} + (1/\pi) \int_{u_0}^{\infty} \frac{du' D_u(s,u')}{u' - u}. \end{aligned} \quad (\text{II.2.5})$$

This form, which is just a special kind of Hilbert transform, is a fixed-s dispersion relation.

If instead of vanishing at infinity the amplitude is bounded by an integral power (of  $t$ ), we can ensure convergence by making a number of subtractions.

### 3. The Mandelstam Representation

An important extension of the single-variable dispersion relation is the double dispersion relation conjectured by Mandelstam (1958), for which a general proof, even in perturbation theory, is lacking. To proceed, we define the discontinuity in  $s$  of  $D_t$  to be

$$\rho_{st}(s,t) = (1/2i)[D_t(s_+,t) - D_t(s_-,t)], \quad s > b_1(t) > 0 \quad (\text{II.3.1})$$

and

$$\rho_{tu}(t,u) = (1/2i)[D_t(u_+,t) - D_t(u_-,t)], \quad u > b_2(t) > 0 \quad (\text{II.3.2})$$

so that

$$D_t(s,t) = (1/\pi) \int_{b_1(t)}^{\infty} \frac{ds'' \rho_{st}(s'',u)}{s'' - s} + (1/\pi) \int_{b_2(t)}^{\infty} \frac{du'' \rho_{tu}(s,u'')}{u'' - u} \quad (\text{II.3.3})$$

The boundary functions  $b_{1,2}$  have been given in general by Kibble (1959). Likewise we can write

$$D_u(s,u) = (1/\pi) \int \frac{ds'' \rho_{su}(s'',u)}{s'' - s} + (1/\pi) \int \frac{dt'' \rho_{tu}(t'',u)}{t'' - t} \quad (\text{II.3.4})$$

Substituting Eqs. (II.3.3) and (II.3.4) into (II.2.5) we get the Mandelstam representation,

$$\begin{aligned} A(s,t) = & \text{Pole terms} + \frac{1}{\pi} \int ds'' \int \frac{dt' \rho_{st}(s'',t')}{(s'' - s)(t' - t)} \\ & + \frac{1}{\pi} \int ds'' \int \frac{du' \rho_{su}(s'',u')}{(s'' - s)(u' - u)} + \frac{1}{\pi} \int dt' \int \frac{du'' \rho_{tu}(t',u'')}{(t' - t)(u'' - u)} \end{aligned} \quad (\text{II.3.5})$$

Notice that the double spectral functions  $\rho_{ij}$  are symmetrically defined.

Thus

$$\begin{aligned} \rho_{st}(s,t) &= (-1/4)[A(s_+,t_+) + A(s_-,t_-) - A(s_+,t_-) - A(s_-,t_+)] \\ &= \left(\frac{1}{2i}\right) \text{Disc}_s D_t(s,t) = \left(\frac{1}{2i}\right) \text{Disc}_t D_s(s,t). \end{aligned} \quad (\text{II.3.6})$$

An understanding of the roles of the three double spectral functions  $\rho_{st}$ ,  $\rho_{su}$ ,  $\rho_{tu}$  is needed for the work of Chapters III and IV. Let us therefore review the connection between signature and double spectral functions.

4. Signatured Amplitudes and the Mandelstam Representation\*

In the  $z_s \equiv \cos \theta_s$  plane there lie right-hand singularities of the scattering amplitude corresponding to t-channel singularities, and left-hand singularities corresponding to u-channel singularities. These are illustrated schematically in Fig. II-3. It is more convenient to work with amplitudes which possess only right-hand singularities. Therefore I construct amplitudes of definite signature (in the s-channel) as follows. Let

$$A(s,t) = A^R(s,t) + A^L(s,t), \quad (\text{II.4.1})$$

where  $A^R$  contains only right-hand singularities and  $A^L$  only left hand ones. Thereupon we can write dispersion relations in  $z_s$  for these functions

$$\left. \begin{aligned} A^R(s,t) &= \sum_{\text{t-poles}} \frac{g_{t_i}(s)}{z_s(s,t_i) - z_s(s,t)} + \frac{1}{\pi} \int_{z_s(s,t_0)}^{\infty} \frac{dz' D_t(s,t')}{z' - z_s(s,t)} \\ A^L(s,t) &= \sum \frac{g_{u_i}(s)}{z_s(s,\Sigma-s-u_i) - z_s(s,t)} + \frac{1}{\pi} \int_{z_0(s,\Sigma-s-u_0)}^{\infty} \frac{dz' D_u(s,t')}{z' - z_s(s,t)} \end{aligned} \right\} \quad (\text{II.4.2})$$

with  $t' = t(z',s)$ .

---

\* Cf. Collins and Squires (1968), Chapter II.

Now define amplitudes of definite signature,

$$A^{\pm}(s,t) = A^R(s,t(s,z_s)) \pm A^L(s,t(s,-z_s)), \quad (\text{II.4.3})$$

each of which has, by definition, only right-hand singularities.

Neglecting for simplicity any bound state poles we may write dispersion relations for  $A^{\pm}$ ,

$$A^{\pm}(s,t) = \frac{1}{\pi} \int_{t_0}^{\infty} \frac{dt' D_t(s,t')}{t' - t} \pm \frac{1}{\pi} \int_{u_0}^{\infty} \frac{du' D_u(s,u')}{u' - t}. \quad (\text{II.4.4})$$

In terms of the double dispersion representation, this becomes

$$\begin{aligned} A^{\pm}(s,t) = & \frac{1}{2\pi} \int ds'' \int dt' \frac{\rho_{st}(s'',t') \pm \rho_{su}(s'',t')}{(s'' - s)(t' - t)} \\ & + \frac{1}{2\pi} \int du'' \int dt' \frac{\rho_{tu}(t',u'') \pm \rho_{tu}(u'',t')}{(u'' - u)(t' - t)}. \end{aligned} \quad (\text{II.4.5})$$

Equation (II.4.5) may be rewritten more compactly as

$$A^{\pm}(s,t) = \frac{1}{\pi} \int_{T_0 = \text{Min}[t_0, t(s, u_0)]}^{\infty} dt' \frac{D_t^{\pm}(s,t')}{t' - t}, \quad (\text{II.4.6})$$

with

$$\begin{aligned} D_t^{\pm}(s,t') = & \frac{1}{\pi} \int \frac{ds''}{(s'' - s)} [\rho_{st}(s'',t') \pm \rho_{su}(s'',t')] \\ & + \frac{1}{\pi} \int \frac{du''}{(u'' - u)} [\rho_{tu}(t',u'') \pm \rho_{tu}(u'',t')]. \end{aligned} \quad (\text{II.4.7})$$

It will be convenient later to define also the  $s$ -discontinuity function

$$D_s^\pm(s,t) = \frac{1}{\pi} \int \frac{dt'}{(t' - t)} [\rho_{st}(s,t') \pm \rho_{su}(s,t')]. \quad (\text{II.4.8})$$

5. The Froissart-Gribov Projection\*

Putting back possible poles into (II.4.6) we have the dispersion relation

$$A^\pm(s,t) = \sum_{t\text{-poles}} g_{t_i} / (M_{t_i}^2 - t) \pm \sum_{u\text{-poles}} g_{u_i} / (M_{u_i}^2 - t) + \frac{1}{\pi} \int_{T_0}^{\infty} dt' \frac{D_t^\pm(s,t')}{t' - t} \quad (\text{II.5.1})$$

$$= \sum_{t\text{-poles}} g_{t_i}(s) / [z_s(s, M_{t_i}^2) - z_s(s,t)] + \sum_{u\text{-poles}} g_{u_i}(s) / [z_s(s, \Sigma - s - M_{u_i}^2) - z_s(s,t)] + \frac{1}{\pi} \int_{z_s(s, T_0)}^{\infty} dz' \frac{D_t^\pm(s,t')}{z' - z_s(s,t)}, \quad (\text{II.5.2})$$

where

$$g_{t_i}(s) = g_{t_i} / 2p_{12} p_{34}; \quad g_{u_i}(s) = g_{u_i} / 2p_{12} p_{34} \quad (\text{II.5.3})$$

and  $z' = z_s(s,t')$ . We now define a partial wave projection,

---

\* See Froissart (1961), Gribov (1961).

$$A(s; \ell) = (1/32\pi) \int_{-1}^1 dz_s P_\ell(z_s) A(s, t[s, z_s]). \quad (\text{II.5.4})$$

Inserting (II.5.2) into (II.5.4), we invert the order of integration and use Neumann's formula\* [HTF 1, Section 3.6 (29)]

$$Q_\ell(z) = (-1/2) \int_{-1}^1 dz' P_\ell(z') / (z' - z) \quad (\text{II.5.5})$$

to perform the  $z$  integral,

$$\begin{aligned} A^\pm(s; \ell) = & (1/16\pi) \sum \{g_{t_i}(s) Q_\ell(z_s[s, M_{t_i}^2]) \\ & \pm g_{u_i}(s) Q_\ell(z_s[s, \Sigma - s - M_{u_i}^2])\} \\ & + (1/16\pi^2) \int_{z_s(s, T_0)}^\infty dz' D_t^\pm(s, t') Q_\ell(z'). \end{aligned} \quad (\text{II.5.6})$$

Suppressing poles, we are able to write two expressions for the partial wave projection of signed amplitudes,

$$A^\pm(s; \ell) = (1/16\pi^2) \int_{z_s(s, T_0)}^\infty dz' D_t^\pm(s, t') Q_\ell(z'), \quad (\text{II.5.7})$$

---

\* References to the Bateman Manuscript are cited as [Name Volume, Section (Equation)] where name is HTF for Higher Transcendental Functions or TIT for Tables of Integral Transforms. See Erdelyi (1953).

and

$$A^{\pm}(s; \ell) = (1/32\pi) \int_{-1}^1 dz' P_{\ell}(z') A^{\pm}(s, t'), \quad (\text{II.5.8})$$

for integer  $\ell$ . Now  $D_{\ell}^{\pm}(s, t)$  is the  $t$ -discontinuity of  $A^{\pm}(s, t)$ .

It therefore exists only for  $z_s \geq z_s(s, T_0)$ . On the other hand, the discontinuity of  $Q_{\ell}(z)$  is

$$\text{Im}\{Q_{\ell}(z)\} = \begin{cases} (-\pi/2) P_{\ell}(z), & -1 < z < 1 \\ 0, & |z| > 1, \ell \text{ integral.} \end{cases} \quad (\text{II.5.9})$$

In consequence we can combine (II.5.7) and (II.5.8) as

$$A^{\pm}(s; \ell) = (-i/32\pi^2) \int_{\rho_1 \text{ or } \rho_2} dz' Q_{\ell}(z') A^{\pm}(s, t'), \quad (\text{II.5.10})$$

where the contours  $\rho_1, \rho_2$  are shown in Fig. II-4. The partial wave series for the signed amplitudes, corresponding to the inverse of (II.5.10), is

$$A^{\pm}(s, t) = 16\pi \sum_{\ell=0}^{\infty} (2\ell + 1) A^{\pm}(s; \ell) P_{\ell}(z_s). \quad (\text{II.5.11})$$

Since  $P_{\ell}(z)$  is even or odd in  $z$  for integer  $\ell$  according as  $\ell$  is even or odd it follows that

$$A(s; \ell) = \begin{cases} A^+(s; \ell), & \ell \text{ even} \\ A^-(s; \ell), & \ell \text{ odd.} \end{cases} \quad (\text{II.5.12})$$

It is also useful to remark here that  $A^\pm(s,t)$  contains the  $\begin{pmatrix} \text{even} \\ \text{odd} \end{pmatrix}$  part of  $A(s,t)$ .

### 6. Singularities in $s$ of the Partial Wave Amplitudes

It is evident from (II.5.10) that  $A^\pm(s; \ell)$  has in the  $s$  plane the same right-hand singularities as  $A^\pm(s,t)$  except that it will not necessarily have all the poles. There will be in addition a set of left-hand singularities generated by the pinching of  $t$ - or  $u$ -channel singularities with the branch points of  $Q_\ell(z)$  at  $z = \pm 1$ . For any singularity of  $A^\pm(s,t)$  at  $t = t_i$ ,  $A^\pm(s; \ell)$  will have a branch point at

$$z_s(s, t_i) = \pm 1. \quad (\text{II.6.1})$$

For nonintegral  $\ell$  the left-hand singularities are rather more complicated, for  $Q_\ell(z)$  has four branch points and is cut between  $z = (-\infty, -1)$ , as well as  $z = (-1, 1)$ . Thus Eq. (II.5.10) remains valid for noninteger  $\ell$  but the contour  $\mathcal{C}_1$  must enclose the real  $z$ -axis, for  $1 > z > -\infty$ . The new contour is represented in Fig. II-5. The generalization of (II.5.9) is given by HTF 1, Section 3.3 (11, 12):

$$\text{Im}\{Q_\ell(z)\} = \begin{cases} (-\pi/2) P_\ell(z), & -1 < z < 1 \\ \sin \pi\ell Q_\ell(-z), & -\infty < z < -1. \end{cases} \quad (\text{II.6.2})$$

This provides us with two expressions for the partial wave projection, namely

$$A^\pm(s; \ell) = (1/16\pi^2) \int_{z_s(s, T_0)}^{\infty} dz' D_t^\pm(s, t') Q_\ell(z'). \quad (\text{II.6.3})$$

as before, and

$$A^{\pm}(s; \ell) = (1/32\pi) \int_{-1}^1 dz' P_{\ell}(z') A^{\pm}(s, t') \\ - (\sin \pi\ell/16\pi^2) \int_{-\infty}^{-1} dz' Q_{\ell}(-z') A^{\pm}(s, t'). \quad (\text{II.6.4})$$

The utility of these equations can be enhanced somewhat through elimination of the extra cut for  $z < -1$ . This may be done (see Collins and Squires, 1968 for the arithmetic) by writing dispersion relations not for the full partial wave amplitude  $A^{\pm}(s; \ell)$  but for the "reduced" partial wave amplitude

$$\hat{A}^{\pm}(s; \ell) = A^{\pm}(s; \ell)/(p_{12}p_{34})^{\ell}. \quad (\text{II.6.5})$$

The results may be summarized as

$$\text{Im}\{\hat{A}^{\pm}(s; \ell)\}_{\text{l.h.}} = (1/32\pi) \int_{-1}^{z_s(s, T_0)} dz' P_{\ell}(-z') D_t^{\pm}(s, t') (-p_{12}p_{34})^{-\ell} \\ + (1/16\pi^2) \int_{\rho_{tu} \neq 0} dz' Q_{\ell}(z') [1 \mp e^{-i\pi\ell}] \rho_{tu}(t', u') (p_{12}p_{34})^{\ell} \quad (\text{II.6.6})$$

on the left-hand cut. For physical  $\ell$  the last term does not contribute.

On the right-hand cut,

$$\text{Im}\{\hat{A}^{\pm}(s; \ell)\}_{\text{r.h.}} = (1/16\pi^2) \int_{z_s(s, T_0)}^{\infty} dz' Q_{\ell}(z') \\ \times [\rho_{st}(s, t') \pm \rho_{su}(s, t')] (p_{12}p_{34})^{-\ell}. \quad (\text{II.6.7})$$

This is a most useful result, for it states the connection between signature and the double spectral functions. We shall find it useful in Chapter IV.

### 7. Sommerfeld-Watson Transforms\*

Heretofore we ignored, for the sake of brevity, the subtractions which might be necessary to ensure convergence of

$$A^\pm(s; \ell) = (1/16\pi^2) \int_{z_s(s, T_0)}^{\infty} dz' D_t^\pm(s, t') Q_\ell(z'). \quad (\text{II.5.7})$$

In reality, this equation is likely to be undefined as it stands for many values of  $s$ . But if  $D_t^\pm(s, t')$  is power-bounded, i.e.

$$\left. \begin{array}{l} D_t^\pm(s, t') \underset{s \rightarrow \infty}{\sim} z_s^{N(s) - \sigma(s)} \\ N(s) \text{ an integer; } 0 < \sigma(s) < 1 \end{array} \right\}, \quad (\text{II.7.1})$$

then we may subtract Eq. (II.5.2)  $N(s)$  times at the point  $z_s = 0$ , whence

$$A^\pm(s, t) = P_{N-1}(s, z_s) + \frac{z_s^{N(s)}}{\pi} \int_{z_s(s, T_0)}^{\infty} \frac{dz' D_t^\pm(s, t')}{(z' - z_s) z_s^{N(s)}}. \quad (\text{II.7.2})$$

In (II.7.2),  $P_{N-1}(s, z_s)$  is a polynomial in  $z_s$  of degree  $N-1$ , and the remaining integral converges. Now applying (II.5.4) we obtain

---

\* See Sommerfeld (1949), Watson (1918), Collins and Squires (1968).

$$A^{\pm}(s; \ell) = (1/32\pi) \int_{-1}^1 dz_s P_{\ell}(z_s) \times \left\{ P_{N-1}(s, z_s) + \frac{z_s^N}{\pi} \int_{z_s(s, T_0)}^{\infty} \frac{dz' D_t^{\pm}(s, t')}{(z' - z) z'^N} \right\} \quad (\text{II.7.3})$$

As  $\int_{-1}^1 dz P_{\ell}(z) z^M = 0$  for  $M < \ell$ , we put

$(z_s/z')^N = [1 + (z_s - z')/z']^N$ , expand in powers, and get

$$A^{\pm}(s; \ell) = (1/16\pi^2) \int_{z_s(s, T_0)}^{\infty} dz' Q_{\ell}(z') D_t^{\pm}(s, t'), \quad (\text{II.7.4})$$

for  $\ell \geq N(s)$ . Since [HTF 1, Section 3.9 (21)]  $Q_{\ell}(z) \underset{z \rightarrow \infty}{\sim} z^{-(\ell+1)}$ , the integral in (II.7.4) will converge.

Providing that the Mandelstam representation is power bounded, the higher partial-waves are given uniquely by the double spectral functions, whereas lower partial-waves may depend on arbitrary subtraction constants. To proceed to the Sommerfeld-Watson transform, we suppose that the signatured partial-wave amplitude  $A^{\pm}(s; \ell)$  defined in (II.5.7) is an analytic function of  $\ell$  (in the physicist's sense) in the right half-plane.\* The import of this assumption is that we can continue (II.7.4) below  $\text{Re}\{\ell\} = N(s)$  to interesting physical values of  $\ell$ . Observe that because the only singularities in  $\ell$  of  $Q_{\ell}(z)$  are simple poles at the negative integers [HTF 1, Section 3.3 (3)], the

---

\* Thus, by analytic we mean that only isolated singularities occur.

amplitude  $A^\pm(s; \ell)$  is holomorphic (free of any singularities) for  $\text{Re}\{\ell\} \geq N(s)$ .

We now replace the partial-wave expansion (II.5.11) by a contour integration in the  $\ell$ -plane,

$$A^\pm(s, t) = \frac{-16\pi}{2i} \int_C \frac{d\ell (2\ell + 1) A^\pm(s; \ell) P_\ell(-z_s)}{\sin \pi \ell}, \quad (\text{II.7.5})$$

which is illustrated in Fig. II-6. The contour includes the nonnegative integers, but avoids any singularities of  $A^\pm(s; \ell)$ . The integrand has a pole at each integer  $n$ , for which  $\sin \pi \ell \rightarrow (-1)^n (\ell - n)\pi$ . Since  $P_n(-z) = (-1)^n P_n(z)$  [HTF 1, Section 3.3 (10)] the pole residues are

$$2i P_n(z_s) A^\pm(s; n) (2n + 1). \quad (\text{II.7.6})$$

With this information it is easy to verify (Cauchy's theorem) that (II.7.5) is equivalent to the partial-wave series

$$A^\pm(s, t) = 16\pi \sum_{\substack{\text{positive,} \\ \text{integral } \ell}} (2\ell + 1) A^\pm(s; \ell) P_\ell(z_s). \quad (\text{II.5.11})$$

We now wish to continue in  $\ell$ , and we assert that  $A^\pm(s; \ell)$  as given by (II.7.4) is the unique analytic continuation of the partial-wave amplitude for integral  $\ell$ . For the proof, we invoke Carlson's theorem (Titchmarsh, 1939). [Although we did not remark upon it in Section II.5, the point of the Froissart-Gribov projection was to build a continuation which satisfies the conditions of Carlson's theorem.]

If  $f(z)$  is regular and of the form

$$O(e^{x|z|}), \quad x < \pi, \quad \text{for } \operatorname{Re}\{z\} > A, \quad \text{and } f(z) = 0$$

for an infinite sequence of integers  $z = A, A+1, \dots$ , then  $f(z) \equiv 0$ .

We notice that

$$Q_\ell(z) \underset{|\ell| \rightarrow \infty}{\sim} C \ell^{-\frac{1}{2}} \exp\left[\left(\ell + \frac{1}{2}\right) \log\left\{z + (z^2 - 1)^{\frac{1}{2}}\right\}\right] \quad (\text{II.7.7})$$

[HTF 1, Section 3.9 (1)]. Thus if the integral (II.7.4) converges, it is the lowest values of  $z'$  in the range of integration which dominate the high partial-waves. That is to say, the high partial waves are controlled by the nearest singularities (in  $t$  or  $u$ ). If the nearest singularity is at  $z_0$ , then (subject to the assumption that the amplitude is power-bounded)

$$A^\pm(s; \ell) \underset{\ell \rightarrow \infty}{\longrightarrow} \phi(s) e^{-\ell[\log\{z_0 + (z_0^2 - 1)^{\frac{1}{2}}\}]}, \quad (\text{II.7.8})$$

where  $\phi(s)$  is a function of  $s$ . The asymptotic form (II.7.8) satisfies the requirements of Carlson's theorem (which is applied to the difference between the "true" amplitude and the Froissart-Gribov continuation), so our continuation in  $\ell$  is unique.

Next we distort the contour  $\rho$  into  $\rho'$ , opening it up with a semicircle at infinity and a line parallel to the imaginary axis at  $\operatorname{Re}\{\ell\} = L$ . This is shown in Fig. II-7. So long as  $L > N(s)$ , no singularities will be encountered as this displacement is made. Thus

$$\int_{\rho_1} = \int_{\rho}. \quad \text{Moreover, the contribution from the semicircle vanishes}$$

because of (II.7.8) and  $|P_\ell(-z_s)/\sin \pi \ell| \xrightarrow[\ell \rightarrow \infty]{} 0$ .<sup>\*</sup> We continue to distort the contour by reducing  $L$ . For  $L \leq N(s)$ , we shall encounter singularities in the  $\ell$  plane. These are swallowed by the contour and we pick up their contributions as prescribed by Cauchy. The situation is shown schematically in Fig. II-8, for  $L = -\frac{1}{2}$ . The result of moving the contour back to  $\text{Re}\{\ell\} = -\frac{1}{2}$  is

$$\begin{aligned}
 A^\pm(s, t) &= \frac{-16\pi}{2i} \int_{-\frac{1}{2}-i\infty}^{-\frac{1}{2}+i\infty} d\ell (2\ell + 1) \frac{A^\pm(s; \ell)}{\sin \pi \ell} P_\ell(-z_s) \\
 &- \sum_{\text{poles}} 16\pi^2 (2\alpha_i(s) + 1) \beta_i(s) P_{\alpha_i(s)}(-z_s) / \sin \pi \alpha_i(s) \\
 &- \sum_{\text{cuts}} \frac{16\pi}{2i} \int_{\mathcal{C}_j} d\ell (2\ell + 1) A^\pm(s; \ell) P_\ell(-z_s) / \sin \pi \ell. \quad (\text{II.7.9})
 \end{aligned}$$

The first term, the background integral, vanishes as  $z_s \rightarrow \infty$ , leaving a sum of Regge poles and Regge cuts.

In order to make the complex angular momentum analysis useful for physics, one has to ensure that the Regge poles and Regge cuts uncovered in the distortion of the contour dominate for large energy over the contribution of the background integral. In (II.7.9), we pushed the contour back to  $\text{Re}\{\ell\} = -\frac{1}{2}$ . For large values of  $z$ ,

$$P_\alpha(z) \underset{z \rightarrow \infty}{\sim} z^{|\alpha + \frac{1}{2}| - \frac{1}{2}}, \quad (\text{II.7.10})$$

---

\* See, e.g., Collins and Squires (1968), Section II.7-9.

if  $\alpha$  is not a negative integer [HTF 1, Section 3.2 (23)]. Therefore the first term in (II.7.9), the background integral, is least important (as  $z \rightarrow \infty$ ) for  $\text{Re}\{\ell\} = -\frac{1}{2}$ ; for example, Regge poles with  $A(s) > -\frac{1}{2}$  will be more important. As  $\text{Re}\{\ell\}$  is decreased from  $-\frac{1}{2}$ , the asymptotic form (II.7.10) of  $P_\alpha$  seems to indicate that the background integral will become asymptotically dominant over the singularities in the right half  $\ell$  plane.

The way out of this difficulty was found by Mandelstam (1962), who demonstrated the dominance of the right-hand singularities as  $z \rightarrow \infty$ , for  $\text{Re}\{\ell\} < -\frac{1}{2}$  in the background contour. We follow the summary of Collins and Squires (1968), Section II.12. Rewrite the partial-wave series (II.5.11) by adding and subtracting a piece:

$$\begin{aligned}
 A^\pm(s, t) = & 16\pi \sum_{\ell=0}^{\infty} \left\{ (2\ell + 1) A^\pm(s; \ell) P_\ell(z_s) \right. \\
 & \left. + \frac{1}{\pi} (-1)^{\ell-1} (2\ell) A^\pm(s; \ell - \frac{1}{2}) Q_{\ell - \frac{1}{2}}(z_s) \right\} \\
 & - 16 \sum_{\ell=0}^{\infty} (-1)^{\ell-1} (2\ell) A^\pm(s; \ell - \frac{1}{2}) Q_{\ell - \frac{1}{2}}(z_s). \quad (\text{II.7.11})
 \end{aligned}$$

Now using [HTF 1, Section 3.3 (3)]

$$\frac{P_\ell(z)}{\sin \pi \ell} - \frac{1}{\pi} \frac{Q_\ell(z)}{\cos \pi \ell} = -\frac{1}{\pi} \frac{Q_{-\ell-1}(z)}{\cos \pi \ell}, \quad (\text{II.7.12})$$

we obtain

$$\begin{aligned}
 A^{\pm}(s,t) &= \frac{16}{2i} \int_{L-i\infty}^{L+i\infty} d\ell(2\ell + 1) A^{\pm}(s; \ell) \frac{Q_{-\ell-1}(-z_s)}{\cos \pi\ell} \\
 &- \sum_{\ell=L'+\frac{1}{2}}^{\infty} \frac{(-1)^{\ell-1}}{\pi} (2\ell) A^{\pm}(s; -\ell-\frac{1}{2}) Q_{\ell-\frac{1}{2}}(-z_s) \\
 &+ (\text{Regge poles}) + (\text{Regge cuts}), \tag{II.7.13}
 \end{aligned}$$

where  $-L'$  is the smallest half-integer greater than  $L$ . Since [HTF 1, Section 3.2 (41)]

$$Q_{\ell}(z) \underset{z \rightarrow \infty}{\sim} z^{-\ell-1}, \tag{II.7.14}$$

the first and second terms in (II.7.13) die as  $z_s^L$  for  $L < -\frac{1}{2}$ , and the dominance of the Regge singularities is assured.

### 8. Mellin Transforms\*

Mellin transforms provide another technique for calculating high-energy behavior by picking out the rightmost singularity in the  $\ell$  plane. The Mellin transform  $F(\alpha)$  of a function  $f(s)$  is defined by

$$F(\alpha) = \int_0^{\infty} ds f(s) s^{-\alpha-1}. \tag{II.8.1}$$

The inverse transform is

---

\* See Bjorken and Wu (1963); Courant and Hilbert (1953); Eden, et al. (1966), p. 151.

$$f(s) = (1/2\pi i) \int_{\sigma-i\infty}^{\sigma+i\infty} d\alpha F(\alpha) s^\alpha, \quad (\text{II.8.2})$$

where  $F(\alpha)$  is analytic on the line  $\text{Re}\{\alpha\} = \sigma$ . These are simply the Fourier integral formulae in the variables  $\ln s$  and  $-i\alpha$ .

An important class of functions  $f(s)$  is given by

$$f(s) = \begin{cases} s^{\alpha_0} (\ln s)^{b-1} & s > 1 \\ 0 & s \leq 1 \end{cases} \quad (\text{II.8.3})$$

for which the Mellin transforms are poles of order  $b$  if  $b$  is integral,

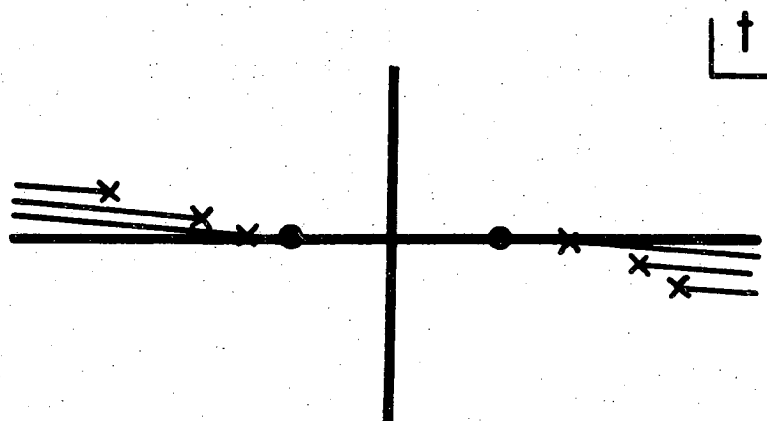
$$F(\alpha) = \Gamma(b)(\alpha - \alpha_0)^{-b}. \quad (\text{II.8.4})$$

For noninteger values of  $b$ ,  $F(\alpha)$  is cut from  $\alpha = -\infty$  to  $\alpha = \alpha_0$ ; then the integration contour specified by the parameter  $\sigma$  must be chosen to avoid the cut.

The application of Mellin transforms is similar to that of Sommerfeld-Watson transforms. For example, if  $F(\alpha)$  is regular in a region, except for poles, then we may displace the contour  $\mathcal{C}(\sigma)$  to the left and obtain a sequence of contributions from the poles encountered. As in the case of Sommerfeld-Watson transforms, the rightmost singularity in  $\alpha$  will dominate the behavior of  $f(s)$ , as  $s \rightarrow \infty$ .

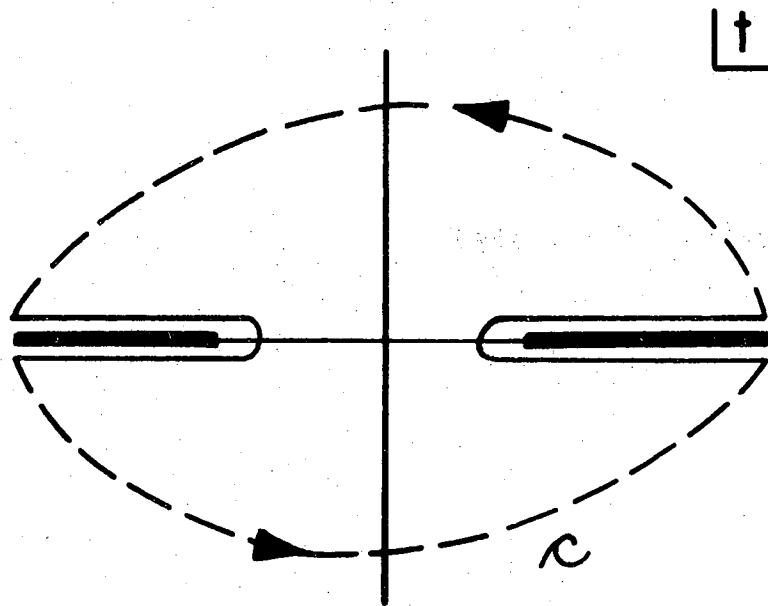
FIGURE CAPTIONS

- Fig. II-1. Branch cuts in the complex  $t$ -plane arising from thresholds in the  $t$ -channel (on the right) and in the  $u$ -channel (on the left) for a fixed value of  $s$ . Two poles are also shown.
- Fig. II-2. The Cauchy contour of integration in the complex  $t$ -plane, used in writing a dispersion relation.
- Fig. II-3. The schematic singularity structure of Fig. II-1, mapped onto the  $z_s$ -plane.
- Fig. II-4. Integration contours in the complex  $z_s$ -plane, for the Froissart-Gribov projection (II.5.10).
- Fig. II-5. Contours of integration in the  $z_s$ -plane for the Froissart-Gribov projection when  $\ell$  is complex.
- Fig. II-6. Integration contour for the Sommerfeld-Watson transformation.
- Fig. II-7. The opened contour with a semicircle at infinity.
- Fig. II-8. The contour pushed back to  $\text{Re}\{\ell\} = -1/2$ . Two schematic Regge poles and one schematic Regge cut are shown.



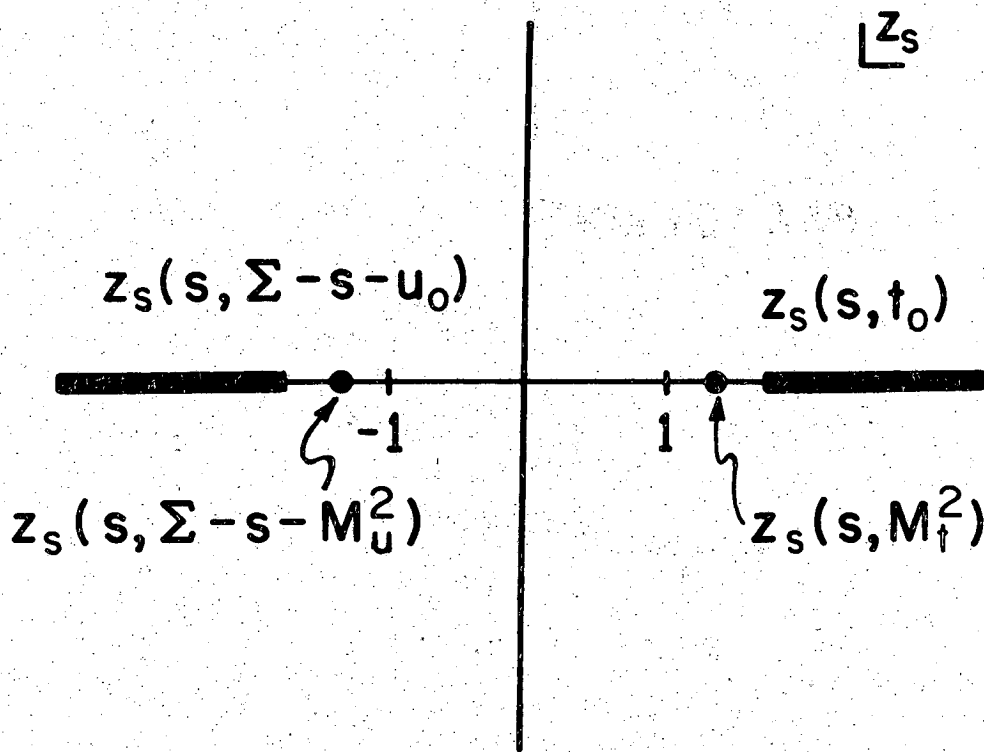
XBL707-3491

Fig. II-1.



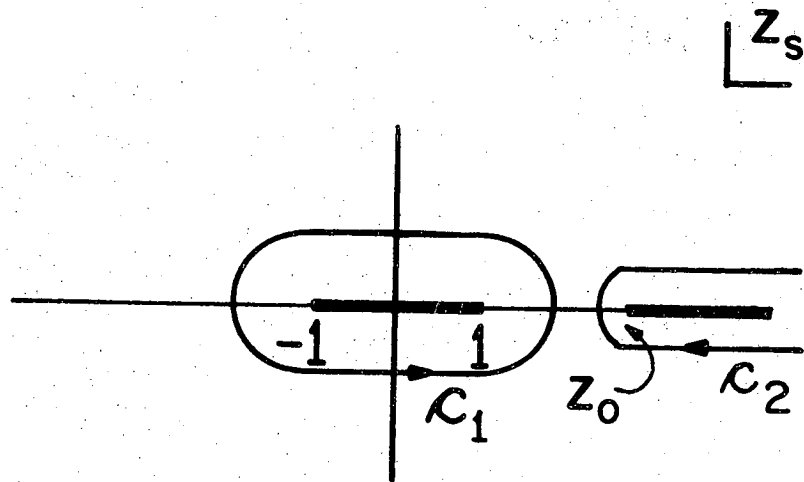
XBL707-3486

Fig. II-2.



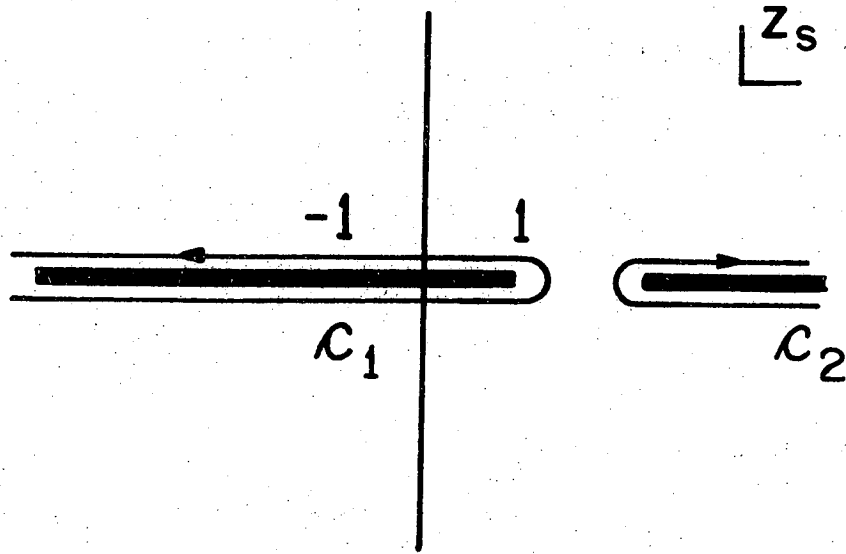
XBL707-3484

Fig. II-3.



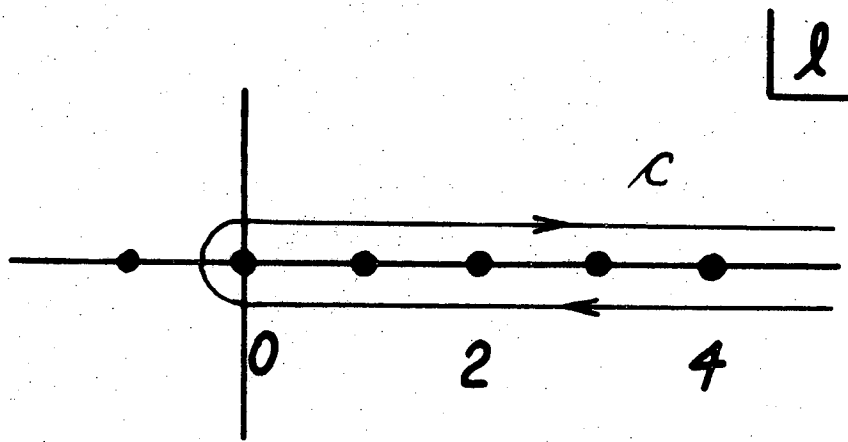
XBL707-3488

Fig. II-4.



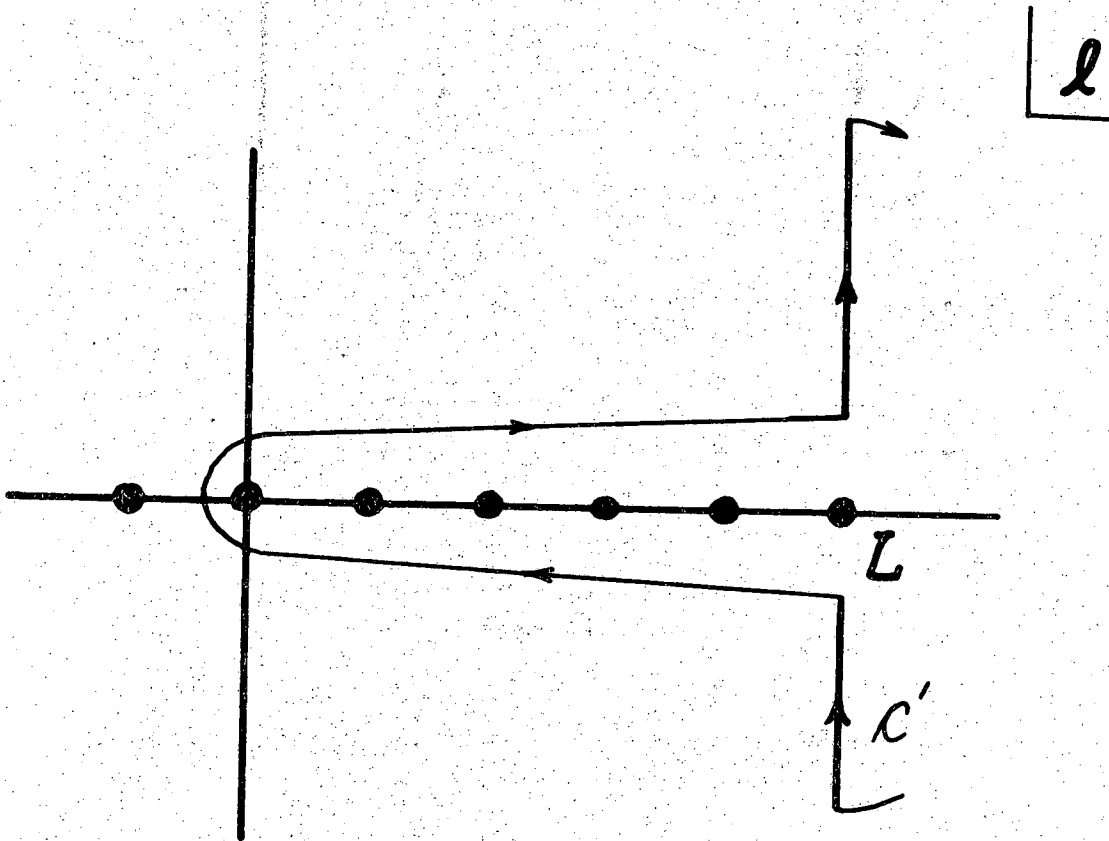
XBL707-3490

Fig. II-5.



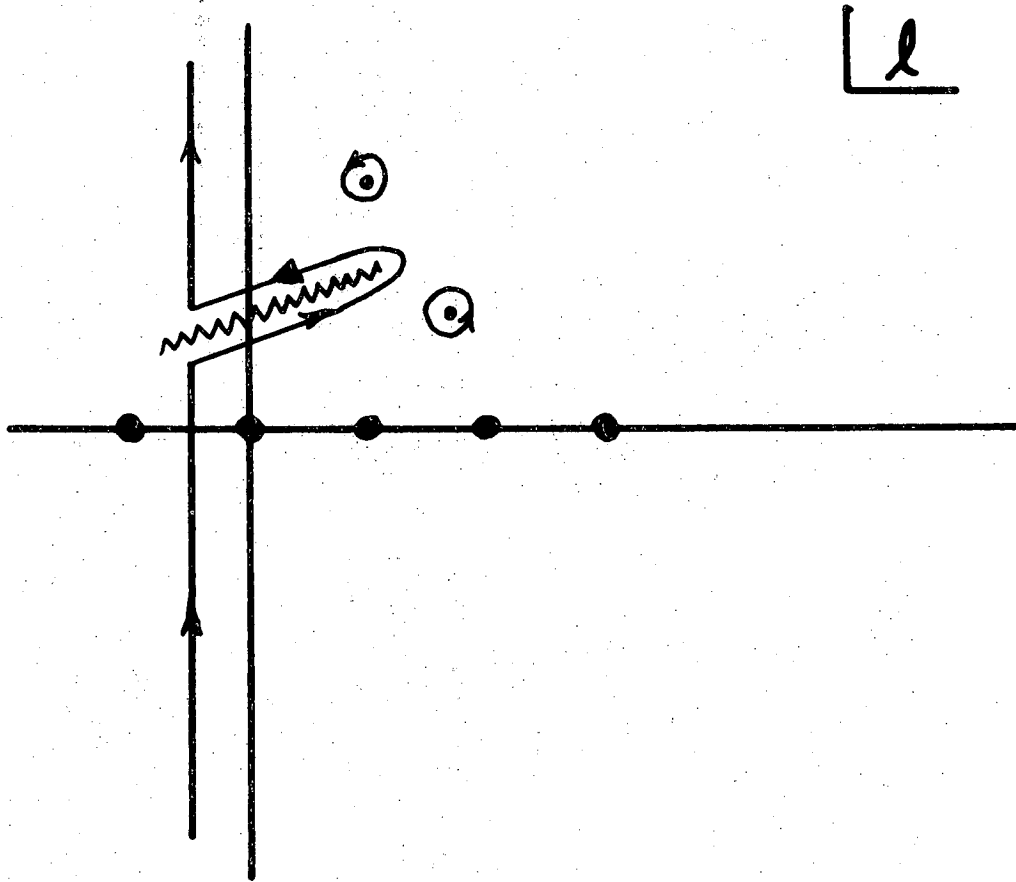
XBL 708-1842

Fig. II-6.



XBL 708-1843

Fig. II-7.



XBL 708-1841

Fig. II-8.

### III. THE AMATI-FUBINI-STANGHELLINI BRANCH CUT

Historically, the possible existence and potential importance of Regge cuts were first acknowledged by Amati, Fubini, and Stanghellini (1962a,b) [hereafter, AFS], in the context of the multiperipheral model. In this simplest case the cuts are only illusory, and result from an unjustified truncation of the unitarity sum (Mandelstam, 1963; Polkinghorne, 1963). I shall review the AFS calculation and discuss the cancellation of the apparent cut by many-body contributions to the unitarity equation. Then I will specify the conditions under which Regge cuts can be generated, and note some consequences of the existence of cuts in the  $j$  plane.

#### 1. Generation of the AFS Cut by Two-Body Unitarity

Amati, Fubini, and Stanghellini considered the effects of  $s$ -channel unitarity upon their multiperipheral model. In the simplest case of a single iteration in the  $s$ -channel, one considers the set of graphs shown in Fig. III-1, where each blob (or bubble) represents a complete sum of Feynman graphs. That is,  is a full (off-mass-shell) scattering amplitude. To study the two Reggeon cut we specialize to the diagram of Fig. III-2 in which the blobs are represented as Regge pole exchange amplitudes. Following AFS, let us call  $T(s,t)$  a Regge pole amplitude and call  $A_1(s,t)$  the absorptive part of the once-iterated amplitude. The Regge pole amplitude is given by

$$T(s,t) = C(t) \xi(t) (s/s_0)^{\alpha(t)}, \quad (\text{III.1.1})$$

where  $\xi(t)$  is the signature factor,  $(\tau + e^{-i\pi\alpha(t)})/\sin \pi\alpha(t)$ . The first iteration gives

$$A_1(s,t) = (8\pi)^{-2} \int d\Omega T_0^*(s,t') T_0(s,t''), \quad (\text{III.1.2})$$

where  $t'$  is the momentum transfer squared through the first Reggeon,  $\Omega$  is the c.m. solid angle between the initial and final states, and  $t''$  is the momentum transfer squared through the second Reggeon. As (III.1.2) is a unitarity equation, the intermediate states are on the mass shell. This expression can be manipulated into the form

$$A_1(s,t) = 2(8\pi)^{-2} s^{-1} \int_{-\infty}^0 dt' \int_{-\infty}^0 dt'' T_0^*(s,t') T_0(s,t'') \kappa(t,t',t''), \quad (\text{III.1.3})$$

where

$$\kappa(a,b,c) = \frac{\theta[-a^2 - b^2 - c^2 + 2ab + 2ac + 2bc]}{[-a^2 - b^2 - c^2 + 2ab + 2ac + 2bc]^{\frac{1}{2}}}.$$

With the amplitudes (III.1.1) as input, this becomes

$$A_1(s,t) = 2(8\pi)^{-2} \int_{-\infty}^0 dt' \int_{-\infty}^0 dt'' C(t') C(t'') \xi(t') \xi(t'') \times \kappa(t,t',t'') (s/s_0)^{\alpha(t')+\alpha(t'')-1}. \quad (\text{III.1.4})$$

This displays explicitly all the  $s$ -dependence in  $A_1$ , and we appear to have produced asymptotic behavior corresponding to a continuous superposition of Regge poles or in other words a Regge cut with branch point at

$$\alpha_{\text{cut}}(t) = \text{Max}\{\alpha(t') + \alpha(t'') - 1\}. \quad (\text{III.1.5})$$

Indeed, by taking a Froissart-Gribov or Mellin projection [for which see Section II.5-8] it can be shown that a Regge cut occurs with branch point at (III.1.5). For more specific results, see Rothe (1967).

In this, the AFS approximation, the s-channel intermediate states are taken to be on the mass shell, and indeed in the approximation of two-body unitarity, Eq. (III.1.4) is exact. However it was soon pointed out by Mandelstam (1963) and by Polkinghorne (1963) that truncation of the unitarity sum with two-body intermediate states only was unwarranted. Specifically, there are contributions to the unitarity sum from "higher order" intermediate states which precisely cancel the AFS cut on the physical sheet in the s plane.

To discuss the cancellation we turn to the Feynman integral technique used by Rothe (1967). This route is rather clumsier for computation than the Sudakov variable method but provides good insight.

## 2. The Rothe Cancellation\*

When Mandelstam demonstrated the absence of the AFS cut in Fig. III-2, he proposed that there should be an uncancelled cut in the double cross diagram shown in Fig. III-3. He further conjectured that cuts should exist only in those diagrams of the form of Fig. III-4 in which both blobs contain third double spectral functions with respect to the t-channel ( $\rho_{su} \neq 0$ ). This conjecture was verified for Feynman graphs by Wilkin (1964), and emerges easily in Rothe's method.

---

\* The calculation is nicely summarized by Landshoff (1969), and by Risk (1970).

Consider Fig. III-2 as a Feynman diagram. The amplitude is

$$A(s,t) = C \int d^4 k_1 \left\{ \frac{1}{-k_2^2 - m^2 + i\epsilon} \cdot \frac{1}{-k_4^2 - m^2 + i\epsilon} \cdot R(s, k_1^2; k_2^2, k_4^2) R(s, k_3^2; k_2^2, k_4^2) \right\} \quad (\text{III.2.1})$$

where  $R(s, -t_i; -\mu_2^2, -\mu_4^2)$  is the off mass shell amplitude associated with the exchange of a Regge pole with trajectory  $\alpha(t_i)$ . Now make the change of variables  $d^4 k_i \rightarrow \prod_{n=1}^4 dk_n^2$ , which is accompanied by the Jacobian

$$\left. \begin{aligned} J &= \theta(D)/D^{\frac{1}{2}} \\ D &= -16 \det |2k_i \cdot k_j|. \end{aligned} \right\} \quad (\text{III.2.2})$$

We assume that the limit  $s \rightarrow \infty$  can be taken inside the Feynman integral, insert the asymptotic form of the Jacobian, and arrive at

$$A(s,t) \approx \frac{C}{4s} \int dk_1^2 \int dk_2^2 \int dk_3^2 \int dk_4^2 \left[ \kappa(-k_1^2, -k_3^2, t) \times \frac{1}{-k_2^2 - m^2 + i\epsilon} \cdot \frac{1}{-k_4^2 - m^2 + i\epsilon} R(s, k_1^2; k_2^2, k_4^2) R(s, k_3^2; k_2^2, k_4^2) \right]. \quad (\text{III.2.3})$$

Consider the  $-k_2^2$  integration. There is a pole from the propagator  $(-k_2^2 - m^2 + i\epsilon)^{-1}$  which appears below the integration contour, by virtue of the  $+i\epsilon$  prescription. There may also be branch points from the two vertex functions that depend on  $k_2^2$ . Drawing upon experience in perturbation theory (for which see Eden, et al., 1966), we assume two properties for the vertex functions:

(i) They have only a right-hand cut in  $-k_2^2$ , which also appears below the integration contour.

(ii) They vanish for large values of  $|k_2^2|$ .

Property (ii) permits us to close the contour of integration with an infinite semicircle in the upper half plane, and property (i) results in the integral vanishing. This is shown pictorially in Fig. III-5. The original contour of Fig. III-5(a) is deformed into the contour sketched in Fig. III-5(b) which, enclosing no singularities, shows that the integral vanishes.

Alternatively we could wrap the contour around the right-hand singularities as indicated in Fig. III-5(c). This must of course give the same answer as Fig. III-5(b), which means that the pole contribution (the on mass shell piece) must be canceled by the integral along the cut. The procedure of Amati, Fubini, and Stanghellini (1962a,b) amounted [Fig. III-5(d)] to picking up only the pole term from the propagator, and ignoring the singularities of the vertex function.

### 3. Diagrams with Cuts

Clearly if we wish to write down a diagram with a Regge cut, we must arrange to have both right-hand and left-hand singularities in  $-k_2^2$ . The presence of left-hand singularities prevents the distortion of the contour which results in Fig. III-5(b) and thereby invalidates the proof that the Regge cut vanishes. The simplest change is to replace the left-hand side of Fig. III-2 by a cross (this substitution is represented in Fig. III-6). After the replacement, the bubbles representing the vertex functions have both left-hand and right-hand singularities in

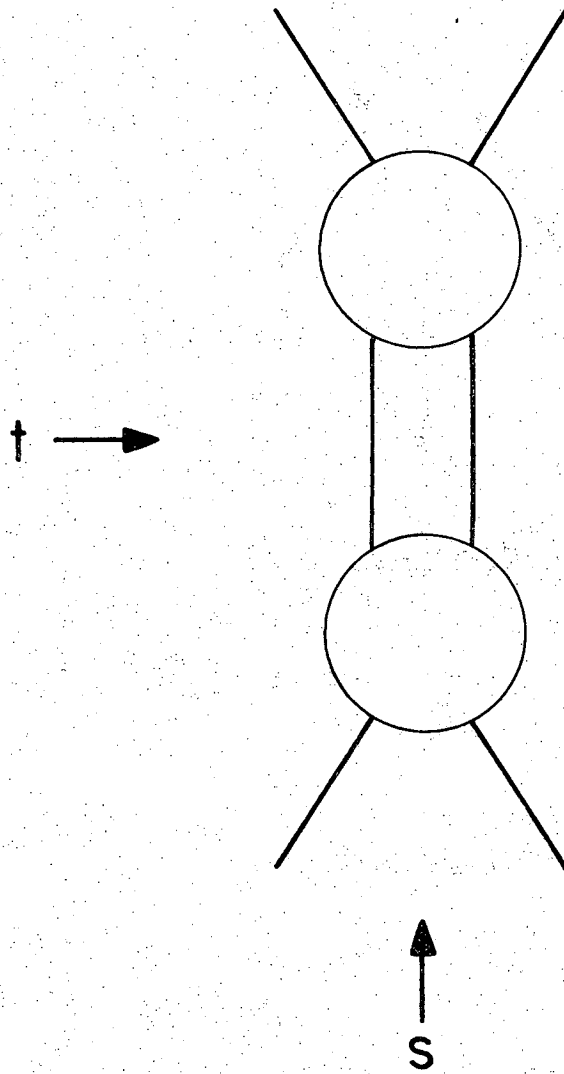
$-k_2^2$  (which is the total energy-squared flowing vertically through the cross). We ignore for the moment variables internal to the cross, and note that because the cross has an  $su$  double spectral function it has both right-hand and left-hand cuts in  $-k_2^2$  at fixed  $t$ . Thus the contour cannot be closed in either the upper or lower half plane, but as the cross tends to zero faster than  $1/k_2^2$  for large  $|k_2^2|$  we can make the deformation of Fig. III-5(c) to obtain an integral over the imaginary part of the cross graph.

Identical arguments apply to the  $-k_4^2$  integration. Therefore to obtain a diagram with a Regge cut we must make insertions having  $su$  double spectral functions into both ends of the graph. These insertions will then have third double spectral functions in the  $t$ -channel sense. Finally we see that the simplest graph with a Regge cut is the Mandelstam graph shown as Fig. III-3. A summary of the calculation of this double cross graph is given in the next chapter.

Cuts in the  $j$  plane weaken the analyticity properties of the scattering amplitude which can be proved from the unitarity equation. In particular the existence of certain fixed- $j$  poles is related to the existence of Regge cuts. Some aspects of the properties of the scattering amplitude when Regge cuts are present are discussed by Collins and Squires (1968), Sections V. 4-6.

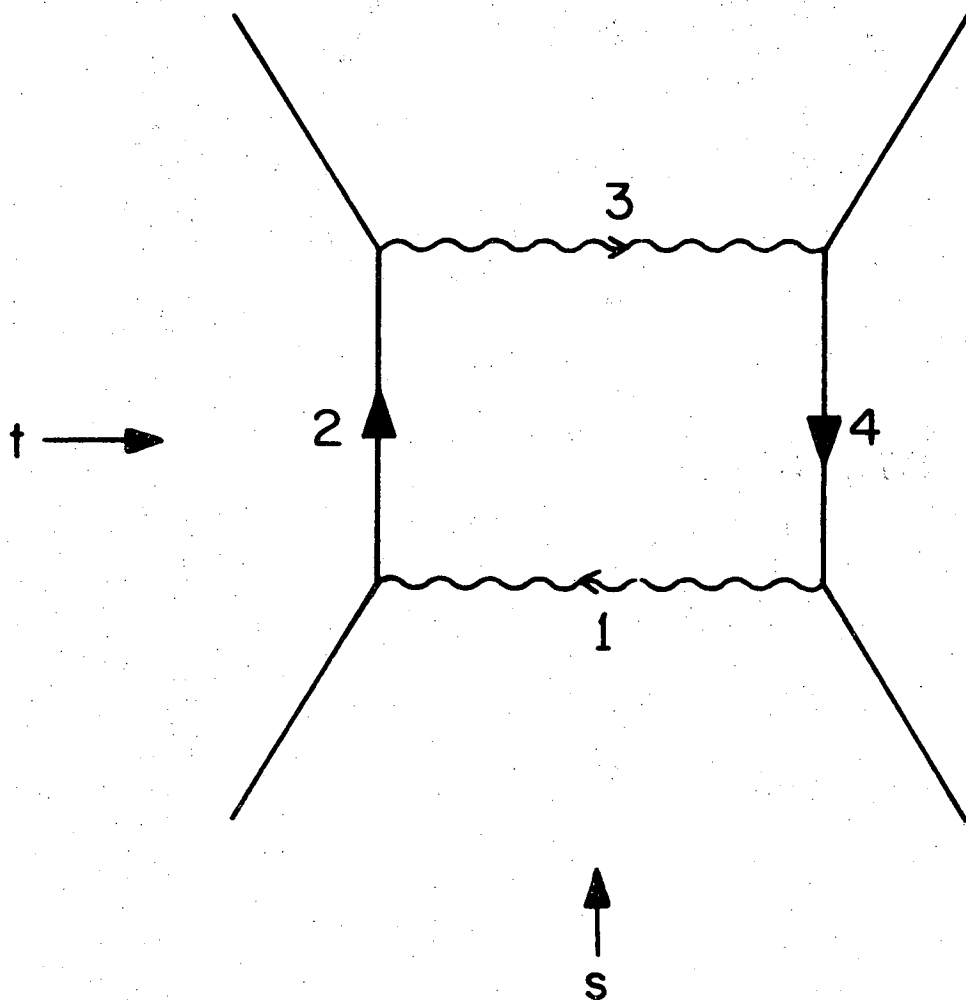
FIGURE CAPTIONS

- Fig. III-1. The set of graphs representing one iteration of the scattering amplitude in the s channel.
- Fig. III-2. A special case of the s-channel iterations corresponding to two-Reggeon exchange. The Reggeons are represented by wavy lines.
- Fig. III-3. The Mandelstam (double cross) diagram.
- Fig. III-4. A general diagram for two Reggeon exchange.
- Fig. III-5. Contours of the  $-k_2^2$  integration in Eq. (III.2.3).  
(a) The original contour, which passes above the on mass shell pole contributed by the  $\delta$ -function part of the propagator, and above the right-hand cut in the vertex functions.  
(b) The contour closed in the upper half plane. (c) The contour wrapped around the right-hand singularities. (d) The AFS approximation, in which the cut contribution is neglected.
- Fig. III-6. Replacing the left-hand portion of Fig. III-2 by a cross.



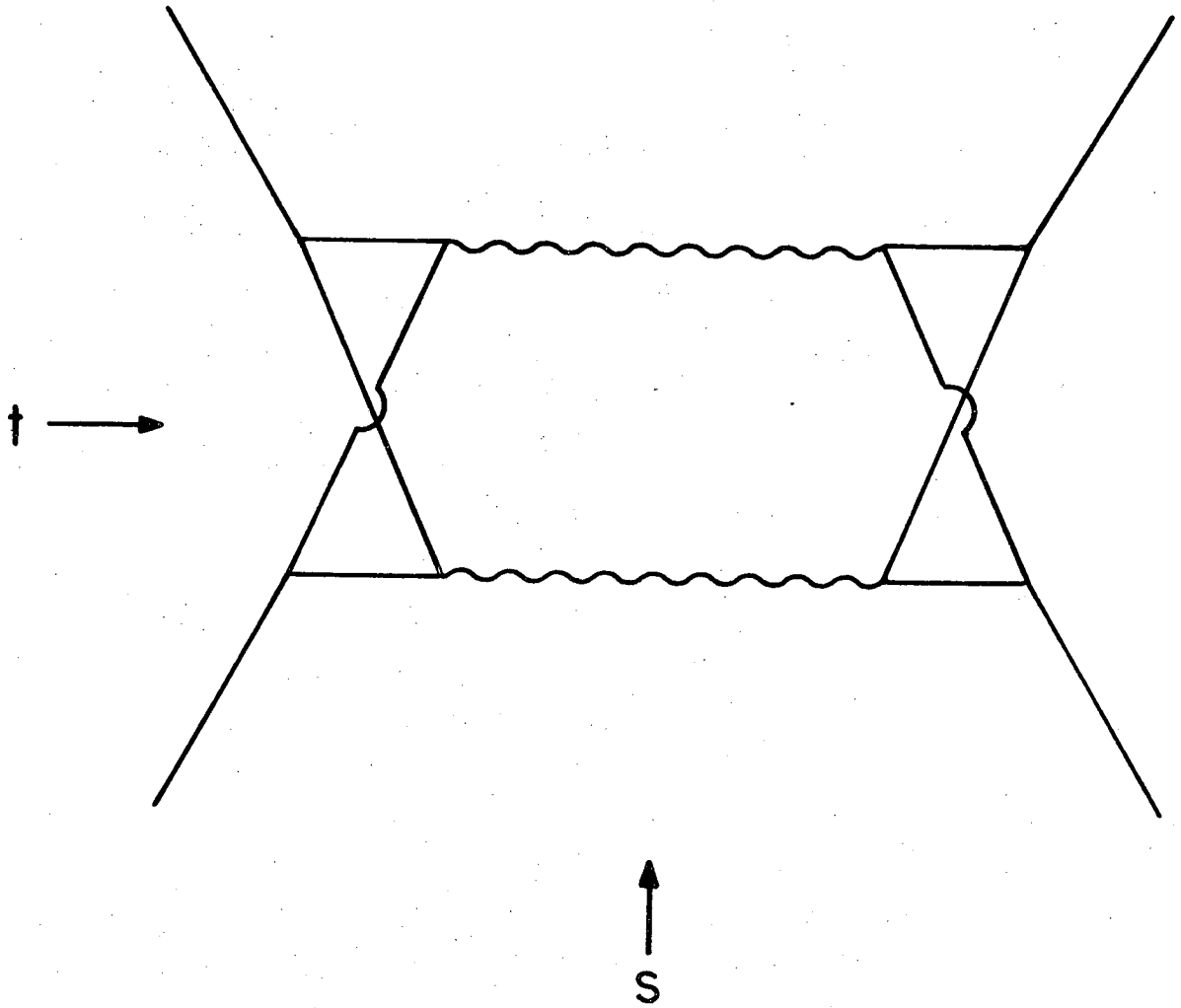
XBL707-3485

Fig. III-1.



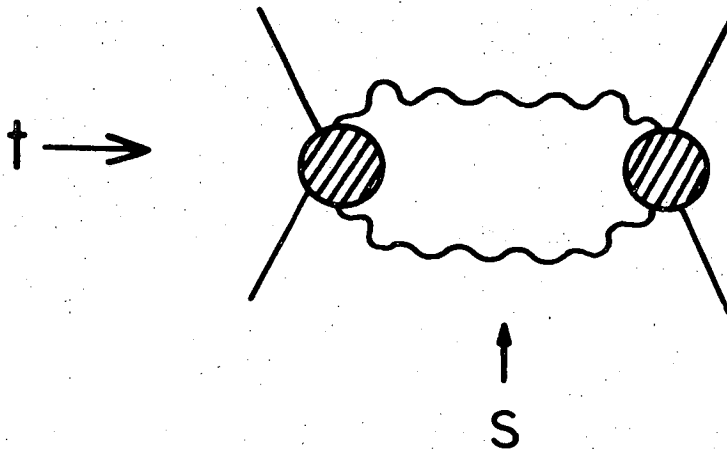
XBL707-3475

Fig. III-2.



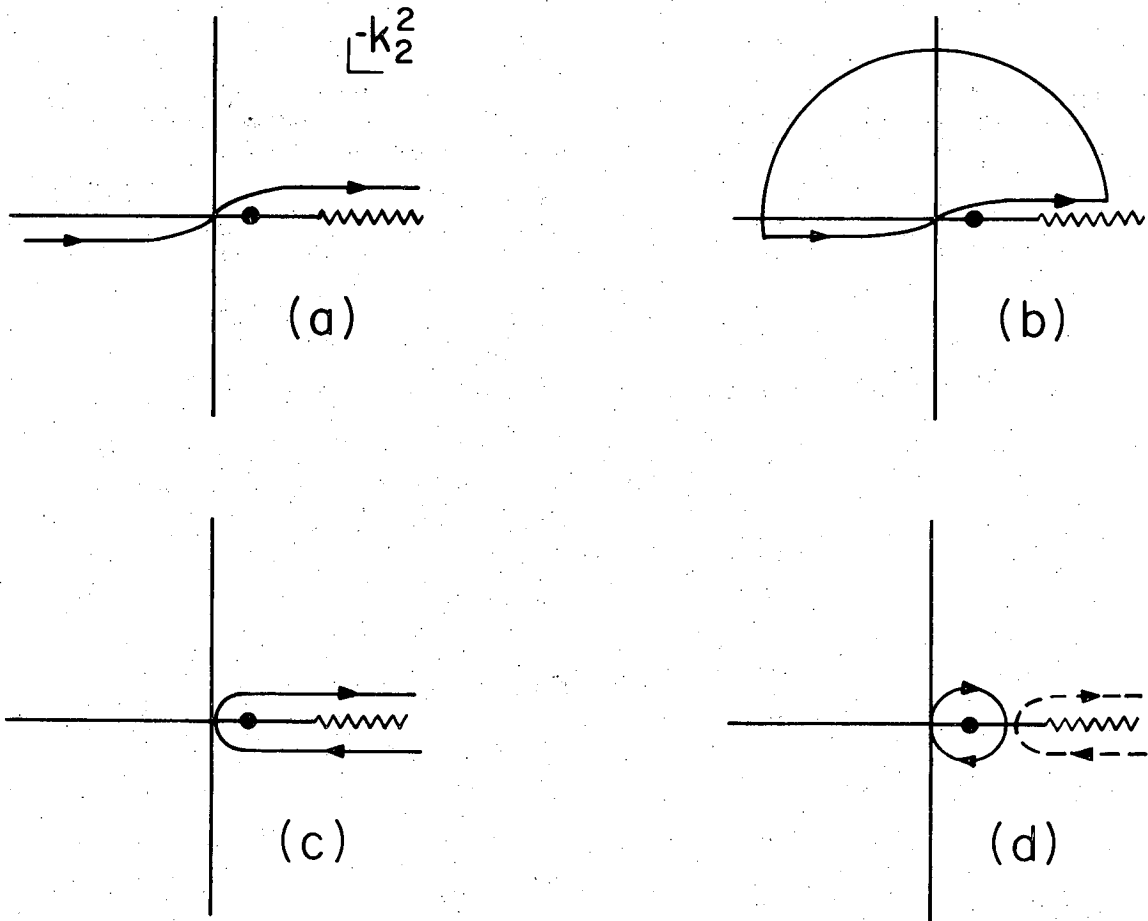
XBL707-3473

Fig. III-3.



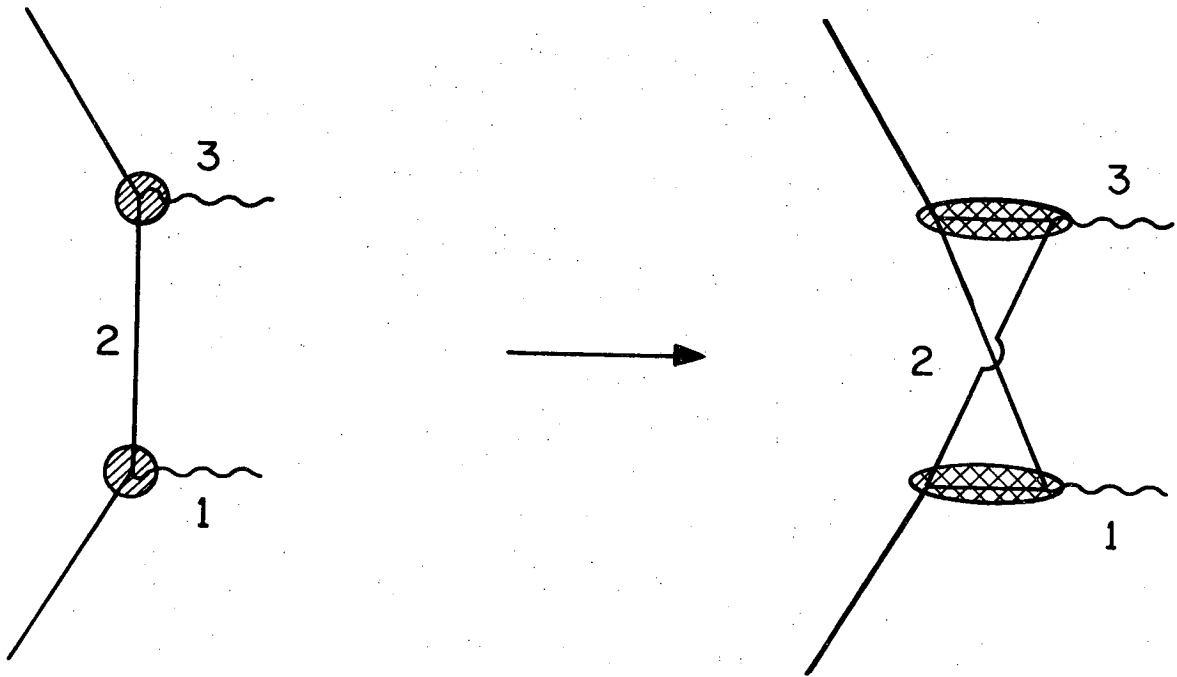
XBL706-3221

Fig. III-4.



XBL707-3469

Fig. III-5.



XBL707-3477

Fig. III-6.

#### IV. THE DOUBLE CROSS DIAGRAM

In this chapter I shall investigate the asymptotic behavior of the double cross diagram suggested by Mandelstam (1963) as a prototype Regge cut diagram. First I will sketch the calculation by Gribov, based on Sudakov's technique. Next I examine a modification of the Gribov work, due to Polkinghorne, which removes some of the arbitrariness in the technical assumptions. After showing how Gribov's result is simplified for use in phenomenology, I state a number of objections to the graphical procedure.

##### 1. Sudakov Variables: A Simple Example

The Sudakov variables (Sudakov, 1956) are particularly suited for the calculation of asymptotic values of Feynman graphs, for they provide a clear separation between negligible and important invariants. As an introductory illustration let us consider the simple two body to two body graph of Fig. IV-1, which represents the lowest-order scattering amplitude in a scalar  $\phi^3$  theory. Define lightlike four-vectors

$$\left. \begin{aligned} p_1' &= p_1 - \rho p_2, \\ p_2' &= p_2 - \rho p_1, \end{aligned} \right\} \quad (\text{IV.1.1})$$

where

$$\rho = (1 - s/M^2) + (s/M^2)(1 - 2M^2/s)^{\frac{1}{2}} \approx M^2/s. \quad (\text{IV.1.2})$$

Then  $(p_i')^2 = 0$  is negligible, whereas  $p_1' \cdot p_2' \sim s$  is not. Let  $k_i$  be the transverse part of  $q_i$  (in the 3-vector sense) in the c.m. frame:

$$k_i \cdot p'_j = 0; \quad k_i^2 \geq 0 \quad (\text{spacelike}). \quad (\text{IV.1.3})$$

The Sudakov variables  $\alpha_i, \beta_i, k_i$  are defined implicitly by

$$q_i = \alpha_i p'_2 + \beta_i p'_1 + k_i. \quad (\text{IV.1.4})$$

What do they mean? Energy-momentum conservation ( $q_1 + q_2 = p_1 + p_2$ ) implies that

$$k_1 + k_2 = 0 \quad (\text{IV.1.5})$$

$$\alpha_1 + \alpha_2 - \rho(\beta_1 + \beta_2) = \beta_1 + \beta_2 - \rho(\alpha_1 + \alpha_2) = 1 \quad (\text{IV.1.6a})$$

or

$$\alpha_1 + \alpha_2 = (1 - \rho)^{-1} = \beta_1 + \beta_2. \quad (\text{IV.1.6b})$$

As a result we can write  $s_{12} \equiv -(q_1 + q_2)^2$  as

$$s_{12} = -2(\alpha_1 + \alpha_2)(\beta_1 + \beta_2)p'_1 \cdot p'_2 = s, \quad (\text{IV.1.7})$$

and the momentum transfer-squared as

$$t_{12} \equiv -(p_1 - q_1)^2 = -k_1^2 - \frac{2p'_1 \cdot p'_2}{(1 + \rho)^2} \left[ -\alpha_1 \beta_2 + \rho(\alpha_1 \beta_1 + \alpha_2 \beta_2) - \rho^2 \alpha_2 \beta_1 \right] \quad (\text{IV.1.8})$$

$$= -k_1^2 + \frac{s(1 - \rho)^2}{(1 + \rho)^2} \left[ -\alpha_1 \beta_2 + \rho(\alpha_1 \beta_1 + \alpha_2 \beta_2) - \rho^2 \alpha_2 \beta_1 \right].$$

For forward scattering, the Sudakov variables become

$$\left. \begin{aligned} \alpha_1 &= \beta_2 = \rho/(1 - \rho^2), \\ \alpha_2 &= \beta_1 = 1/(1 - \rho^2). \end{aligned} \right\} \quad (\text{IV.1.9})$$

Having studied the Sudakov variables in a very simple example, let us move on to a description of Gribov's evaluation of Mandelstam's graph.

## 2. The Two Reggeon Branch Point

In this section I sketch the evaluation, using the Sudakov technique, of a specific diagram which has a Regge cut, the double cross diagram which is labeled for kinematics in Fig. IV-2. This calculation has been done already by Gribov (1967) and by Winbow (1969), and I refer to their work for details. Momentum conservation yields

$$\left. \begin{aligned} p_1 + p_2 &= p_3 + p_4 \\ k_1 + k_2 &= k_3 + k_4 \\ k &= k_1 - k_3 = -k_2 + k_4 \\ q &= p_1 - p_3 = -p_2 + p_4, \end{aligned} \right\} \quad (\text{IV.2.1})$$

and as usual  $s \equiv -(p_1 + p_2)^2$  and  $t \equiv -(p_1 - p_3)^2$ . The graph is to be computed as a function of the asymptotic forms of the bubble amplitudes  $f(k_1, k, k_2)$  and  $f'(p_1 - k_1, q - k, p_2 - k_2)$  in the limit as  $s \rightarrow \infty$  for fixed  $t$ . In this limit it is supposed that each bubble amplitude is a Regge pole exchange amplitude. It is further assumed that the bubble amplitudes vanish if the momentum transfer (through the

bubble) or any of the external masses tends to infinity (Mandelstam, 1963; Rothe, 1967). This assumption, once accepted, motivates some otherwise ad hoc assumptions about the significant region of integration.

For simplicity, assume that all the particles (the solid lines in Fig. IV-2) are scalar and have the same mass  $M$ . The Sudakov parametrization [compare Eq. (IV.1.1)] is

$$\left. \begin{aligned} k &= \alpha p'_2 + \beta p'_1 + k_{\perp} \\ k_1 &= \alpha_1 p'_2 + \beta_1 p'_1 + k_{1\perp} \\ k_2 &= \alpha_2 p'_2 + \beta_2 p'_1 + k_{2\perp} \end{aligned} \right\} \quad (\text{IV.2.2})$$

The volume element is  $d^4k = \frac{1}{2}|s|d\alpha d\beta d^2k_{\perp}$ . Consider the left-hand part of the diagram (Fig. IV-3): it involves the denominators

$$d_1 \equiv -k_1^2 - M^2 + i\epsilon = \alpha_1 \beta_1 s (1 - \rho)^2 - k_{1\perp}^2 - M^2 + i\epsilon, \quad (\text{IV.2.3a})$$

$$\begin{aligned} d_2 \equiv & -(p_1 - k_1)^2 - M^2 + i\epsilon = \alpha_1 s (1 - \rho)(1 + \rho)^{-1} [\beta_1 (1 - \rho)^2 - 1] \\ & + \rho s (1 + \rho)^{-2} [1 - \beta_1 (1 - \rho^2)] - k_{1\perp}^2 - M^2 + i\epsilon, \end{aligned} \quad (\text{IV.2.3b})$$

$$\begin{aligned} d_3 \equiv & -(k_1 - k)^2 - M^2 + i\epsilon = (\alpha_1 - \alpha)(\beta_1 - \beta)(1 - \rho)^2 s \\ & - (k_{1\perp} - k_{\perp})^2 - M^2 + i\epsilon, \end{aligned} \quad (\text{IV.2.3c})$$

$$\begin{aligned} d_4 \equiv & -(p_1 - k_1 + k - q)^2 - M^2 + i\epsilon = [(1 - \rho^2)^{-1} - \beta_1 + \beta + q^2/s] \\ & \times [-\rho(1 - \rho^2)^{-1} - \alpha_1 + \alpha - q^2/s](1 - \rho)^2 s \\ & - (k_{1\perp} - k_{\perp} + q_{\perp})^2 - M^2 + i\epsilon. \end{aligned} \quad (\text{IV.2.3d})$$

Now let us assume that the amplitudes  $f(k_1, k, k_2)$  and  $f'(p_1 - k_1, q - k, p_2 - k_2)$  are large when their energy variables

$$\left. \begin{aligned} s_1 &= -(k_1 + k_2)^2 \\ s_2 &= -(p_1 + p_2 - k_1 - k_2)^2 \end{aligned} \right\} \quad (\text{IV.2.4})$$

are large, i.e. of order  $s$ , at the same time their momentum transfers  $-k^2$ ,  $-(q - k)^2$  and masses  $[-k_1^2, -k_2^2, -(k_1 - k)^2, -(k_2 + k)^2 \dots]$  are of order unity ( $s^0$ ). If any of these last variables becomes large, the amplitude becomes small--by assumption--and the corresponding region is unimportant in the integral. This is the "finite mass hypothesis" made explicit. Winbow (1969) gave an elegant summary of the calculation, which I shall follow here. The asymptotic form of the denominators  $[d_1 d_2 d_3 d_4]^{-1}$  is proportional to

$$\delta(\alpha_1) \delta(\alpha - \alpha_1) / s^2. \quad (\text{IV.2.5})$$

The factor  $\delta(\alpha_1)$  arises from a pinch between  $d_1$  and  $d_2$ , whereas the factor  $\delta(\alpha - \alpha_1)$  is caused by a pinch between  $d_3$  and  $d_4$ . Contributions of parts of the integration region of  $\alpha_1$  and  $\beta_1$  away from the pinches are of lower order in  $s$ . Thus the proof of (IV.2.5) hinges upon the finite mass assumption, specifically on the finiteness of  $k_{1\perp}^2$  and  $(k_{1\perp} - k_{\perp})^2$ .

Similarly one obtains from the right hand cross an asymptotic contribution proportional to

$$\delta(\beta_2) \delta(\beta_2 - \beta) / s^2 \quad (\text{IV.2.6})$$

which arises from pinches which are compatible with those in the left hand cross. Consequently, for very large  $s$  we find

$$\alpha = 0 = \beta, \quad (IV.2.7)$$

a result that also may be seen in a more pedestrian analysis of the implications of the finite mass hypothesis.

Assume that the bubble amplitudes factor (as Regge pole amplitudes, to which we shall immediately specialize, do) in the form

$$f(k_1, k, k_2) = g_1(k_1^2, (k - k_1)^2, k^2) g_2(k_2^2, (k_2 + k)^2, k^2) \times G(k^2, 2k_1 \cdot k_2) \quad (IV.2.8)$$

where the functions  $g_1$  and  $g_2$  of external masses and momentum transfers are Regge residues. A similar form is assumed for  $f'$ . We write the function  $G$  as a Mellin transform,

$$\begin{aligned} G(k^2, 2k_1 \cdot k_2) &= - \int \frac{d\ell_1}{4i} \xi_{\ell_1} G_{\ell_1}(k^2) (2k_1 \cdot k_2)^{\ell_1} \\ &= - \int \frac{d\ell_1}{4i} \xi_{\ell_1} G_{\ell_1}(k^2) (\alpha_2 \beta_1 s)^{\ell_1}, \end{aligned} \quad (IV.2.9)$$

where  $\xi_{\ell_1} = [\tau + \exp(-i\pi\ell_1)]/\sin \pi\ell_1$  is the signature factor, and  $\tau$  is the signature. For Regge pole exchange the Mellin transform is

$$G_{\ell_1}(k^2) = [l_1 - \phi(k^2)]^{-1} \quad (IV.2.10)$$

with  $\phi(k^2)$  the Regge trajectory.

Because of the condition (IV.2.7) the asymptotic form of the Feynman integral factorizes and one obtains the result (Gribov, 1967; Winbow, 1969)

$$A(s, t) = \frac{i\pi}{2|s|} \int \frac{dl_1}{2\pi i} \int \frac{dl_2}{2\pi i} \xi_{l_1} \xi_{l_2} \int \frac{d^2 k_{\perp}}{(2\pi)^2} \times \left\{ N_{l_1 l_2} \right\}^2 s^{l_1 + l_2} [l_1 - \phi_1(k_{\perp}^2)]^{-1} [l_2 - \phi_2((q_{\perp} - k_{\perp})^2)]^{-1}, \quad (\text{IV.2.11})$$

where

$$N_{l_1 l_2} = \frac{\lambda^2 s^2}{8\pi^{\frac{1}{2}}} \int \frac{d^2 k_{\perp}}{(2\pi)^4} \int d\alpha_1 \int d\beta_1 \int d\alpha \frac{g_1 g'_1 \beta_1^{l_1} (1 - \beta_1)^{l_2}}{d_1 d_2 d_3 d_4}, \quad (\text{IV.2.12})$$

and  $\lambda$  is the  $\phi^3$  coupling constant. Evidently  $N_{l_1 l_2}$  is independent of  $s$ . Furthermore (Gribov, 1967; Winbow, 1969)  $N_{l_1 l_2}$  is real for  $-q^2 \lesssim 0$ , so the signature factors determine the imaginary part of  $A$  by the factor

$$\text{Re}[\xi_{l_1} \xi_{l_2}] = \gamma_{l_1 l_2}. \quad (\text{IV.2.13})$$

Finally, using the Mellin projection

$$a_j(q^2) = \int_{s_0}^{\infty} ds s^{-j-1} \text{Im} A(s, q^2),$$

important cases of which are listed in (II.8.3,4), one exposes the branch point in the  $j$  plane at

$$j_{\text{cut}} = \text{Max}_{[k_{\perp}^2]} \{ \phi_1(k_{\perp}^2) + \phi_2((k_{\perp} - q)^2) - 1 \}, \quad (\text{IV.2.14})$$

the same location as we found for the AFS cut in Eq. (III.1.5).

### 3. Polkinghorne's Modification

The use of the finite mass hypothesis to pick out the significant region of integration is somewhat distasteful, because it makes the calculation very qualitative. Thus the corrections to the asymptotic form are difficult to estimate. Polkinghorne (1970) has invented an appealing alternative which is based on the use of Veneziano (1968) amplitudes to represent the Reggeons. While the beta functions do not have the rapid decrease with external mass required in the Gribov theory, the Feynman integrals may be evaluated by the method of stationary phase. The result is completely analogous to (IV.2.11).

### 4. Application to Physical Processes

It is convenient to rewrite (IV.2.12) as

$$N_{\ell_1 \ell_2} = \int_{-\infty}^{\infty} \frac{ds_1}{2\pi i} A_{\ell_1 \ell_2}(s_1, k_1, k_2) \quad (\text{IV.4.1})$$

where

$$A_{\ell_1 \ell_2}(s_1, k_1, k_2) = \frac{i\lambda^2 s\pi^{\frac{1}{2}}}{4(2\pi)^4} \int d\alpha_1 \int d\beta_1 \int \frac{d^2 k_{\perp 1} g_1 g'_1 \beta_1^{\ell_1} (1 - \beta_1)^{\ell_2}}{d_1 d_2 d_3 d_4} \quad (\text{IV.4.2})$$

is the particle-Reggeon scattering amplitude and  $s_1 = -(p_1 + k_1)^2 = \alpha s$ .

We distort the contour of integration [shown in Fig. IV-4(a) for Eq.

(IV.4.1)] to close on the right-hand cut of  $A_{\ell_1 \ell_2}(s_1, k_1, k_2)$  in the

$s_1$  plane. The final configuration, which appears in Fig. IV-4(b), leads to

$$N_{\ell_1 \ell_2}(k_1, k_2) = \frac{1}{\pi} \int_{s_1(0)}^{\infty} ds_1 \operatorname{Im} \{ A_{\ell_1 \ell_2}(s_1, k_1, k_2) \}, \quad (\text{IV.4.3})$$

where  $s_1(0)$  is the right-hand branch point. Gribov and Migdal (1968) wrote this form for  $N$  and gave a plausibility argument that the absorptive part of  $A_{\ell_1 \ell_2}(s_1, k_1, k_2)$  should satisfy a unitarity condition analogous to the one for normal scattering amplitudes. The first few terms of such a "unitarity" sum are depicted in Fig. IV-5.

Kaidalov and Karnakov (1969a,b) retained only the first term in the sum and assumed that the single particle intermediate states could be replaced by a sum of narrow resonances. In this approximation [cf. (IV.2.11)] the amplitude for  $a \rightarrow b$  is given by

$$A(s, t) = \frac{i}{8\pi^2 |s|} \sum_n \int d^2 k_{\perp} A_1^{[n \leftarrow a]}(s, k_{\perp}) A_2^{[b \leftarrow n]}(s, k_{\perp} - q), \quad (\text{IV.4.4})$$

where  $A^{[n \leftarrow a]} = \xi_{\alpha} g_1 g_2 (s/s_0)^{\alpha}$  is the contribution of the pole  $\alpha$  to the amplitude for  $a \rightarrow n$ , and  $n$  is the two-particle intermediate state corresponding to the poles in  $N$ . This procedure is similar in spirit to the one advocated by Henyey and Risk, as reported by Risk (1970). Further restriction of the sum  $\sum_n$  to include only  $n = (a, b)$  reduces (IV.4.4) to a statement of the absorption model (for which see, e.g. Sopkovich, 1962; Jackson, 1965a; Arnold, 1967; Cohen-Tannoudji, Morel, and Navelet, 1967).

## 5. Objections to the Graphical Approach

While much has been learned--and is to be learned--from the graphical approach it is easy to raise significant objections to the results deduced from Feynman diagrams. Even accepting the utility of graphs, one is forced to admit that it would be overly optimistic to expect that a few graphs contain a credible theory of high energy scattering. To be fair I must remark that Gribov's program is to obtain Feynman rules for Reggeon diagrams (a Reggeon calculus) which would permit the evaluation of arbitrarily complicated graphs. A set of Feynman rules was indeed given by Gribov (1967) and checked by Winbow (1969) in some more complicated cases. Even in this circumstance the interpretation of results remains ambiguous. To pose a few unanswered questions, what is meant by the input Reggeon? What is the effect of t-channel iterations (do they just renormalize the Regge pole)? It may be that in the present embryonic stage of the theory of Regge cuts we should take a more operational point of view and assign these questions only secondary importance.

But metaphysical objections aside, I am troubled by more practical uncertainties. In the Gribov-Migdal-Kaidalov-Karnakov approach or in the equivalent Henyey-Risk model it is necessary to impute internal structure to the s-channel intermediate states. This is certainly required in the diagram picture because third double spectral functions must be built in to both ends of every graph. It seems to me defensible to fabricate specific diagrams which have cuts and then to abstract from them a plausible form for the two Reggeon branch cut. Thus I should be

willing to tolerate ideas gleaned from the study of individual graphs if the imputed structures seemed physically realistic.

With this in mind I wish to voice a new objection to the derivations from Feynman graphs, which is rooted in phenomenology. The point is not subtle and surely has occurred to others, although I have never seen it stated explicitly. Recall that the diagram which was in the end regarded as a useful approximation to the general two Reggeon exchange graph is the one shown in Fig. IV-6, where the s-channel intermediate states consist of two physical particles, each on its mass shell. Recall, too, that cuts are "second-order in the third double spectral function" (Matsuda, 1969), i.e. both halves of the box must contain nonvanishing  $\rho_{su}(s,u)$  if the diagram is to produce a Regge cut in the t channel. As  $\rho_{su}$  is the second double spectral function in the s-channel sense, it is responsible for the signature of the s-channel intermediate states. If the s-channel states are assumed to lie on exchange degenerate Regge trajectories,<sup>\*</sup> signature is unimportant and the effects of  $\rho_{su}$  are negligible. Thus if exchange degeneracy is exact, no t-channel Regge cut exists in the graph of Fig. IV-6. From a purely theoretical point of view exchange degeneracy is a most attractive hypothesis, and it appears to be approximately satisfied in the hadron spectrum. Furthermore, only one of the intermediate particles need be unsigned (i.e. have  $\rho_{su} = 0$ ) in order for the cut to be absent. This argument, which is not based on details of the graphs, but only

---

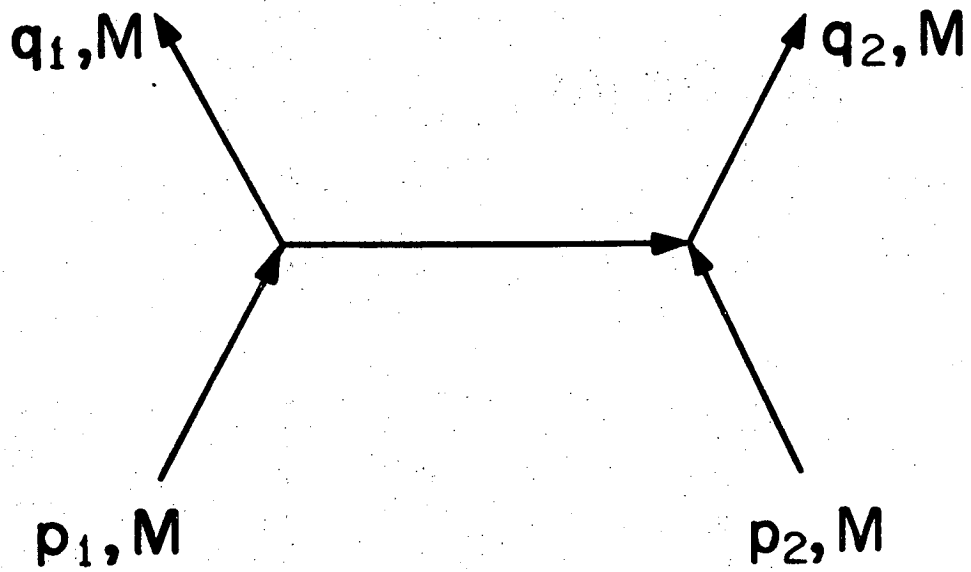
\* The reader who is unfamiliar with the idea of exchange degeneracy will find an elementary discussion in Section VI.1.

upon the known (or indeed, hoped for) properties of the particles which are identified as intermediate states, strongly challenges the derivations of the absorption model from Feynman graphs. (See Gribov and Migdal, 1968; Kaidalov and Karnakov, 1969a; Risk, 1970.) Moreover, this flaw seems more immediate and damaging than the deeper questions to which I alluded above.

I close this discussion on a hopeful note. Many of the same issues which appeared in this section have been debated for several years in the context of the Glauber theory for hadron-deuteron scattering. (See the review by Joachain and Quigg, 1970, for details and original references.) In that field, as in this closely allied one, the effect of graphical derivations has been rather to disprove the model, than to prove it. Thus the Glauber formula contains a Regge cut whereas the Feynman graph with which the Glauber formula has been identified does not. An instructive potential scattering calculation (Harrington, 1969) demonstrates that the Glauber formula corresponds to a sum of Feynman graphs, some of which contain higher than double scattering terms (in the Feynman graph sense) and that a conspiracy between the various terms yields precisely the Glauber formula, in the eikonal limit. The relevance of potential scattering to relativistic problems is always questionable, but Harrington's example makes it clear that proofs (or disproofs!) of the Glauber (or of the absorption) model based on a small number of graphs are probably specious. It may be--this is the attitude I will take for the remainder of this thesis--that absorptive models are appropriate for hadron physics, quite apart from the detailed derivations considered above.

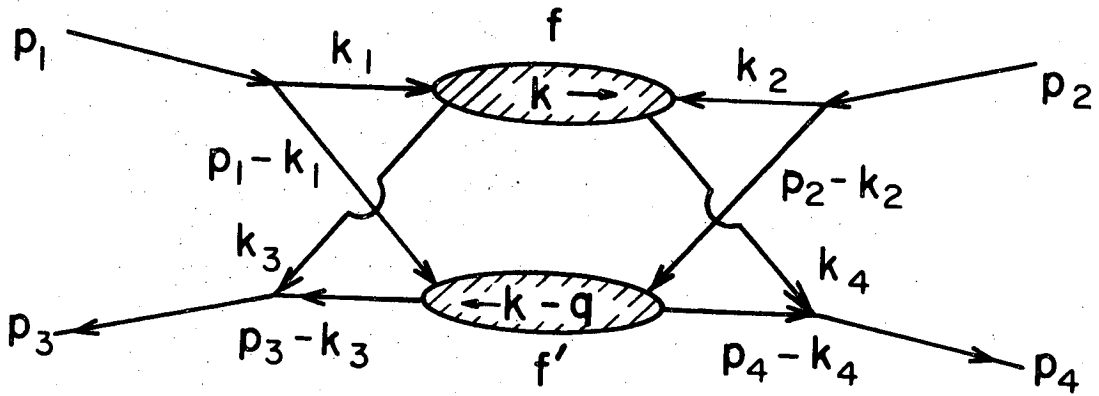
FIGURE CAPTIONS

- Fig. IV-1. Kinematical diagram to elucidate the meaning of Sudakov variables.
- Fig. IV-2. Kinematics of the double cross diagram.
- Fig. IV-3. The left hand side of the double cross graph.
- Fig. IV-4. (a) The contour of integration in Eq. (IV.4.1). (b) The contour wrapped around the right-hand singularities, for Eq. (IV.4.3).
- Fig. IV-5. "Unitarity" sum for  $\text{Im } A_{\ell_1 \ell_2}(s_1, k_1, k_2)$ . The lines bearing crosses represent particles on the mass shell.
- Fig. IV-6. The diagram evaluated as an approximation to the general Reggeon box diagram. The lines bearing crosses represent particles on the mass shell.



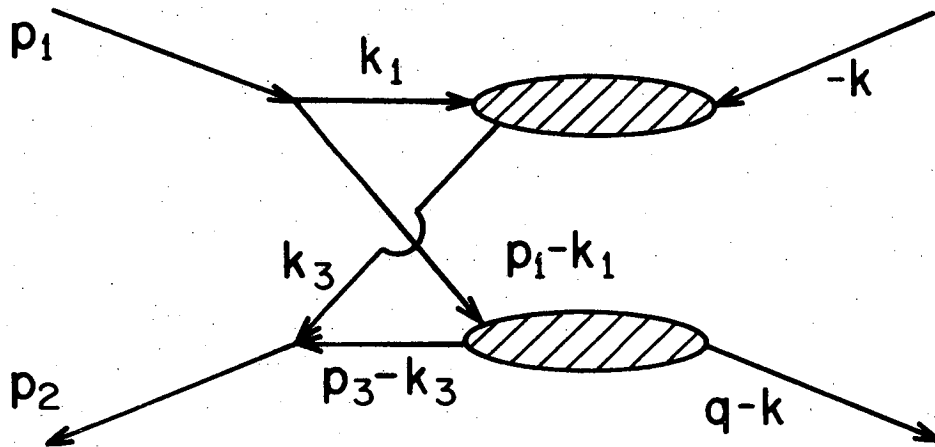
XBL707-3481

Fig. IV-1.



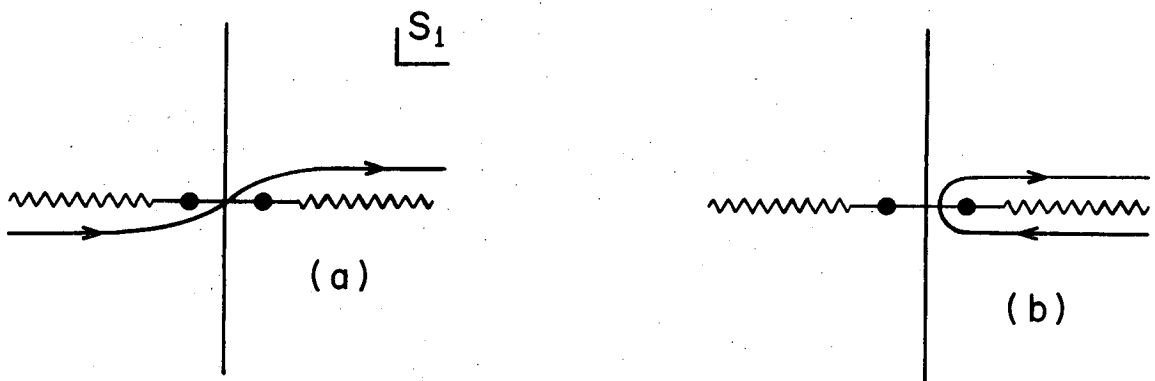
XBL707-3494

Fig. IV-2.



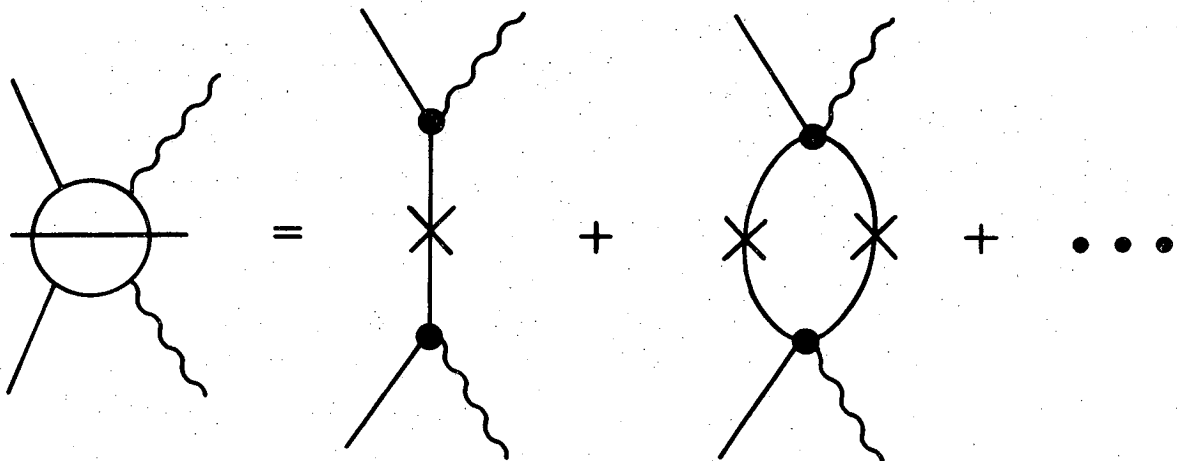
XBL707-3493

Fig. IV-3.



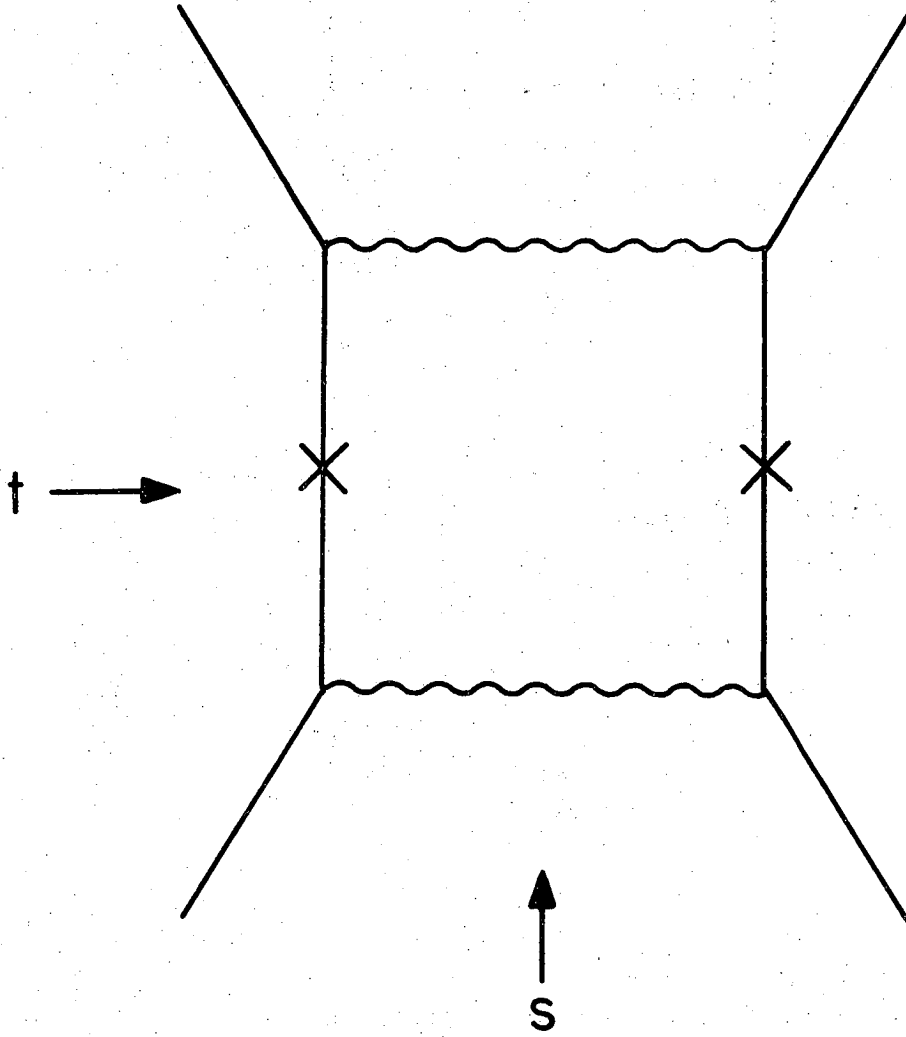
XBL 707-3495

Fig. IV-4.



XBL707-3498

Fig. IV-5.



XBL707-3474

Fig. IV-6.

## V. A PHENOMENOLOGICAL MODEL OF REGGE CUTS

The desirability of having a plausible model with which to confront the high-energy data argues against the pessimism of the previous chapter and demands a pragmatic approach. Thus I am led to construct an amplitude for two Reggeon exchange by fiat rather than orderly derivation. The result is not startling; it is in fact the answer one expects from the derivations described before, if indeed the derivations could rigorously be concluded. The model amplitude contains elements dictated by physical ideas and motivated principally by the relative success of the peripheral model with absorption. A novel feature is the incorporation in a phenomenologically useful way of s-u crossing.

I begin by reminding the reader of the Sopkovich (1962) prescription for absorptive corrections to single particle, or as now seems more sensible, single Reggeon exchange. This formula serves as a prototype for the case in which two Reggeons, of which one and only one is a Pomeranchuk trajectory, are exchanged. Let  $R_J(s)$  be an s-channel helicity partial-wave amplitude for the exchange of a Regge pole in the reaction  $ab \rightarrow cd$ . Then according to the guess of Sopkovich the influence of competing channels is included in the full s-channel partial-wave helicity amplitude  $H_J(s)$  by means of the prescription

$$H_J^{cd:ab}(s) = [S_J^{ab:ab}]^{\frac{1}{2}} R_J^{cd:ab} [S_J^{cd:cd}]^{\frac{1}{2}}, \quad (V.1.1)$$

where  $S_J$  is the partial-wave S-matrix element for elastic scattering of the initial or final particles. The elastic scattering amplitudes

need not be diagonal in the helicities but I suppress any such dependence for the moment to make the equations more succinct. The equation (V.1.1) is based on the distorted-wave Born approximation, which has been used by many authors after Sopkovich (1962) with qualitatively similar results. (A few of the important references are Gottfried and Jackson, 1964; Durand and Chiu, 1964; Ross and Shaw, 1964; Jackson, 1965; Jackson, et al., 1965.) I take the liberty of replacing the geometric mean of the elastic S-matrices by the arithmetic mean. Then with

$$S_J = 1 + 2i E_J \quad (V.1.2)$$

I obtain

$$H_J^{cd:ab} = R_J^{cd:ab} \{1 + i[E_J^{ab:ab} + E_J^{cd:cd}]\}, \quad (V.1.3)$$

which is represented graphically in Fig. V-1. This recipe has enjoyed wide acceptance up to the present day, usually with the additional assumption  $E^{ab:ab} = E^{cd:cd}$ .

An obvious shortcoming of (V.1.3) is that it fails to satisfy s-u crossing or what is known in Regge theory as line reversal. Thus in general one obtains one result if he absorbs in the s-channel and crosses to the u-channel, and another result if he absorbs in the u-channel directly. If only the Pomeranchuk singularity contributed to  $E_J$ , and if all elastic scattering amplitudes were equal, there would be no difficulty in practice. In principle, however, a contradiction exists which should be eliminated before we proceed to the general two Reggeon case. It is easy to see that s-u crossing is restored by adding the

graphs of Fig. V-2 to those of Fig. V-1. Crossed graphs lack the intuitive appeal of the box diagrams that enter (V.1.3), for they involve the elastic scattering of an initial-state particle with a final-state particle. Such an occurrence is contrary to the strict time ordering implicit in the Sopkovich picture, but apparently intuition must be sacrificed for crossing. On the other hand, time-ordering is an essentially nonrelativistic concept which should not be expected to be a reliable guide for high-energy scattering. (The relevance of this point to Glauber theory is explained by Joachain and Quigg, 1970.)

The Reggeon graphs I have drawn in Figs. V-1,2 are useful as mnemonics but the reader will be aware, after the discussion of chapter IV, that they are not to be regarded as Feynman graphs. In order to specify with care what is meant by the crossed graphs it is useful to define a line reversal operator  $\mathcal{L}$  which crosses a graph (and the corresponding helicity partial-wave amplitude) from the s-channel to the u-channel. The action of  $\mathcal{L}$  on the single Reggeon exchange graph is illustrated in Fig. V-3(a). It amounts to

$$\mathcal{L} \cdot R_{J[ab]}^{cd:ab} = R_{J[\bar{c}\bar{b}]}^{\bar{a}\bar{d}:\bar{c}\bar{b}} \quad (\text{V.1.4})$$

By the notation  $J[xy]$  I indicate that the partial-wave projection is to be performed in the direct channel implied by the helicity amplitude in question. It is of course these full helicity amplitudes which have simple properties under s-u crossing.\*

---

\* See Appendix C.

The similar action of  $\mathcal{L}$  on a two Reggeon graph is shown in Fig. V-3(b). As  $\mathcal{L}^2 = 1$ , the contribution of the crossed graph in Fig. V-3(b) can be written as

$$\begin{aligned} -iH_J^{cd:ab}(\text{crossed graph}) &= \mathcal{L} \cdot \{R_J^{\bar{a}d:\bar{c}b} E_J^{\bar{c}b:\bar{c}b}\} \\ &= \mathcal{L} \cdot \{ \mathcal{L} \cdot [R_J^{cd:ab}] \mathcal{L} \cdot [E_J^{cb:cb}] \}. \end{aligned} \quad (\text{V.1.5})$$

To summarize, the action of  $\mathcal{L}$  is to (i) sum the helicity partial-wave series, (ii) line-reverse the full helicity amplitude, and (iii) reproject the desired partial-wave in the new direct channel. In this context it is important to emphasize that the cut generated by Reggeons with signatures  $\tau_1, \tau_2$  has signature  $\tau_1 \tau_2$ . This was deduced in Chapter IV from the double cross diagram, and we assume it to be true in general. An ambiguity to be faced is whether to add the crossed graphs to the usual box graphs, or to average the two sets. I will argue below, after discussing normalization with more care, that the correct procedure is to average them. With this rule, the (explicitly s-u crossing symmetric) absorbed amplitude will be

$$\begin{aligned} H_J^{cd:ab} &= R_J^{cd:ab} \{1 + \frac{i}{2} [E_J^{ab:ab} + E_J^{cd:cd}]\} \\ &+ \frac{i}{2} \mathcal{L} \{ \mathcal{L} (R_J^{cd:ab}) [ \mathcal{L} (E_J^{cb:cb}) + \mathcal{L} (E_J^{\bar{a}d:\bar{a}d}) ] \}. \end{aligned} \quad (\text{V.1.6})$$

Then under the extreme assumptions that the elastic amplitudes are helicity independent, diagonal in the helicities, and independent of the scattering particles, the absorbed amplitude simplifies to

$$H_J^{cd:ab}(s) = R_J^{cd:ab}(s)[1 + 2i E_J(s)]. \quad (V.1.7)$$

This is precisely the result given by the usual absorptive prescription in the same simple circumstances. It is necessary to emphasize that (V.1.7) refers to a trivial limit of Pomeranchuk-Regge pole cuts, and not to an amplitude for pole-pole cuts, to which we now turn.

At this point I am able to construct, in analogy with the absorptive model, the general model amplitude for two Reggeon exchange. It is built of the graphs of Fig. V-4, and I write it as

$$(1 + \delta_{12}) H_J^{cd:ab} = R_{1J}^{cd:ab} + R_{2J}^{cd:ab} + \frac{i}{2} \sum_{e,f} (R_{1J}^{ef:ab} R_{2J}^{cd:ef} + R_{1J}^{cd:ef} R_{2J}^{ef:ab} + \mathcal{L}[R_{1J}^{\bar{e}f:\bar{c}b} R_{2J}^{\bar{a}d:\bar{e}f} + R_{1J}^{\bar{a}d:\bar{e}f} R_{2J}^{\bar{e}f:\bar{c}b}]). \quad (V.1.8)$$

The factor  $(1 + \delta_{12})$  is inserted to avoid double counting if Reggeons 1 and 2 are the same. The labels  $a, b, \dots, f$  represent helicities as well as particle identities. The amplitude (V.1.8) is implicit in the hybrid model work of Chiu and Finkelstein (1969), which in turn is related to the formulation of Arnold (1967). The normalization in (V.1.8) and in the equations leading to it has been schematic, to make it possible for the reader to compare figures and formulae with a minimum of confusion. Having obtained the partial-wave amplitude (V.1.8) in this schematic and hopefully understandable manner I now state the result for the full  $s$ -channel helicity amplitude with normalization which corresponds precisely to my conventional choices listed in Sections A.1-3. The resulting amplitude is

$$\begin{aligned}
 (1 + \delta_{12}) H_s^{cd:ab} &= H_{s(1)}^{cd:ab} + H_{s(2)}^{cd:ab} + \frac{i}{64\pi} \sum_J^{\infty} (J + \frac{1}{2}) d_{\lambda\mu}^J(\theta_s) \\
 &\cdot \left\{ \sum_{e,f} [h_{J(1)}^{ef:ab} h_{J(2)}^{cd:ef} + h_{J(1)}^{cd:ef} h_{J(2)}^{ef:ab} \right. \\
 &\quad \left. + \mathcal{L} (h_{J(1)}^{\bar{e}f:\bar{c}b} h_{J(2)}^{\bar{a}d:\bar{e}f} + h_{J(1)}^{\bar{a}d:\bar{e}f} h_{J(2)}^{\bar{e}f:\bar{c}b}) \right\}. \quad (V.1.9)
 \end{aligned}$$

Here  $H_{s(i)}$  is the contribution of the Regge pole "i" to the s-channel helicity amplitude, and  $h_{J(i)}$  is its partial-wave projection which is given by

$$h_{J(i)}^{cd:ab}(s) = \int_{-1}^1 d(\cos \theta_s) H_{s(i)}^{cd:ab}(s, \cos \theta_s) d_{\lambda\mu}^J(\theta_s). \quad (A.3.16)$$

Notice that because the sum  $\sum_{e,f}$  runs over all possible two body on-mass-shell intermediate states, this model includes possible "coherent inelastic states" in the Reggeized absorption model case that one of the Reggeons is a Pomeranchuk trajectory. (See Henyey, et al., 1969.) I do not wish to discuss the magnitude of these contributions in any detail because the diffractive production data for reactions such as  $pp \rightarrow N^*p$  and  $\pi p \rightarrow A_1 p$  seem to me inconclusive. I should be very surprised, however if the total contribution of inelastic intermediate states turned out to be more than 30% of the elastic scattering component (in the amplitude). Thus I disagree with the Michigan group (Henyey, et al., 1969), who believe the strength of the absorptive cuts to be approximately twice the strength implied by the elastic scattering amplitudes alone.

It is instructive to see that the crossed Reggeon graphs are already included, at least in principle, in the diagram versions of the theory discussed in Chapter IV.\* How this comes about may be seen in Fig. V-5. The uncrossed Reggeon box graph is identified with a particular double cross graph which imputes a specific internal structure to the vertices. Similarly the crossed graph is identified with a particular double cross graph with crossed Reggeons. When the latter diagram is untwisted (by pulling on the constituent lines of the right-hand vertices) it becomes an ordinary double cross graph, but with the vertex particles at the initial and final vertices on the right-hand side going to different Reggeons. Since in principle all the various possibilities are put into the Reggeon-particle vertices the general set of diagrams would seem to contain the crossed graphs. Indeed if one is willing to be tied to particular vertex structures it is possible to argue, by returning to the integration contours of Fig. IV-4, that it is correct to average the crossed graphs with the uncrossed ones. Thus the integral over the contour in Fig. IV-4(a) is equal to one-half the integral along the contour in Fig. IV-4(b) around the right-hand singularities plus one-half the integral around the left-hand singularities (contour not shown). The proof is completed by identifying the right-hand singularities with vertex structures from the uncrossed graphs, and the left-hand singularities with vertex structures from the crossed graphs. The argument can be made less model dependent: notice that in untwisting the Gribov graph in Fig. V-5 we line-reversed one of

---

\* I owe this observation to Professor Jackson.

the vertex functions. In Gribov and Migdal's nomenclature, a Reggeon-particle scattering amplitude was line-reversed. For the narrow resonance scheme, this has the effect of replacing  $\rho_{su}(s,t)$  by  $\rho_{su}(u,t)$ , so that by dispersing in the Reggeon-particle subenergy one picks up contributions from states on mass shell in the u-channel.

A simpler principle (for fixing the normalization) is that the absorption model recipe should be recovered when enough simplifying assumptions are made. We saw this to be the case in Eq. (V.1.7).

The crossed graph prescription is, therefore, a way of taking into account the complexity of the vertex structures, in phenomenological calculations. It has the attractive property of satisfying s-u crossing manifestly, which is certainly an important feature to preserve in abstracting a phenomenological model from a theoretical one. In the simplifying limit discussed in obtaining (V.1.7), the added complexity of my recipe (compared with the usual box graph model) makes no difference in the final result. Does it ever make a difference? More to the point, does the new formulation reproduce any desirable result which would have to be imposed by hand on the simpler model? The answer is that it does make a difference, that is nicely illustrated in the reaction  $K^-p \rightarrow K^+\Xi^-$ , which we shall study in detail in Chapter VI.

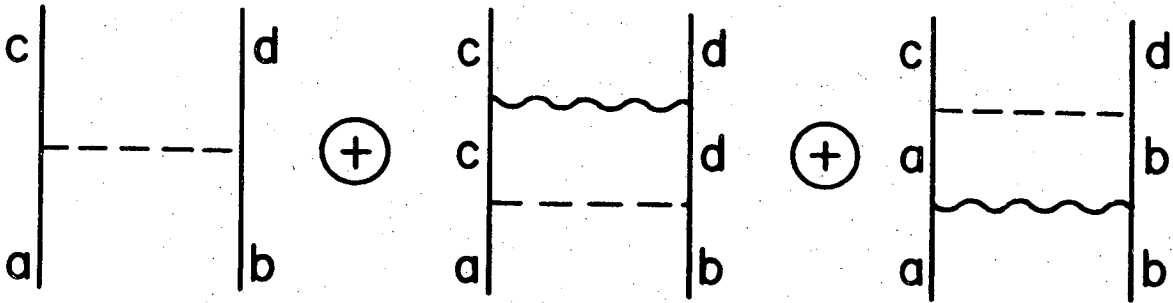
A priori, there are contributions from the  $K^* - K^*$ ,  $K^{**} - K^{**}$ , and  $K^* - K^{**}$  Regge cuts. If for concision we restrict our attention to  $\pi^0 Y^0$  intermediate states, the amplitude for the exchange of two Reggeons can be represented by the graphs in Fig. V-6. Upon untwisting the crossed graphs as described above, we find the resulting amplitude

to be  $(1 + \tau_1 \tau_2)$  times the contribution of the box graphs alone (times the factor  $1/2$  which occurs because we are averaging boxes and crosses). Consequently the contribution of the  $K^* - K^{**}$  cut vanishes and we are left with only the even signature  $K^* - K^*$  and  $K^{**} - K^{**}$  cuts. This is a correct result, which in the conventional box diagram approach would have to be imposed as a symmetry on the vertex functions (compare Appendix C). By building in crossing, we have taken care of such discrete symmetries explicitly.

Thus the crossing-symmetric model is expected to have two practical, phenomenological advantages over the box graph model. First, some cancellations due to discrete symmetries are made explicit. Second, by averaging over narrow resonances in two channels, we may hope to obtain a better approximation to the actual Regge cut amplitude than would be the case in either channel separately.

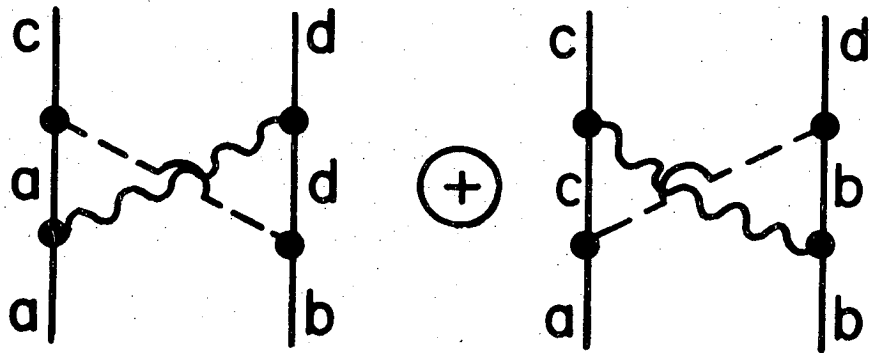
FIGURE CAPTIONS

- Fig. V-1. Reggeon exchange graphs for the conventional absorption model.
- Fig. V-2. The graphs which when added to those of Fig. V-1 restore crossing symmetry.
- Fig. V-3. (a) Action of the line reversal operator  $\mathcal{L}$  on the single Reggeon exchange diagram which represents a helicity partial-wave amplitude. (b) Effect of the line reversal operator on the two Reggeon cross diagram. If the wavy line represents the Pomernanchuk (or specifically, elastic scattering), then  $e = c$  and  $f = b$ .
- Fig. V-4. Graphical representation of the model for two Reggeon exchange.
- Fig. V-5. Identification of some Reggeon graphs considered in this chapter with some Gribov graphs, to elucidate the role of the crossed Reggeon graphs.
- Fig. V-6. The set of graphs relevant for the reaction  $K^-p \rightarrow K^+\Xi^-$ , which proceeds by  $(K^*, K^{**})$  exchange.



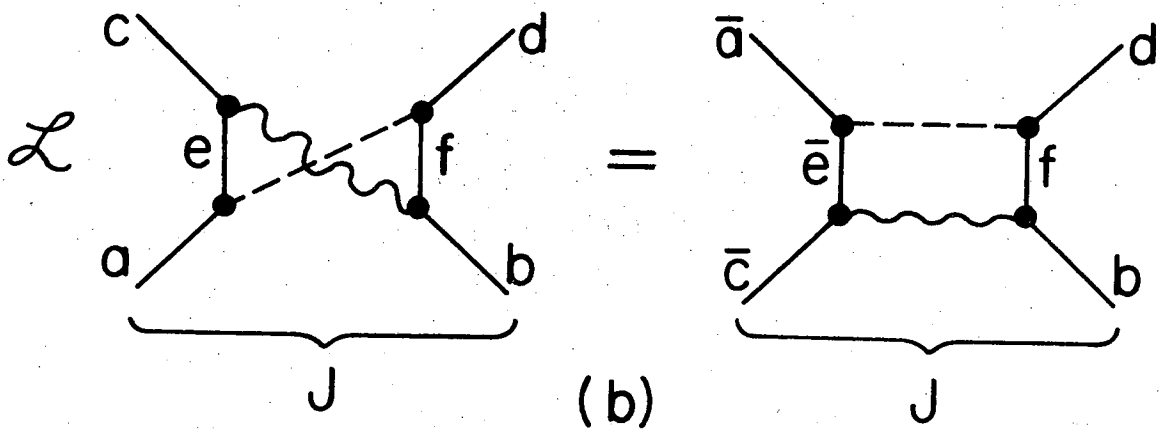
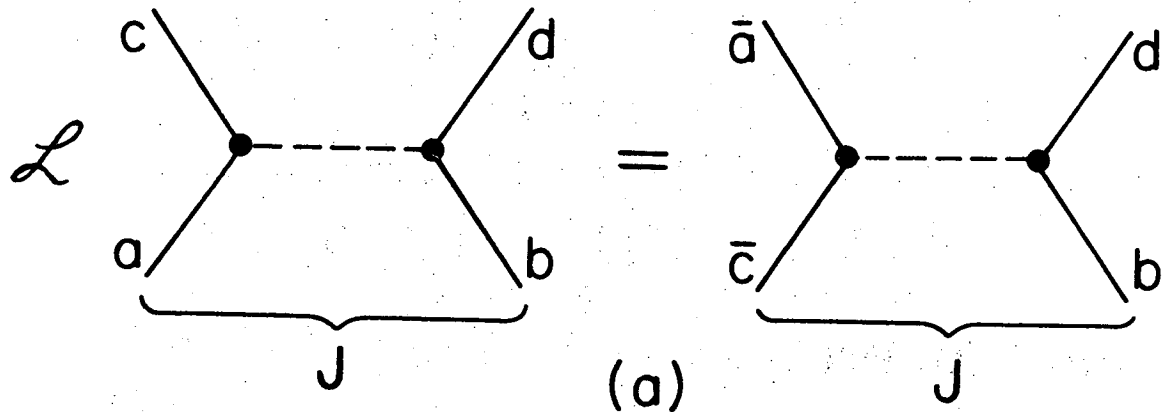
XBL707-3478

Fig. V-1.



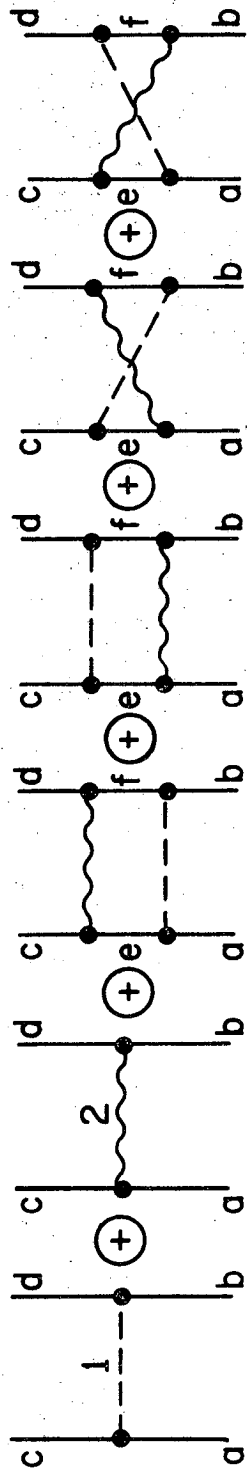
XBL707-3476

Fig. V-2.



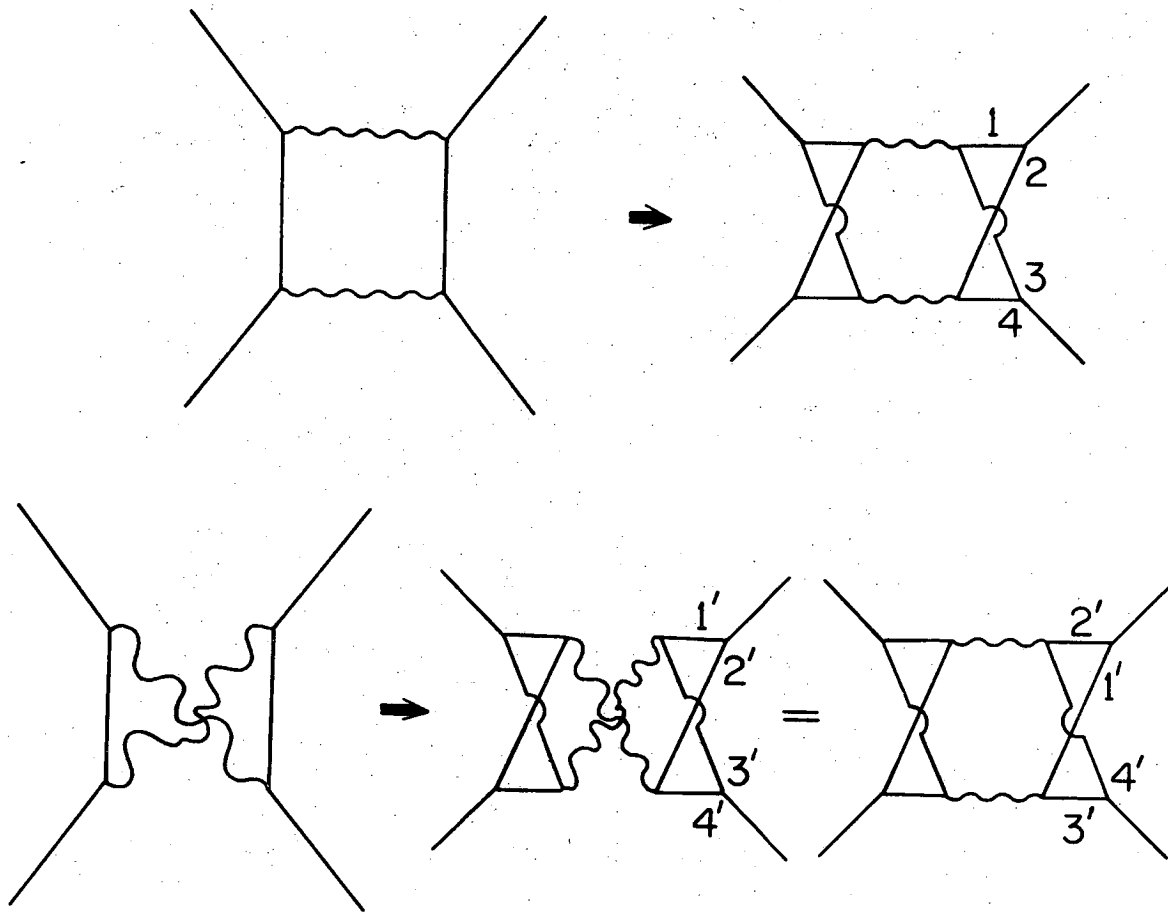
XBL707-3468

Fig. V-3.



XBL707-3497

Fig. V-4



XBL707-3471

Fig. V-5.

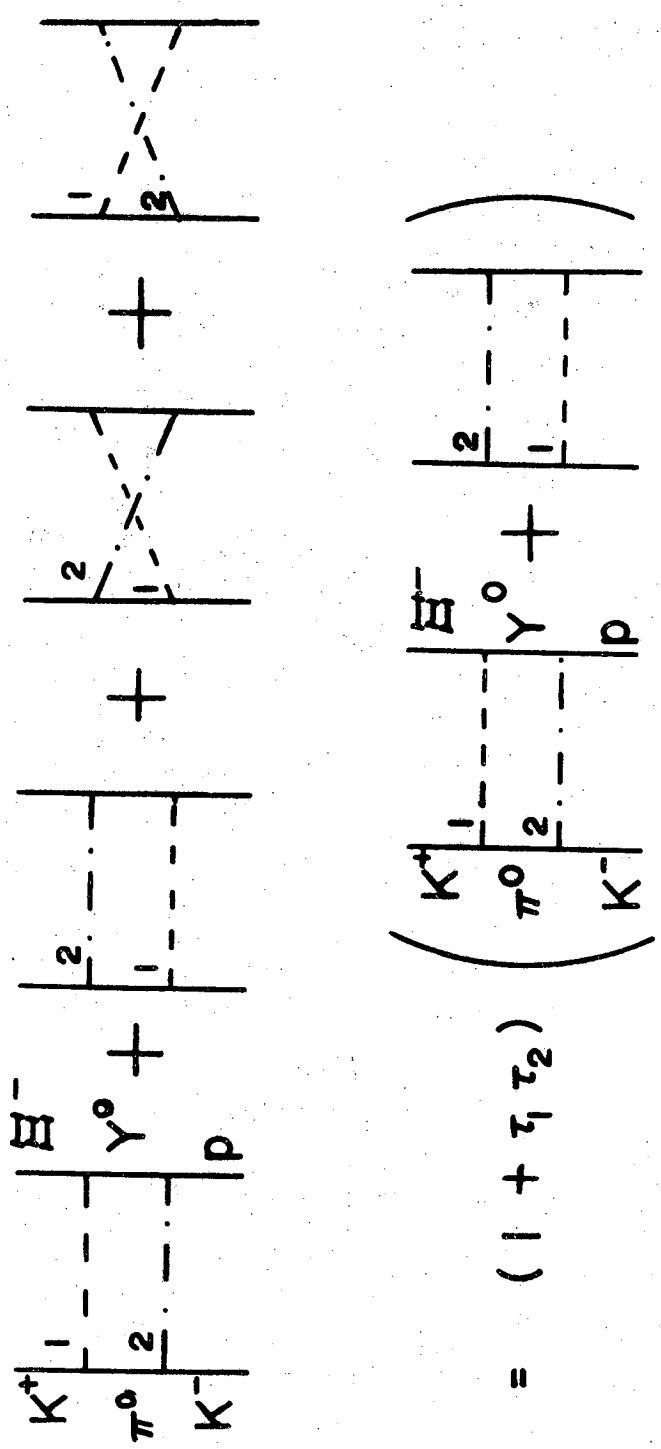


Fig. V-6.

## VI. REGGE CUTS AND EXCHANGE DEGENERACY

In this chapter I consider some applications of the Regge cut model formulated above. These are very much in the nature of model calculations which serve to answer some questions about the effects of absorptive cuts on high-energy amplitudes. Thus I shall fit no data, but try to make semiquantitative observations that will shed some light on possible connections between exchange degeneracy breaking and Regge cuts. The model calculations form part of a larger program which will be reported elsewhere (Fox and Quigg, 1970).

### 1. Regge Cuts and Duality

I mentioned in Chapter IV a possible conflict between exact exchange degeneracy and the popular formulations of Regge cuts, namely the requirement that third double spectral functions be nonzero if cuts are to exist, whereas exchange degeneracy implies the absence of third double spectral functions. Accordingly the simple Reggeon box diagram interpreted as a Feynman graph gives no Regge cut if the world is exchange degenerate. However, I swept such difficulties under the rug by arguing in analogy with potential scattering off deuterons that conclusions based on a small number of Feynman graphs could well be misleading.

Another obvious question to pose is whether Regge cuts in general and specifically those generated by the absorptive prescription I employ are compatible with finite energy sum rules (FESR) or equivalently with "global duality" (Dolen, Horn, and Schmid, 1967, 1968).\*

---

\* For a synopsis of work on FESR's, see Jackson (1970).

data of infinite precision over a wide range of energies it might be possible to distinguish poles from cuts on the basis of their different energy dependences, but this is notoriously difficult. What can be shown is that FESR's cannot distinguish between different classes of models, given the present state of the low-energy data. An explicit demonstration of this was given for charged pion photoproduction by Jackson and Quigg (1969) who constructed a number of models with evasive  $\pi$  and  $A_2$  exchange and "conspiring" absorptive cuts to fit the high-energy data and the sum rules.

On the operational level, cuts may be duality-preserving or duality-breaking with respect to the prediction of exchange degeneracy (if it is legitimate to ignore possible conflicts between exchange degeneracy and the existence of cuts). Indeed it has been proposed (e.g. Michael, 1969b; Lovelace, 1969) that exchange degeneracy might be broken only by the effects of Regge cuts. This is one of the ideas I wish to elucidate here. Already in Chapter IV I gave a rather formal statement of what exchange degeneracy means, to wit  $\rho_{su}(s,t) = 0$ . An explanation of the connection between the absence of exchange forces and exchange degeneracy may be found in Section V-3(b) of Jackson (1970), or in Arnold (1965).

As an example let us consider as the u-channel  $K^+p \rightarrow K^0\Delta^{++}$ , a quark model exotic channel in which no strong resonances have been observed. I label the other channels as shown in Fig. VI-1, so the s-channel contains resonances on the  $\rho, A_2$  trajectories and the

t-channel contains resonances on the  $\Sigma_\alpha, \Sigma_\gamma$  trajectories.\* As there are no u-channel forces, we conclude that the  $\rho$  and  $A_2$  Reggeons are exchange degenerate, that is they are described by a single trajectory function  $\alpha(t)$  and by one residue function for each  $p\bar{\Delta}$  helicity state. The example of  $\rho, A_2$  exchange degeneracy is classical; see Mathews (1969) for a detailed phenomenological study. Tests of exchange degeneracy for the trajectory functions recently have been made by Cline, Matos, and Reeder (1969) and by Lai and Louie (1970). By relabeling the channels we may repeat the argument for the  $\Sigma_\alpha, \Sigma_\gamma$  trajectories and prove them exchange degenerate. This pair has been studied by Schmid (1969). The fragmentary evidence from the resonance spectrum for  $\rho, A_2$  and  $\Sigma_\alpha, \Sigma_\gamma$  degeneracy is collected in Fig. VI-2. The spectrum itself only provides plausibility; more concrete evidence that the exchange degeneracy is at least approximately satisfied is given in the references cited. The conclusion is that scattering in an exotic channel is governed by exchange degenerate trajectories in the crossed channels.

The duality diagrams of Harari (1969) and Rosner (1969) are neat mnemonics for the predictions of  $SU(3)$ , exchange degeneracy, and factorization. Each particle is represented by its quark constituents, which rearrange themselves during the collision. If the initial quarks can be connected to the final quarks so that no quark lines cross, the duality diagram is said to be planar and the corresponding amplitude

---

\* There are four classes of baryon trajectories, distinguished by the quantum numbers  $(\tau, P)$ :  $\alpha = (+, +)$ ;  $\beta = (+, -)$ ;  $\gamma = (-, -)$ ;  $\delta = (-, +)$ .

has a  $t$ -dependent phase. If not, the graph is nonplanar, and the amplitude must be purely real. For illustration, consider the forward charge-exchange reaction



for which the  $s$ - $t$  duality diagram is drawn in Fig. VI-3(a). The graph is nonplanar so the amplitude for  $\rho, A_2$  exchange is predicted to be real. The line-reversed reaction



has a planar diagram which is obtained simply by untwisting the graph for reaction (VI.1.1). Shown in Fig. VI-3(b), it implies an amplitude proportional to  $\exp[-i\pi\alpha(t)]$ . Whereas the derivations of duality graphs can only be taken seriously for forward ( $0^\circ$ ) scattering, I will assume that their predictions hold for all values of  $t < 0$ . For easy reference I list in Table VI-1 the quark composition of some common hadrons.

## 2. Systematics of Exchange Degeneracy Breaking

In fact, exchange degeneracy is not an exact symmetry, or at least does not appear to be in the intermediate energy regime ( $5 \text{ GeV}/c \lesssim p_{\text{lab}} \lesssim 10 \text{ GeV}/c$ ) in which quasi-two body reactions have so far received careful experimental attention. As the references cited in the previous section testify, it is approximately satisfied and therefore a useful phenomenological tool. One could of course stop at this point and accept exchange degeneracy as an approximate truth, but it is appealing to view exchange degeneracy instead as a broken symmetry, i.e.

a symmetry broken in a particular (simple!) way. The motivation for this viewpoint may be more visceral than rational. Yet I can cite a few reasons why such an approach may be sensible. For example there is considerable evidence that  $SU(3)$  predictions, when modified by physical mass kinematics (phase space corrections) are satisfied rather well. Here is evidence for an exact symmetry, broken in a simple way. The elegance of the Veneziano (1968) representation, to which exact exchange degeneracy is built in, suggests a perturbative approach in which the final amplitude satisfies exchange degeneracy in an approximate way. It is tempting (Lovelace, 1969) to suppose that the exchange degeneracy breaking, which presumably is the outcome of unitarization of the Veneziano formula (Kikkawa, Sakita, and Virasoro, 1969), might be adequately described by the absorptive corrections given by Regge cuts. With unbridled optimism one might thereby hope to elucidate the nature of exchange degeneracy breaking and the role of Regge cuts at one swoop. Such optimism is at least partially sustained by the discovery of the systematics described below.

[My understanding of the ideas discussed here has evolved in the collaboration with G. C. Fox cited above, in the course of the past year. However, as I hope to make clear through references, these notions are not ours alone; many of them have indeed been published already by others.]

A key observation is that for a pair of reactions related by line reversal, the one with amplitudes predicted to be real by duality diagrams seems in all cases to have a larger cross section than the one

with amplitudes proportional to  $\exp(-i\pi\alpha)$ . This behavior is predicted by the scheme of  $SU(3)$  for Regge pole residues plus exchange degeneracy--broken by the use of physical trajectories. The same scheme also accounts for the observed failures of exchange degeneracy in pairs of reactions for which, because of G-parity restrictions, one trajectory of the possibly degenerate pair is exchanged in each of the reactions. That exotic (in the sense of duality graphs) channels always have larger inelastic cross sections suggests that there is more absorption in the nonexotic channels.\* The greater absorption in turn suggests that nonexotic channels have larger total cross sections, as is observed. Let us consider these regularities in more detail

For notational convenience I will abbreviate exchange degeneracy (equal trajectories and equal residues) as EXD. Equal trajectories but unequal residues corresponds to "weak" exchange degeneracy, or WEXD. Finally I define residue exchange degeneracy, REXD, to mean equal residues but unequal trajectories.

The amplitude  $A_\tau$  for exchange of a trajectory with signature  $\tau$  is

---

\* This seems contradictory at first sight, for absorption is actually the inelasticity caused by competing reaction channels. It may be that there exist more reaction channels with smaller individual cross sections which communicate with the nonexotic channel.

$$A_+ \propto \frac{1 + e^{-i\pi\alpha_+}}{2 \sin \pi\alpha_+} = \frac{\cot \pi\alpha_+/2 - i}{2} \quad (\text{VI.2.1})$$

$$A_- \propto \frac{1 - e^{-i\pi\alpha_-}}{2 \sin \pi\alpha_-} = \frac{i + \tan \pi\alpha_-/2}{2}$$

Thereby in the EXD limit

$$A_+ + A_- \propto \csc \pi\alpha(t) \quad (\text{VI.2.2})$$

is purely real, whereas

$$A_+ - A_- \propto e^{-i\pi\alpha(t)} \csc \pi\alpha(t) \quad (\text{VI.2.3})$$

has a rotating phase. An amplitude which should on the basis of duality diagrams be purely real will be called DDRe; the amplitude related by line-reversal, which should have a rotating phase will be called DDPh. Consider now the case of REXD, with  $\alpha_+ = \alpha$ ;  $\alpha_- = \alpha + \delta$ . Then

$$\begin{aligned} A_+ + A_- &= \frac{1}{2} [\cot \pi\alpha/2 + \tan \pi(\alpha + \delta)/2] \\ &= \frac{\csc \pi\alpha}{1 - \tan \pi\alpha/2 \tan \pi\delta/2} \end{aligned} \quad (\text{VI.2.4})$$

is still purely real.\* This implies a cross section proportional to

---

\* Obviously this cannot be exactly true over an infinite range of energies, but in the intermediate energy regime it is accurate to the extent that  $(s/s_0)^\delta \approx 1$ .

$$\begin{aligned}
 |A_+ + A_-|^2 &= \frac{\csc^2 \pi\alpha}{(1 - \tan \pi\alpha/2 \tan \pi\delta/2)^2} \\
 &= |A_+ + A_-|_{\text{EXD}}^2 / (1 - \tan \pi\alpha/2 \tan \pi\delta/2)^2,
 \end{aligned}
 \tag{VI.2.5}$$

which is larger than the one predicted by EXD if  $\tan \pi\alpha/2 \tan \pi\delta/2 > 0$ . For  $\delta$  small and for all the trajectories which enter into near-forward scattering, an equivalent condition is  $\alpha\delta > 0$ .

The DDPH combination is only slightly more complicated:

$$\begin{aligned}
 A_+ - A_- &= -i + \cot \pi\alpha - \frac{\frac{1}{2} \tan \pi\delta/2 \sec^2 \pi\alpha/2}{1 - \tan \pi\alpha/2 \tan \pi\delta/2} \\
 &= e^{-i\pi\alpha} \csc \pi\alpha - \frac{\frac{1}{2} \tan \pi\delta/2 \sec^2 \pi\alpha/2}{1 - \tan \pi\alpha/2 \tan \pi\delta/2}.
 \end{aligned}
 \tag{VI.2.6}$$

The implied cross section is decreased from the EXD value if  $\cot \pi\alpha$  and  $\tan \pi\delta/2$  have the same sign, or increased if the signs are different. Again I ignore the effect of  $(s/s_0)^\delta$  upon the imaginary part.

In the peripheral region,  $\alpha > 0$  for the vector and tensor trajectories. Thus if a vector trajectory lies above its tensor partner,  $\alpha\delta > 0$  and  $\sigma(\text{DDRe}) > \sigma(\text{DDPh})$ .<sup>\*</sup> To be specific, let us consider the charge-exchange reactions (VI.1.1,2), which proceed by  $\rho, A_2$  exchange. It appears (see for example Mathews, 1969) that  $\delta \approx 0.1$  and  $\alpha_{A_2}(0) \approx 0.45$ . The REXD scheme predicts, therefore,

---

\* Here  $\sigma$  may be taken to mean  $d\sigma/dt$ , near the forward direction.

$$\sigma(K^+n \rightarrow K^0p) > \sigma(K^-p \rightarrow \bar{K}^0n), \quad (\text{VI.2.7})$$

in apparent agreement with the rather low-energy data ( $p_{\text{lab}} \leq 5.5$  GeV/c) considered by Cline, Matos, and Reeder (1969). The effect does not, however, appear to persist experimentally at higher energies. Thus the differential cross section for  $K^+n \rightarrow K^0p$  at 12 GeV/c recently reported by Firestone, et al. (1970) is equal to the 12.3 GeV/c  $K^-p \rightarrow \bar{K}^0n$  cross section of Astbury, et al. (1966).

In proposing a REXD model, Auvil, et al. (1970)\* have noted that in the comparison implied by Eqs. (VI.2.5,6) the difference between cross sections should change sign at  $\alpha_{A_2} = 0$ , i.e. near  $-t = 0.5$ . In fact this is far from the case, at least at low energies, where the ratio

$$\frac{\frac{d\sigma}{dt}(K^+n \rightarrow K^0p)}{\frac{d\sigma}{dt}(K^-p \rightarrow \bar{K}^0n)} \quad (\text{VI.2.8})$$

is maximal at around  $-t = 0.5$ . The remedy proposed by Auvil, et al. is to include a pair of lower trajectories  $(\rho', A'_2)$  which account for the observed  $t$ -dependence. Such a complication just pushes the implications of the straightforward REXD model to higher energies.

---

\* There is a minor error in this paper. In Table 1 a comparison should correctly be made of  $K^-p \rightarrow \pi^0\Lambda$  with  $\frac{1}{2}$  the cross section for  $\pi^-p \rightarrow K^0\Lambda$ .

Similar considerations may be brought to bear on the hypercharge-exchange reactions mediated by  $K^*, K^{**}$  exchange. Assuming  $\alpha_{K^*} > \alpha_{K^{**}}$  we again predict the DDRe cross sections to be systematically higher than the DDPH cross sections. The results of Birnbaum, et al. (1970) indicate that, up to 16 GeV/c,

$$\frac{\frac{d\sigma}{dt}(K^- p \rightarrow \pi^- \Sigma^+)}{\frac{d\sigma}{dt}(\pi^+ p \rightarrow K^+ \Sigma^+)} \approx 2, \quad (\text{VI.2.9})$$

in qualitative agreement with the REXD prediction.\*

Predictions based upon the REXD idea can also be made for reactions that proceed by  $\tau P$ -exchange, e.g. for  $\pi$  and B exchange. For the latter example we expect on esthetic grounds that  $\alpha_B < \alpha_\pi < 0$ , which would again imply that DDRe cross sections should be larger than DDPH cross sections. A typical prediction is that

$$\frac{\rho_{00} \frac{d\sigma}{dt}(K^+ p \rightarrow K^{*0} \Delta^{++})}{\rho_{00} \frac{d\sigma}{dt}(K^- n \rightarrow \bar{K}^{*0} \Delta^-)} > 1, \quad (\text{VI.2.10})$$

in the peripheral region. In a world where Regge cuts may be important it is of course very difficult to separate the contributions of individual Regge poles, even when one considers particular moments of decay angular distributions. Thus it may be hard to perform tests like (VI.2.10) in convincing fashion, particularly when the lower-lying  $\tau P$ -trajectories are involved.

---

\* See also Kirz (1970).

The three competing hypothesis of EXD, WEXD, and REXD are all quite splendid theoretical ideas which lead to distinct and definite, if only qualitative predictions. Each has a simplicity or elegance that makes its potential value for increasing our understanding enormous. Thus it is essential to answer experimentally, and at high energies (for the study of quasi-two body inelastic reactions, this means  $10 \text{ GeV}/c \lesssim p_{\text{lab}} \lesssim 30 \text{ GeV}/c$ ) questions of the following kinds:

(i) Are line reversal tests satisfied? An affirmative answer confirms WEXD, without making any statement about the residues.

(ii) Do violations of line reversal tests, and thereby of WEXD, occur systematically? If so, does the particular pattern  $\sigma(\text{DDRe}) > \sigma(\text{DDPh})$  persist to higher energies? An affirmative answer will lend support to REXD schemes and may suggest ways of refining them.

(iii) Is EXD satisfied? In particular, are DDRe amplitudes actually real? Such tests (e.g. the absence of polarization in DDRe reactions) are especially delicate, and hard to assess quantitatively; it is difficult to know how to assign errors if an amplitude is "almost" real. It is appropriate to inject here a bit of theoretical bias, which diminishes the appeal of the REXD scheme. In the absence of a "higher" symmetry imposed on hadron dynamics from without, it is hard to see how REXD could be less badly broken than WEXD. Thus the trajectories, which are determined dynamically by a large number of channels, are observed to be approximately, but not exactly, degenerate. It seems plausible that for some processes the residues must be very badly broken from REXD. Consequently unless there is a dynamical miracle, WEXD is probably closer to the truth than REXD.

As we have no complete theory for high-energy collisions, it is hard to overestimate the importance of sorting out regularities such as those bearing on EXD, REXD, and WEXD. Some lists of useful line-reversal tests may be found in the papers of Gilman (1969), Quigg (1970), and Auvil, et al. (1970). Other suggestive hints of systematic behavior are to be found in the review by Rosner (1970). There is no paucity of simple ideas; what we need is large amounts of good data.

### 3. Regge Cuts and the Breaking of Exchange Degeneracy

If exchange degeneracy is broken in some systematic manner, it will be useful to understand how the breaking occurs. For example in the REXD model described in the preceding section the burden is placed on the observed mass splittings of the hadrons, which one may regard either as God-given or as needing explanation on a deeper level. Alternatively, it may be appealing to suppose that Regge cut corrections, applied to EXD input Regge poles, might produce scattering amplitudes which violate the predictions of EXD and agree with the data. As I stressed above, systematic experimental tests are only beginning to emerge, so it is difficult to know which direction to take. Apparently present Regge cut models are sufficiently flexible that many reactions must be studied simultaneously and in detail before success ceases to be guaranteed by a surfeit of parameters. What I am considering here is whether a simple pattern exists, that is instantly explicable in terms of Regge cuts.

To clarify the possible effects of Regge cuts upon EXD input poles, I have done the simplest calculation imaginable. Starting with s-channel nonflip and flip amplitudes appropriate for DDRe and DDPh

reactions, I have computed the absorptive corrections corresponding to an elastic scattering amplitude given by a fixed-pole Pomernanchuk (i.e. a positive imaginary elastic amplitude). For simplicity I took

$$H_{s,\text{elastic}}^{+:+} = i\sigma_{\text{total}} \left(\frac{s}{s_0}\right) e^{at/2}, \quad (\text{VI.3.1})$$

$$H_{s,\text{elastic}}^{-:+} = 0,$$

and used the familiar Fourier-Bessel representation\* for Eq. (V.1.8), which yields

$$H_s^{+:+}(s,t) = H_{s,\text{Regge}}^{+:+}(s,t) - \frac{aC}{2} \int_{-\infty}^0 dt' e^{a(t+t')/2} I_0[a(tt')^{\frac{1}{2}}] \times H_{s,\text{Regge}}^{+:+}(s,t')$$

$$H_s^{-:+}(s,t) = H_{s,\text{Regge}}^{-:+}(s,t) - \frac{aC}{2} \int_{-\infty}^0 dt' e^{a(t+t')/2} I_1[a(tt')^{\frac{1}{2}}] \times H_{s,\text{Regge}}^{-:+}(s,t'). \quad (\text{VI.3.2})$$

Here  $I_n$  is a modified Bessel function of the first kind, of order  $n$ ;  $a = 8(\text{GeV}/c)^{-2}$  is the slope of the forward diffraction peak, and  $C$  is a dimensionless parameter, given in principle by

$$C = \sigma_{\text{total}}/4\pi a. \quad (\text{VI.3.3})$$

---

\* See, for example, Jackson (1970), Section IV.4.

For the input Regge pole amplitudes I followed the recipe developed in Appendix C, so that the DDRe amplitudes are

$$H_{s, \text{Regge}}^{+:+}(s, t) = 2\Gamma(1 - \alpha(t))(s/s_0)^{\alpha(t)}, \quad (\text{VI.3.4})$$

$$H_{s, \text{Regge}}^{-:+}(s, t) = 2(-t/s_0)^{\frac{1}{2}} \Gamma(1 - \alpha(t))(s/s_0)^{\alpha(t)}.$$

The DDPH amplitudes are the same, times an extra factor of  $e^{-i\pi\alpha(t)}$ . In the example I will discuss I chose  $\alpha(t) = \frac{1}{2} + t$ ,  $s_0 = 1(\text{GeV}/c)^2$ , and  $(s/s_0) = 10$ .

In Fig. VI-4 I have plotted the results for the nonflip amplitude. The absolute square of the input pole amplitude is the solid line; it is the same for both the DDRe and the DDPH cases. The contribution of the Regge cut (for  $C = 1$ , which corresponds roughly to total absorption of the s-wave) in the DDRe case is plotted with long dashes. It is smaller than the pole contribution at  $t = 0$ , but is less peripheral. The absolute square of the output, "pole minus cut," amplitude is plotted with short dashes, for the DDRe case. It is more peripheral than the input was, for the effect of the absorptive corrections is to subtract out low partial waves. There is a zero in the amplitude caused by complete destructive interference between pole and cut, at  $-t \approx 0.37 (\text{GeV}/c)^2$ . When the input is the DDPH amplitude one expects (Michael, 1969b) a smaller cut for a given value of  $C$ , since the rotating phase of the input pole enhances the possibility of cancellations in the convolution integral. Also the destructive interference between pole and cut will not be total, for the pole and cut will in general have different phases. Both these features are shown by the DDPH output,  $|\text{Pole minus cut}|^2$ ,

which appears as a dotted line in Fig. VI-4. It lies above the DDRe output, reflecting a smaller cut subtraction, and has only a shoulder at  $-t \approx 0.35$ , rather than a zero. What is somewhat surprising is that the ratio

$$|H_{s,DDPh}^{+:+}|^2 / |H_{s:DDRe}^{+:+}|^2 \approx 1.5 \quad (\text{VI.3.5})$$

is so large. (As expected it is  $>1$ , whereas the REXD mnemonic predicts  $<1$ .)

The same effects are seen in the calculation for the flip amplitude, the results of which are plotted in Fig. VI-5. Again the DDRe output has a zero [at  $-t > 1.0(\text{GeV}/c)^2$ ] but the DDPh output has only a shallow dip; again the ratio

$$|H_{s;DDPh}^{-:+}|^2 / |H_{s,DDRe}^{-:+}|^2 \approx 1.5 \quad (\text{VI.3.6})$$

is rather large. Some calculations similar to these were published recently by Meyers and Salin (1970), which agree qualitatively with my conclusions.

As expected Regge cuts even when generated by a flat Pomeranchuk invalidate the predictions of WEXD (although not in a manner consistent with experiment). While this theory is wrong--and therefore unrealistic--it may be worthwhile to remark that it preserves the prediction of no polarization in the DDRe reaction (both flip and nonflip amplitudes remain purely real) but breaks the EXD prediction of no polarization in the DDPh reaction. This is because the phases of the flip and nonflip amplitudes are altered in different ways. In my examples, the flip-

nonflip phase difference is small for  $-t \lesssim 0.3(\text{GeV}/c)^2$  in the DDPH reaction and also for  $\tau^+$  and  $\tau^-$  exchange separately.

From the perspective of duality graphs, the REXD predictions have a natural explanation in terms of absorptive cuts generated by full (not just Pomeranchuk) elastic amplitudes. In the computation reported above I assumed that the elastic scattering amplitudes were equal in the initial and final states and were equal in the DDRe and DDPH channels. Now in fact this is not so. The "exotic" channels which give rise to nonplanar quark graphs for inelastic processes have smaller total cross sections (thus smaller forward elastic amplitudes) than the channels to which they are related by line reversal. Thus the DDRe amplitudes should be absorbed less than the DDPH amplitudes. If elastic scattering amplitudes are represented in terms of Regge poles (or poles and cuts) this means that the difference between DDRe and DDPH cross sections should be explained by two-Reggeon cuts, in which neither Reggeon is a Pomeranchuk trajectory. Thus the REXD recipe might serve to take account of the effects of two-Reggeon cuts. However REXD, in the simple form stated above, treats flip and nonflip amplitudes in the same way, so does not account for polarization, whereas two Reggeon cuts may well do so. The importance of two Reggeon cuts, with neither Reggeon a Pomeranchuk trajectory, was suggested by Michael (1969b). Recent work along the same lines has been reported by O'Donovan (1970). Some relevant model calculations are discussed below.

A final comment derived from the model calculation discussed here bears on the vaunted dip systematics of the Michigan strong cut model (see Ross, et al., 1970). In Fig. VI-6 I have shown the values of

$t$  for which dips are generated in the flip and nonflip amplitudes, as functions of the strength of the Regge cut. Although my input poles, in having conventional nonsense zeroes, differ from the input of the Michigan model, the dips appear at the expected positions for a cut of Michigan strength ( $C \approx 1.5$ ). In the DDRe case the dips are quite dramatic, representing excursions through two or more decades in  $|H_s^{++}|^2$ , even when the observed real part of the elastic amplitude is tacked on by the substitution

$$C \rightarrow C[1 - i(\text{Real part}/\text{Imaginary part})]. \quad (\text{VI.3.7})$$

In contrast the structure in the DDPh case is a break or a shallow dip. Some care is therefore required, precisely to state the predictions of the Michigan model in specific reactions. The strong cut systematics may be every bit as fuzzy as those of the classical Regge pole model. Obviously this remark applies equally to proponents and detractors of the strong cut model.

Krzywicki and Tran Thanh Van (1969) [see also Krzywicki, 1970] investigated the effects on polarization predictions of cuts generated by a nonflat Pomeranchuk trajectory. Their discussion utilizes a very simplified parametrization which cannot be taken seriously for quantitative features (such as the magnitude of polarizations), but two natural predictions of the model stand out. First, near the forward direction, the polarization  $P$  is of the same sign in the DDRe and DDPh reactions related by line reversal. Second,  $P(\text{DDRe})$  has a constant sign over a substantial range in  $t$ , whereas  $P(\text{DDPh})$  changes sign at some small

value of  $-t$ . Despite these attractive features, which appear to be present in the data, it is unlikely that this scheme can accommodate all the experimental features. The cut corrections to DDRe amplitudes will exceed those to DDPH amplitudes and thereby disagree with what is observed.

#### 4. Reggeon-Reggeon Cuts and Line-Reversal Violations

The model calculation described in the preceding section illustrated the conclusion that the recipe of exchange degenerate Regge poles plus pole-Pomeranchuk cuts does not account for the experimental fact that  $\sigma(\text{DDRe}) > \sigma(\text{DDPh})$ , at intermediate energies. It is therefore of obvious interest to assess the effects of two-Reggeon cuts, when neither Reggeon is the Pomeranchuk trajectory. To accomplish this, I have calculated the non-Pomeranchuk contributions to the reactions

$$\text{DDPh: } \pi^+ \pi^- \rightarrow \pi^+ \pi^-, \quad (\text{VI.4.1a})$$

$$\text{DDRe: } \pi^- \pi^- \rightarrow \pi^- \pi^-, \quad (\text{VI.4.1b})$$

i.e. the  $P' + \rho$  poles and the  $(P' + \rho) \otimes (P' + \rho)$  cut. The restriction to a spinless reaction is made for technical simplicity, to avoid becoming bogged down in details of flip to nonflip ratios, etc.

For the Regge pole amplitudes I chose

$$H_S [\pi^+ \pi^- \rightarrow \pi^+ \pi^-] = -2g\Gamma(1 - \alpha(t)) (\alpha(s))^{\alpha(t)} e^{-i\pi\alpha(t)}, \quad (\text{VI.4.2a})$$

$$H_S [\pi^- \pi^- \rightarrow \pi^- \pi^-] = -2g\Gamma(1 - \alpha(t)) (\alpha(s))^{\alpha(t)}, \quad (\text{VI.4.2b})$$

corresponding to amplitudes for  $P'$  and  $\rho$  exchange

$$H_{(\rho)} = -g\Gamma(1 - \alpha(t))(\alpha(s))^{\alpha(t)}(1 - e^{-i\pi\alpha(t)}), \quad (\text{VI.4.3})$$

$$H_{(P')} = -g\Gamma(1 - \alpha(t))(\alpha(s))^{\alpha(t)}(1 + e^{-i\pi\alpha(t)}).$$

The trajectory function  $\alpha(x) = 0.48 + 0.9x$ , and the coupling constant  $g = 16\pi$  were taken from the paper by Shapiro (1969). The prescription (V.1.9) gives

$$H_{s,\text{total}}(s,t) = H_{(\rho)}(s,t) + H_{(P')}(s,t) + \frac{i}{16\pi} \sum_{J=0}^{\infty} (J + \frac{1}{2}) d_{00}^J(\theta_s) \{ h_{J(\rho)} h_{J(P')} + \frac{1}{2} [ (h_{J(\rho)})^2 + (h_{J(P')})^2 ] \}, \quad (\text{VI.4.4})$$

where

$$h_{J(i)} = \int_{-1}^1 d(\cos \theta_s) H_{(i)}(s, \cos \theta_s) d_{00}^J(\theta_s). \quad (\text{VI.4.5})$$

In practice I truncated the partial-wave expansion at  $J < 30$ , and performed the partial-wave projection by 96-point Gaussian quadrature on the CDC 6600. Numerous checks were made to verify the orthonormality of my  $d_{00}^J$  functions, and the ability of the projecting and resumming routines to reproduce various input functions. Each of the examples discussed below required about 3 seconds of computer time.

Figure VI-7 shows the contributions of the various components in (VI.4.4) for the parameters chosen, at  $s = 10 \text{ GeV}^2$ . Broken down in this way, the pieces are the same--in magnitude--in the two reactions.

The weakness of the  $\rho$ - $\rho$  cut is due to the vanishing of the  $\rho$  Regge pole amplitude at  $-t \approx 0.58$ . The integrated cross section contributed by the poles is  $\sigma_{el} \approx 2\text{mb.}$ , a not unreasonable value. In Fig. VI-8 I have plotted the contributions of the cuts as they occur in the two reactions of interest. The DDRe cut, for  $\pi^- \pi^- \rightarrow \pi^- \pi^-$  is the result of convoluting the real amplitude (VI.4.2b) with itself. As expected, it is somewhat larger than the DDPh cut, which is the convolution of the rotating phase amplitude (VI.4.2a) with itself. In the DDRe case, the cut contribution is a real number times the explicit factor of  $i$  that appears in (VI.4.4). Consequently the cut and pole contributions add incoherently, for the reaction  $\pi^- \pi^- \rightarrow \pi^- \pi^-$ . Near the forward direction, the effect of the  $(P' + \rho) \otimes (P' + \rho)$  cut is insignificant (in  $\pi^- \pi^- \rightarrow \pi^- \pi^-$ ), as evidenced by the near equality of the DDRe and Input (= poles only) curves in Fig. VI-8.

The situation is completely different in the DDPh case. The phase of the cut piece at any value of  $t$  is approximately twice the phase of (VI.4.2a) at  $t/4$ , plus  $\pi/2$  (from the explicit factor of  $i$ ). At  $t = 0$ , the input amplitude (VI.4.2a) is  $\alpha + i$ . Thus at  $t = 0$ , the cut is roughly negative imaginary; it interferes destructively with the pole amplitude, as stated by Michael (1969b). For my choice of the coupling constant, the cross section is diminished by about 20%, for  $s = 10 \text{ GeV}^2$ , in the forward direction. The effect is larger at larger values of  $-t$ , because the cut amplitude is less peripheral than the pole amplitude. Amusingly, indeed encouragingly, the violations of line reversal in KN charge exchange are bigger at moderate values of  $-t$  than at  $t = 0$ .

To give a feeling for the energy dependence of the pole-pole cuts I have plotted the same quantities at  $s = 5$  and  $20 \text{ GeV}^2$  in Figs. VI-9,10. Alternatively, these can be interpreted as reflecting the sensitivity of the results to the coupling constant  $g$ . These very simplified calculations show that the pole-pole cuts do contribute with the right phases to make  $\sigma(\text{DDRe}) > \sigma(\text{DDPh})$ , and may be substantial in magnitude at low energies. (It is worth remarking that if the DDPH input had been  $\alpha - i$ , the poles and cuts would have interfered constructively.) In addition, the cut corrections become more important at nonforward angles. Rather remarkably (at first sight) the cuts have an energy dependence characterized by  $\alpha_{\text{eff}}(0) < 2\alpha(0) - 1$ , at these low energies. (See Figs. VI-8,9,10.) Thus the argument of Cline, et al. (1970) that the energy dependence of pole-pole cuts is too gentle to account for the probable diminution with increasing energy of the line reversal violation in KNCEX is too naive, and therefore misleading. O'Donovan (1970) points out that his estimates of pole-pole cut corrections to KNCEX fade away faster with increasing energy than  $\alpha_{\text{cut}}(0) = 2\alpha(0) - 1$  would lead one to expect. He ascribes this rapid energy variation to complicated pole-cut interferences. This misses the point. As shown by Figs. VI-8,9,10 the cut pieces alone behave as  $\alpha_{\text{eff}}(0) < 2\alpha(0) - 1$ . This merely reflects the fact that the cut amplitude is not proportional to  $(\alpha(s))^{\alpha_{\text{cut}}}$ , but to  $(\alpha(s))^{\alpha_{\text{cut}}} / [\ln(\alpha(s)) - i\pi/2]^\beta$ . For small values of  $\alpha(s)$ , the logarithm varies rapidly, and the net energy dependence will resemble that characterized by a power somewhat lower than  $\alpha_{\text{cut}}$ . (For a more explicit demonstration, see Fig. 18 of Jackson, 1970.) Thus

describing the energy dependence of the cut as  $s^{\alpha_{\text{cut}}}$  at small values of  $s$  is dangerous and may lead to wrong conclusions. The question of energy dependence recurs in the discussion of exotic exchanges, which follows.

### 5. Exotic Quantum Number Exchange

It has been recognized for some time that two-Reggeon exchange graphs provide a mechanism for the exchange of exotic quantum numbers, without the necessity of exotic trajectories (e.g. Chiu and Finkelstein, 1969). The formalism constructed in Chapter V needs only the existence of reliable amplitudes for the individual rungs of the box diagrams to be quantitatively useful. Our work in progress on  $(K^*, K^{**})$  exchange soon will yield amplitudes which should permit reliable statements to be made about production angular distributions, absolute normalizations, and so on. As an example of the kind of results which will be the outcome of this program, I present here a calculation of the near-forward differential cross section for the reaction

$$K^- p \rightarrow K^+ \Xi^-, \quad (\text{VI.5.1})$$

assumed to proceed (as discussed in Section V.2) by double  $K^*$  or by double  $K^{**}$  exchange. Although such calculations have been talked about before (Chiu and Finkelstein, 1969; Rivers, 1968), this seems to be the first one actually carried through. I hasten to add that for the reaction (VI.5.1) the dominant mechanism is assumed to be baryon  $(Y = 0, I = 0, 1)$  exchange. The present calculation is thus an attempt to estimate the magnitude and shape of the contribution at small  $t$

generated by two successive nonexotic mesonic exchanges, and not an attempt to fit the observed cross section over the whole angular range.

For simplicity, and to facilitate the discussion of qualitative features, we take the amplitudes for the allowed associated production reactions  $K^- p \rightarrow \pi^0 Y^0$  from an EXD Regge pole fit to the available high-energy data. The amplitudes for  $\pi^0 Y^0 \rightarrow K^+ \Xi^-$  are obtained by SU(3) rotations. We neglect intermediate states in which  $\eta$  replaces  $\pi^0$ , for lack of useful data on  $K^- p \rightarrow \eta Y^0$ , although these states in principle contribute. We then have

$$\begin{aligned}
 H_s^{\lambda' : \lambda}(s, t) = & \frac{i}{32\pi} \sum_{J, \mu} (J + \frac{1}{2}) \{ h_{J(K^*)}^{\mu : \lambda} \text{I}(s) h_{J(K^*)}^{\lambda' : \mu} \text{III}(s) \\
 & + h_{J(K^*)}^{\mu : \lambda} \text{II}(s) h_{J(K^*)}^{\lambda' : \mu} \text{IV}(s) + h_{J(K^{**})}^{\mu : \lambda} \text{I}(s) h_{J(K^{**})}^{\lambda' : \mu} \text{III}(s) \\
 & + h_{J(K^{**})}^{\mu : \lambda} \text{II}(s) h_{J(K^{**})}^{\lambda' : \mu} \text{IV}(s) \} d_{\lambda, \lambda'}^J(\theta_s)
 \end{aligned} \tag{VI.5.2}$$

where the individual reactions are denoted by

- I:  $K^- p \rightarrow \pi^0 \Lambda$
- II:  $K^- p \rightarrow \pi^0 \Sigma^0$
- III:  $\pi^0 \Lambda \rightarrow K^+ \Xi^-$
- IV:  $\pi^0 \Sigma^0 \rightarrow K^+ \Xi^-$

To parametrize the single meson exchange allowed reactions we make the usual decomposition into invariant amplitudes

$$M = \bar{u}_2 \{A - (i/2)\gamma \cdot (q_1 + q_2)B\} u_1, \quad (\text{VI.5.3})$$

where  $q_1$  ( $q_2$ ) is the c.m. four momentum of the incoming (outgoing) meson. The s-channel helicity amplitudes are then

$$H_S^{++} = \{A\eta_- + B[\eta_+(s)]^{\frac{1}{2}} - \frac{(m_1 + m_2)}{2} \eta_-\} \cos \theta_s/2, \quad (\text{VI.5.4})$$

$$H_S^{-+} = \{A\eta_+ + B[\eta_-(s)]^{\frac{1}{2}} - \frac{(m_1 + m_2)}{2} \eta_+\} \sin \theta_s/2, \quad (\text{VI.5.5})$$

where  $m_1$  ( $m_2$ ) is the mass of the incoming (outgoing) baryon, and we define

$$\eta_{\pm} = [E_1 + m_1]^{\frac{1}{2}} [E_2 + m_2]^{\frac{1}{2}} \left\{ 1 \pm \frac{p_1 p_2}{(E_1 + m_1)(E_2 + m_2)} \right\}, \quad (\text{VI.5.6})$$

in which  $p$  and  $E$  are respectively the baryon momentum and energy in the center of mass system. We define the quantities  $T^{\lambda':\lambda}$  which are related to the t-channel helicity amplitudes by factors that remove the kinematical singularities:

$$T^{++} = A' [(m_1 + m_2)^2 - t]^{\frac{1}{2}}, \quad (\text{VI.5.7})$$

$$T^{+-} = \nu B \{-t / [(m_1 + m_2)^2 - t]\}^{\frac{1}{2}}, \quad (\text{VI.5.8})$$

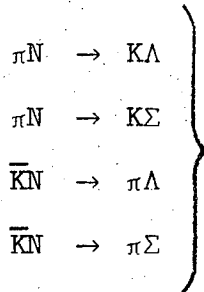
with  $\nu = (s - u)/2$ ,  $A' = A + xB$ , and

$$x = \frac{(m_1 + m_2)}{(m_1 + m_2)^2 - t} \left\{ \nu + \frac{(m_1 - m_2)(\mu_1^2 - \mu_2^2)}{2(m_1 + m_2)} \right\}. \quad (\text{VI.5.9})$$

For each reaction, the amplitudes  $T^{\lambda';\lambda}$  are characterized by four parameters. Thus

$$T^{+;\pm} = -\frac{[\tau + \exp(-i\pi\alpha(t))]}{2\Gamma(1 + \alpha(t))\sin \pi\alpha(t)} \left(\frac{\nu}{\nu_0}\right)^{\alpha(t)} C^{\pm} e^{at} \quad (\text{VI.5.10})$$

is the contribution of the Regge pole with signature  $\tau$ . We require the  $K^*$  and  $K^{**}$  to be EXD, and fix the slope of the trajectory  $\alpha' = 0.9 \text{ GeV}^{-2}$  and the scale factor  $\nu_0 = 1 \text{ GeV}^2$ . There remain as parameters the intercept  $\alpha(0)$ , the vertex exponential  $a$ , and two coupling constants  $C^+$  and  $C^-$ . As the intercept must be the same for all reactions we have a total of seven free parameters to fit the reactions



when the constraints of factorization and isospin conservation are imposed. The fits to associated production will be discussed in detail elsewhere (see Fox and Quigg, 1970). It suffices, for present purposes, to know that the EXD fit yields a fair overall fit ( $\chi^2 = 891/220$  differential cross section points;  $\chi^2 = 234/48$  polarization data which are irrelevant for the fit since  $P \equiv 0$  in the model). The data considered are summarized in Table VI-2; for details and references, consult our paper. The best fit parameters are given in Table VI-3, together with the coupling constants for  $\pi Y^0 \rightarrow K^{\pm}\Xi^{\mp}$  obtained from them by  $SU(3)$  rotations. We chose the vertex exponentials for  $\bar{Y}^{\pm}$

equal to the one for  $\bar{p}\Sigma$ , which was much better determined than the one for  $\bar{p}\Lambda$ .

The differential cross sections computed (from EXD poles alone) from these parameters at 5 GeV/c are plotted in Fig. VI-11. [The reaction  $K^-p \rightarrow \pi^- \Sigma^+$  is plotted rather than  $K^-p \rightarrow \pi^0 \Sigma^0$  which cross section nearly coincides with the one for  $\pi^0 \Lambda \rightarrow K^+ \Xi^-$ .] Details, such as the forward dip for  $\pi^0 \Sigma^0 \rightarrow K^+ \Xi^-$ , should not be taken too seriously, as the couplings for  $K^-p \rightarrow \pi^0 \Lambda$  are quite uncertain. However the magnitude of the cross sections is probably reliably estimated by our simple model. The spin content of the cross sections, expressed through the useful parameter

$$A \equiv \frac{|H_s^{+:+}|^2 - |H_s^{+:-}|^2}{|H_s^{+:+}|^2 + |H_s^{+:-}|^2} \quad (\text{VI.5.11})$$

is conveyed by Fig. VI-12. As one would guess from the previous figure, all the reactions but  $\pi^0 \Sigma^0 \rightarrow K^+ \Xi^-$  are dominated by nonflip amplitudes for small values of  $-t$ . Since we are assuming EXD, Fig. VI-12 applies separately to the  $K^*$  and  $K^{**}$  contributions, as well. Each cross section is an incoherent sum of the  $K^*$  and  $K^{**}$  components, which are shown in Figs. VI-13 and VI-14, respectively. The presence of the nonsense, wrong-signature zero in the  $K^*$  contribution suggests-- compare the  $\rho \otimes \rho$  cut computed in Section 4--that double  $K^*$  exchange will be unimportant compared with double  $K^{**}$  exchange. We will see below that this is indeed the case.

In Fig. VI-15 I have displayed the results of the calculation of  $K^-p \rightarrow K^+ \Xi^-$  with the pole-pole cut. The thick, solid line marked

"All" is the full cross section implied by (VI.5.2). The contribution from graphs with a  $\Sigma^0$  intermediate state ( $\Sigma$ ) is negligible. This suppression is a consequence of the forward dip in  $\pi^0 \Sigma^0 \rightarrow K^+ \Xi^-$ . The graphs with  $\Lambda^0$  intermediate state ( $\Lambda$ ) contribute nearly the entire cross section. Similarly, the  $K^{**} - K^{**}$  graphs ( $K^{**}$ ) are responsible for most of the cross section, and the  $K^* - K^*$  graphs ( $K^*$ ) are of little importance. To summarize the content of Fig. VI-15, we may remark that for the model based on (VI.5.2)  $K^{**} - K^{**}$  exchange in the two-step process  $K^- p \rightarrow \pi^0 \Lambda \rightarrow K^+ \Xi^-$  is the dominant mechanism for a peripheral (small  $t$ ) peak in  $K^- p \rightarrow K^+ \Xi^-$ . The  $K^{**}$  dominance is an expected, qualitative feature, whereas the unimportance of the  $\Sigma^0$  intermediate state is model-dependent. The  $A$  parameter for  $K^- p \rightarrow K^+ \Xi^-$ , plotted in Fig. VI-16, shows that the calculated cross section is dominated by the nonflip amplitude.

The calculated near-forward cross section for  $p_{\text{lab}} = 2, 3, \text{ and } 5$  GeV/c is shown in Fig. VI-17. The cross section is quite small:  $d\sigma/dt (t = 0) = 605, 166, 32 \text{ nb/GeV}^2$  at  $p_{\text{lab}} = 2, 3, 5$  GeV/c. These are rather less than the value of  $2 \mu\text{b/GeV}^2$  at 3.5 GeV/c estimated by Rivers (1968) or the estimate of  $2.6 \mu\text{b/GeV}^2$  at 3.4 GeV/c deduced in a rescattering quark model by Dean (1968). Measured production angular distributions for the incident momentum range 1.2 to 3.5 GeV/c are collected in Fig. VI-18. The prominent feature of these distributions is a backward peak suggestive of baryon exchange. At the lower momenta (particularly at 1.8 GeV/c) there is some evidence for forward peaking as well, but this is probably a result of s-channel resonance formation.

At the higher momenta there is no hint of a (forward) peripheral peak. The "high-energy" data of Fig. VI-18g,h,i are shown in Figs. VI-19,20,21 respectively. [Some of the data evidently were revised after the compilation of Lyons (1966), from which Fig. VI-18 was taken, was made.]\* The cross sections in the forward bins are tabulated in Table VI-4. The apparent absence of peripheral peaks agrees with our prediction of rather small forward cross sections, but the number of events in the forward bins is greater than we expect. Possibly the tail of the baryon exchange production angular distribution can account for these events. We may also compare the total peripheral cross section predicted by the model with the observed peripheral u-channel cross sections. From the curves shown in Fig. VI-17 we find  $\sigma_{\text{cut}} \approx 180, 44, 7 \text{ nb.}$  at  $P_{\text{lab}} = 2, 3, 5 \text{ GeV/c}$ , whereas the experimental cross sections are  $175 \pm 16 \mu\text{b}$  at  $1.70 \text{ GeV/c}$ ,  $58 \pm 6 \mu\text{b}$  at  $2.64 \text{ GeV/c}$  (Dauber, et al., 1969); and  $21 \pm 3.5 \mu\text{b}$  at  $3.0 \text{ GeV/c}$  (Badier, et al., 1966).

It has been hoped (Michael, 1969a) that exotic trajectory exchange might be identified by some characteristic energy dependence, such as

$$\frac{d\sigma}{dt} \propto s^{-10},$$

which is easily distinguished from the behavior expected of Regge cuts,

$$\frac{d\sigma}{dt} \propto s^{2[\alpha_1(0)+\alpha_2(0)-1]-2},$$

---

\* See also Fig. 2 of Dauber, et al. (1969), in which their statistically superior results are summarized.

near  $t = 0$ , if  $\alpha(0)$  corresponds to an established, high-lying trajectory. In the preceding Section I noticed that the logarithmic energy dependence of the Regge cut can confound such simple estimates. In  $j$ -plane language, the cut discontinuity is large below the branch point, thus  $\alpha_{\text{effective}} < \alpha_{\text{cut}}$ . The present calculation gives another illustration of this effect. Determining  $\alpha_{\text{eff}}(t = 0)$  from the 2, 3, and 5 GeV/c predictions, we obtain  $\alpha_{\text{eff}}(t = 0) \approx -0.55$ , whereas  $\alpha_{\text{cut}}(t = 0) \approx -0.31$ . It is worth remarking that for baryon ( $\Lambda, \Sigma$ ) exchange,  $\alpha_{\text{eff}} \approx -1$  and hence the pole-pole cut contribution may eventually dominate. However the energy at which it dominates will be extremely large, because of the factor of  $10^3$  in magnitude that must be overcome.

Let me further caution that such energy dependence arguments are not rigorous, for Reggeon box graphs can in fact generate contributions that vanish rapidly with increasing  $s$ . A specific example was given by Wilkin (1964) who showed that a diagram with  $\rho_{\text{su}}(s, t) \equiv 0$  has an amplitude which goes as  $s^{\alpha_1(-\infty) + \alpha_2(-\infty) - 1}$ , for  $t = 0$ . In a ladder model for Regge poles,  $\alpha(-\infty) = -1$ , so that

$$\frac{d\sigma}{dt} \propto s^{-8}, \quad (\text{VI.5.12})$$

which is uncomfortably close to  $s^{-10}$ . It would indeed be disgusting if nonleading contributions from two-Reggeon exchange diagrams played an important role in any reaction. On the other hand this (admittedly far-fetched) example weakens any arguments in favor of exotics based on anomalously low effective Regge pole intercepts. There are no doubt assorted weird objects lurking in the left-half  $j$  plane. Thus we shall

have evidence for exotics either when an exotic resonance is established or when quantitative two-Reggeon-exchange calculations fail.

The present calculation, which gives an unobservably small cross section, is somewhat academic (as befits a thesis!), but it is sufficiently simple that it can be explained concisely. It was intended to illustrate an approach to Regge cut calculations, and to demonstrate some features of my  $s$ - $u$  crossing symmetric prescription. Other, more experimentally interesting reactions come to mind. Many of these are more complicated calculations, in terms of the number of Regge poles and diagrams involved, than the simple example treated here, but are still of finite difficulty. I intend to consider some of these more interesting examples in the near future.

Table VI-1. Quark compositions of some hadrons.

<u>Hadron</u>	<u>Constituents</u>
$\pi^+$	$\bar{p}n$
$\pi^0$	$(\bar{p}p + n\bar{n})/\sqrt{2}$
$\pi^-$	$\bar{p}n$
$K^+$	$\bar{p}\lambda$
$K^0$	$n\bar{\lambda}$
$\bar{K}^0$	$\bar{n}\lambda$
$K^-$	$\bar{p}\lambda$
$p$	$ppn$
$n$	$pnn$
$\Lambda$	$pn\lambda$
$\Sigma^+$	$pp\lambda$
$\Sigma^0$	$pn\lambda$
$\Sigma^-$	$nn\lambda$
$\Xi^0$	$p\lambda\lambda$
$\Xi^-$	$n\lambda\lambda$
$\Delta^{++}$	$ppp$
$\Delta^+$	$ppn$
$\Delta^0$	$pnn$
$\Delta^-$	$nnn$
$\Omega^-$	$\lambda\lambda\lambda$

Table VI-2. Associated production data.

Reaction	Minimum $p_{lab}$	$d\sigma/dt$ points	Polarization points
$\pi^- p \rightarrow K^0 \Lambda$	2.95 GeV/c	7	9
$\pi p \rightarrow K \Sigma$	5	54	30
$\pi^- p \rightarrow K^0 (\Lambda + \Sigma^0)$	6	72	-
$K N \rightarrow \pi \Lambda$	3.7	43	9
$K N \rightarrow \pi \Sigma$	3.7	44	0

Table VI-3. Parameters for  $K^*(890)$  exchange.

Reaction	$a(\text{GeV}^{-2})$	$c^+$	$c^-$
$K^- p \rightarrow \pi^0 \Sigma^0$	2.64	45.6	-73.5
$K^- p \rightarrow \pi^0 \Lambda^0$	0.254	-47.3	-59.49
$\pi^0 \Lambda^0 \rightarrow K^+ \Xi^-$	2.64	-57.0	42.4
$\pi^0 \Sigma^0 \rightarrow K^+ \Xi^-$	2.64	-6.7	-73.1

$$\alpha(0) = 0.35$$

Table VI-4. Forward cross sections for  $K^-p \rightarrow K^+\Xi^-$ .

$p_{\text{lab}}, \text{ GeV}/c$	$-t_1$	$-t_2$	$d\sigma/dt (\text{nb.}/\text{GeV}^2)$
2.24	0.02	0.27	$\sim 4000 \pm 3000$
3.0	0.007	0.391	$2291 \pm 1599$
3.5	0.005	0.481	$0 \pm 1979$

FIGURE CAPTIONS

- Fig. VI-1. Labeling of the  $s, t,$  and  $u$  channels for the proofs of  $\rho, A_2$  and of  $\Sigma_\alpha, \Sigma_\gamma$  exchange degeneracy. No strong resonances occur in the  $u$ -channel, which has exotic quantum numbers.
- Fig. VI-2. Evidence from the hadron spectrum for  $\rho, A_2$  and  $\Sigma_\alpha, \Sigma_\gamma$  exchange degeneracy.
- Fig. VI-3. (a) Nonplanar duality graph for the reaction  $K^+ n \rightarrow K^0 p$ ;  
 (b) Planar graph for  $K^- p \rightarrow \bar{K}^0 n$ .
- Fig. VI-4. Absolute squares of various components of the  $s$ -channel nonflip amplitude, as functions of  $t$ . Solid line--pole term; long dashes--cut contribution in the DDRe case; short dashes--full amplitude in the DDRe case; dots--full amplitude in the DDPh case. See the text for explanation.
- Fig. VI-5. Same as Fig. VI-4, for the  $s$ -channel flip amplitude.
- Fig. VI-6. Location of the dips arising from cut-pole interference, as a function of the cut strength. Solid line--nonflip amplitude; broken line--flip amplitude.
- Fig. VI-7. Contributions of the  $P'$  and  $\rho$  poles, and of the  $P' \otimes P', P' \otimes \rho,$  and  $\rho \otimes \rho$  cuts to  $\pi\pi$  scattering at  $s = 10 \text{ GeV}^2$ .
- Fig. VI-8. Contributions of the  $P'$  and  $\rho$  poles, and of the  $(P' + \rho) \otimes (P' + \rho)$  cuts to the reactions  $\pi^+ \pi^- \rightarrow \pi^+ \pi^-$  (DDPh) and  $\pi^- \pi^- \rightarrow \pi^- \pi^-$  (DDRe) at  $s = 10 \text{ GeV}^2$ . The pole contribution is marked Input. The curves marked DDRe, DDPh represent the (coherent) sum of poles and cuts.

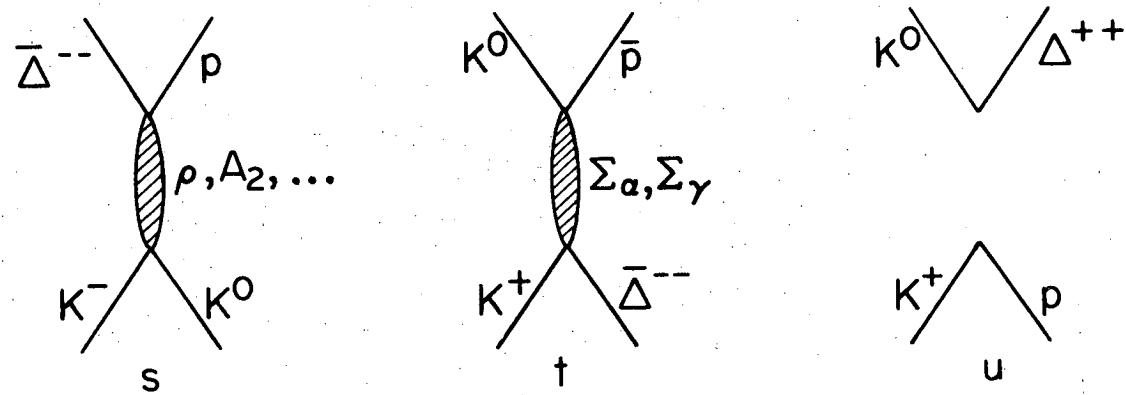
- Fig. VI-9. Same as Fig. VI-8, for  $s = 5 \text{ GeV}^2$ .
- Fig. VI-10. Same as Fig. VI-9, for  $s = 20 \text{ GeV}^2$ .
- Fig. VI-11. Differential cross sections for the  $(K^*, K^{**})$  exchange reactions discussed in the text, computed from the EXD fit to high-energy associated production, at  $5 \text{ GeV}/c$  incident momentum.
- Fig. VI-12. The spin rotation parameter  $A$  for the reactions exhibited in Fig. VI-11, which are labeled by their baryon vertices.
- Fig. VI-13. Contribution of  $K^*$  exchange to the reactions of interest. Note the nonsense, wrong-signature zero near  $-t = 0.4 \text{ (GeV}/c)^2$ .
- Fig. VI-14. Contribution of  $K^{**}$  exchange to the reactions under discussion.
- Fig. VI-15. Predicted cross section for  $K^-p \rightarrow K^+\Xi^-$  at  $5 \text{ GeV}/c$ . The full calculation is represented by the thick, solid line. The components from  $K^*-K^*$  graphs,  $K^{**}-K^{**}$  graphs,  $\pi^0 \Lambda^0$  intermediate states, and  $\pi^0 \Sigma^0$  intermediate states are also shown separately.
- Fig. VI-16. The  $A$  parameter predicted for  $K^-p \rightarrow K^+\Xi^-$  at  $5 \text{ GeV}/c$ .
- Fig. VI-17. Predicted differential cross sections for  $K^-p \rightarrow K^+\Xi^-$  at  $2, 3,$  and  $5 \text{ GeV}/c$  incident momentum.
- Fig. VI-18. Production angular distributions for the reaction  $K^-p \rightarrow K^+\Xi^-$  for the incident momentum range  $1.2$  to  $3.5 \text{ GeV}/c$  (from Lyons, 1966). The data up to  $1.6 \text{ GeV}/c$  are from Alvarez, et al. (1962). (a)  $1.2 \text{ GeV}/c$ , 33 events;

(b) 1.3 GeV/c, 56 events; (c) 1.4 GeV/c, 47 events;  
(d) 1.5 GeV/c, 207 events; (e) 1.6 GeV/c, 41 events;  
(f) 1.8 GeV/c, 96 events, Ticho (1962); (g) 2.24 GeV/c,  
38 events, Bertanza, et al. (1962); (h) 3.0 GeV/c, 28  
events, Badier, et al. (1964); (i) 3.5 GeV/c, 17 events,  
B-G-L-O-R Collaboration (1965).

Fig. VI-19. Production angular distribution for  $K^-p \rightarrow K^+\Xi^-$  at 2.24 GeV/c, from London, et al. (1966).

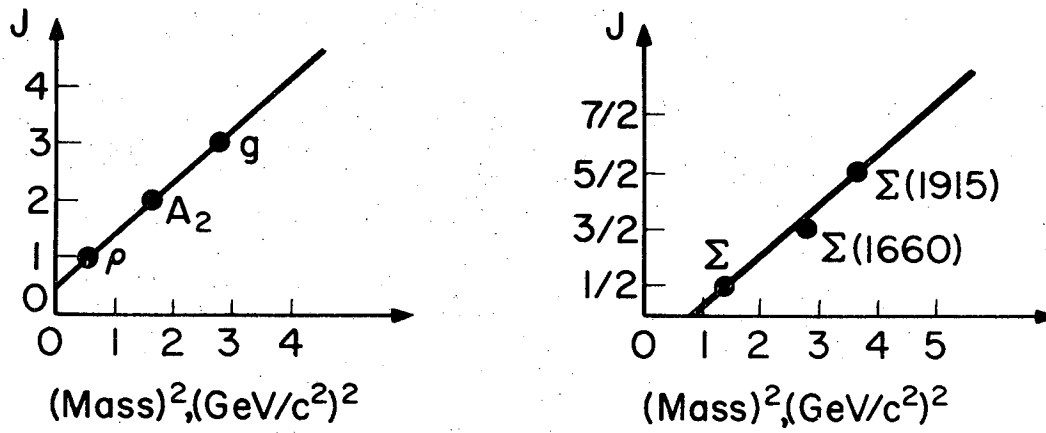
Fig. VI-20. Production angular distribution for  $K^-p \rightarrow K^+\Xi^-$  at 3.0 GeV/c, from Badier, et al. (1966).

Fig. VI-21. Production angular distribution for  $K^-p \rightarrow K^+\Xi^-$  at 3.5 GeV/c, from B-G-L-O-R (1966).



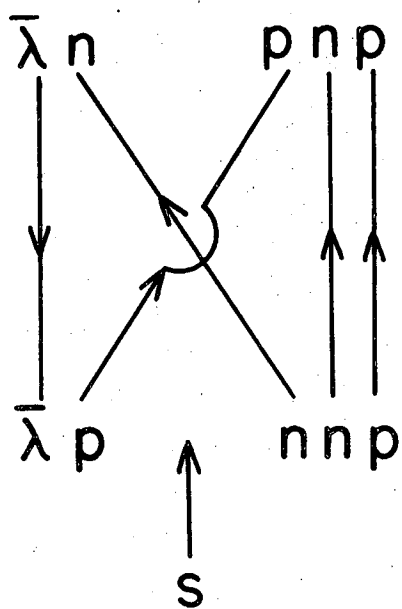
XBL707-3470

Fig. VI-1.

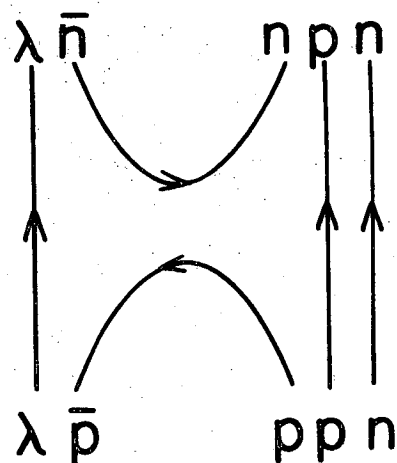
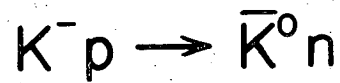


XBL707-3492

Fig. VI-2.



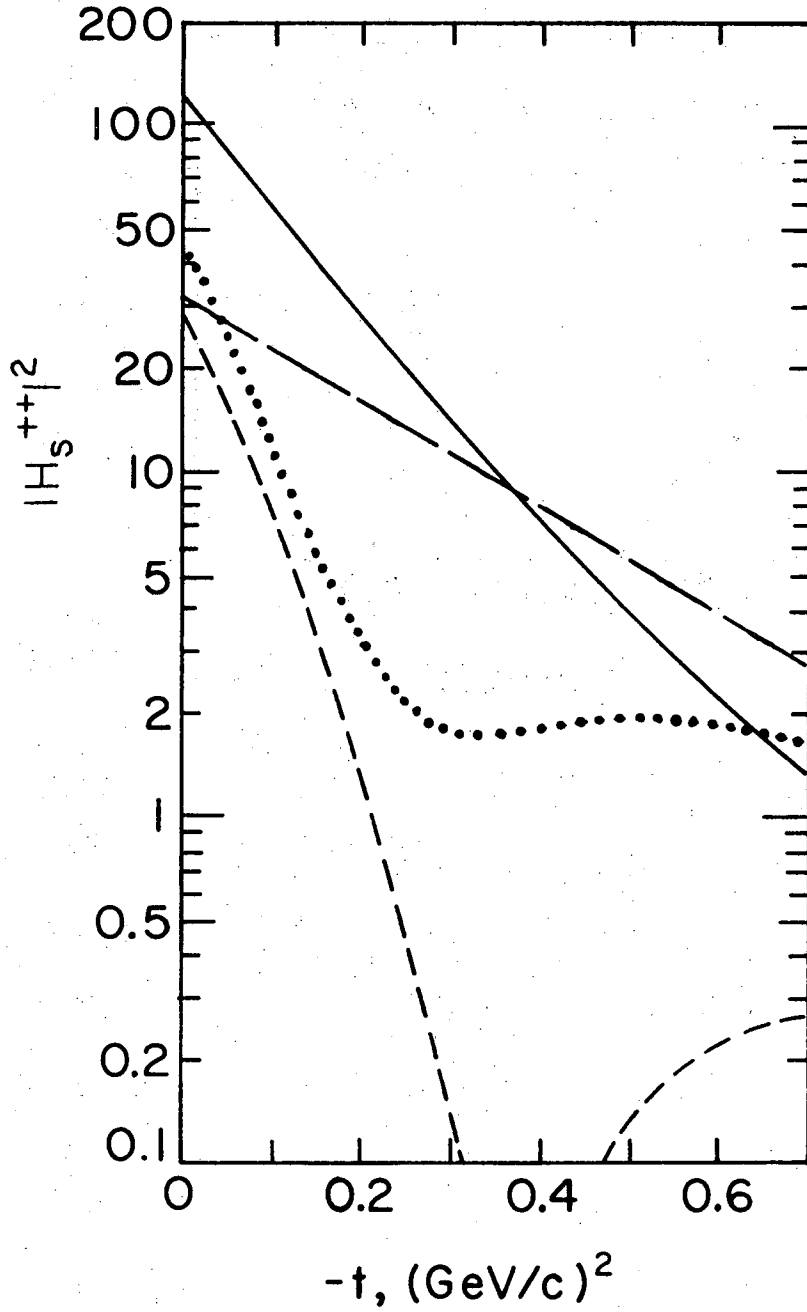
(a)



(b)

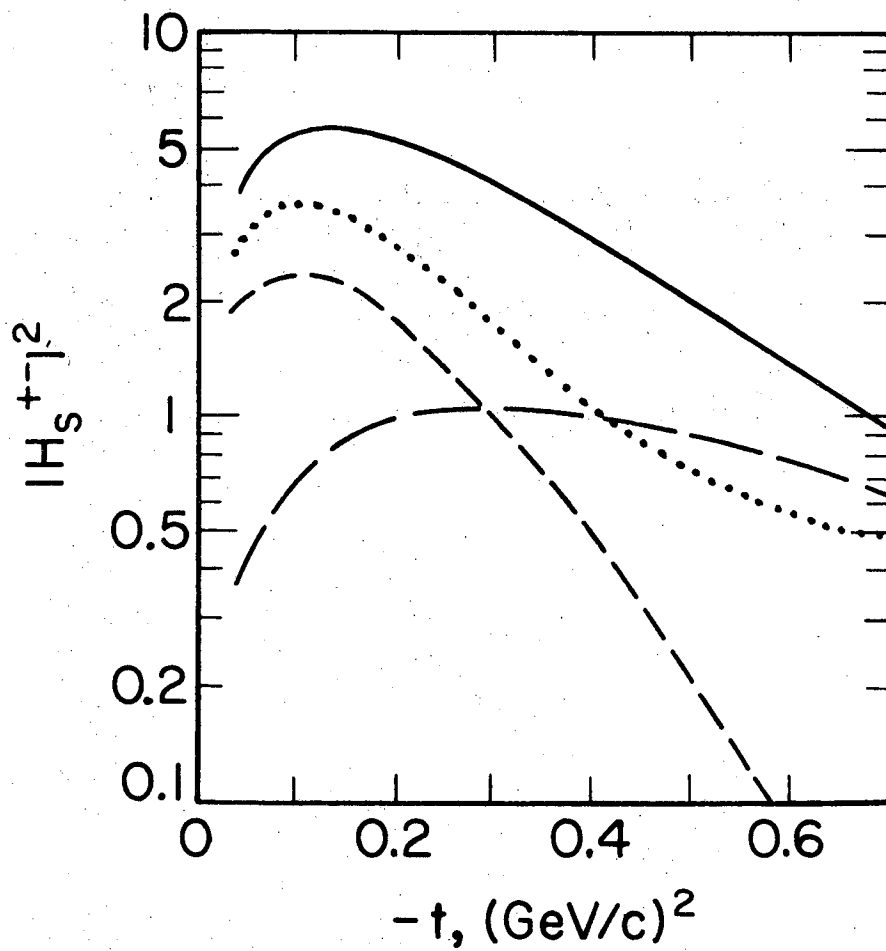
XBL707-3496

Fig. VI-3.



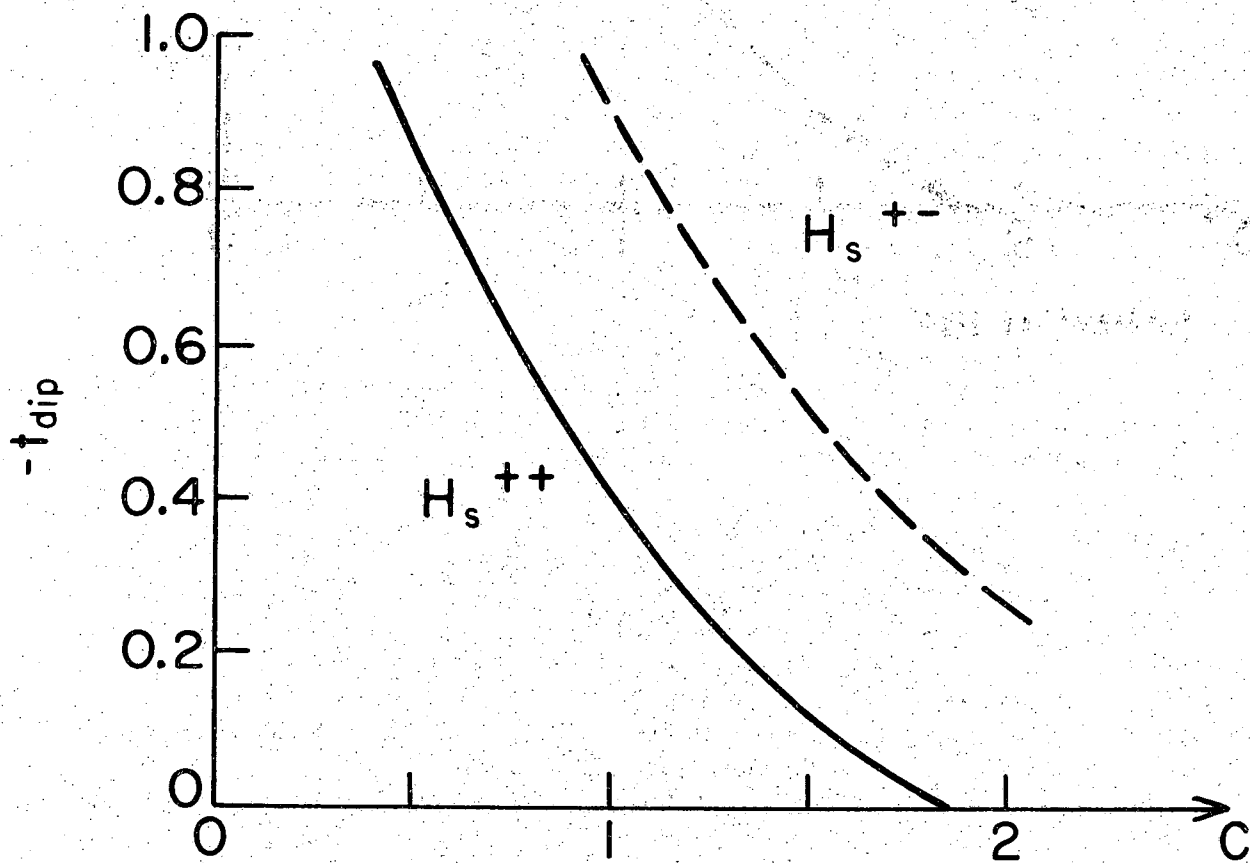
XBL707-3499

Fig. VI-4.



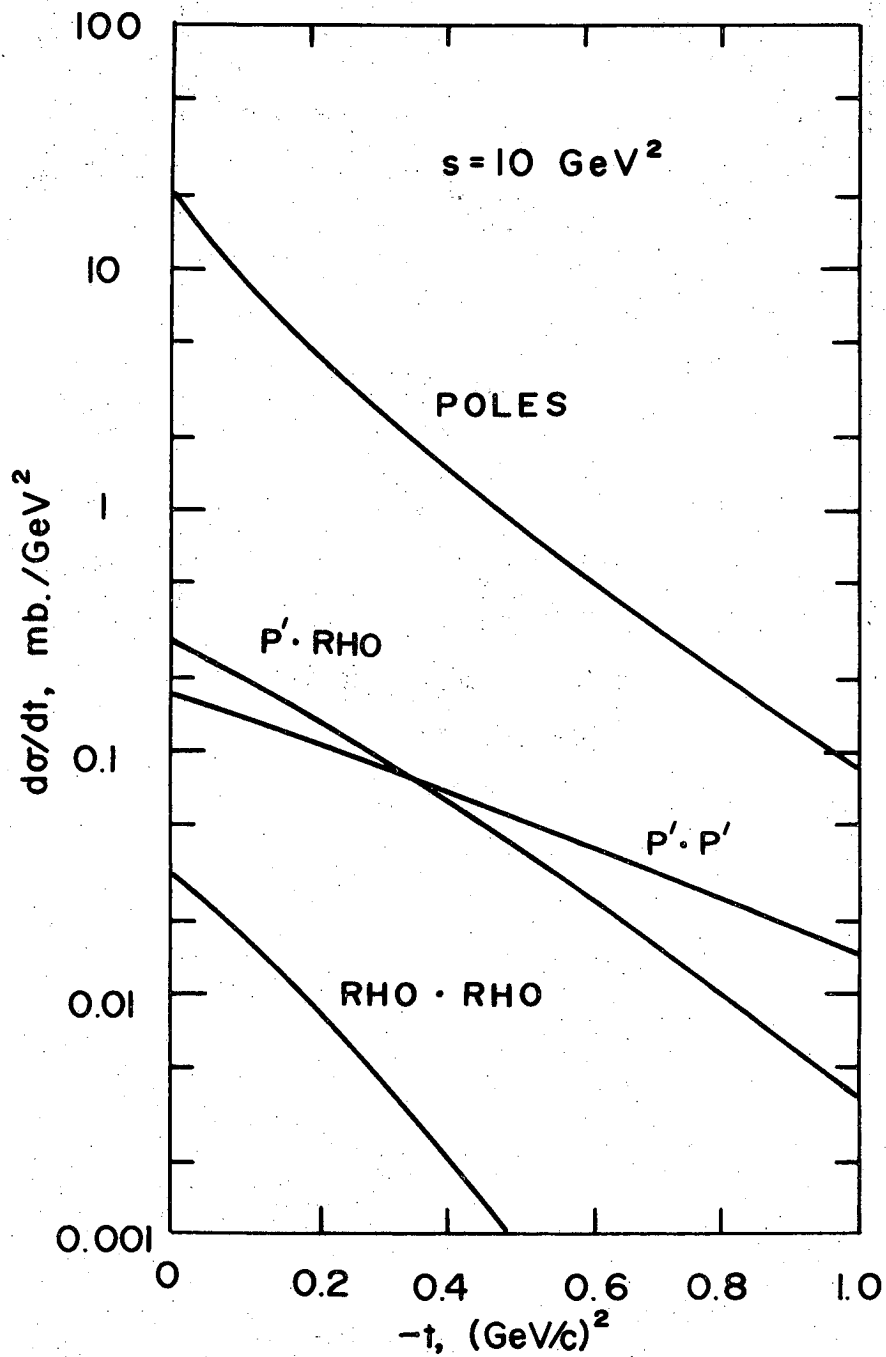
XBL707-3487

Fig. VI-5.



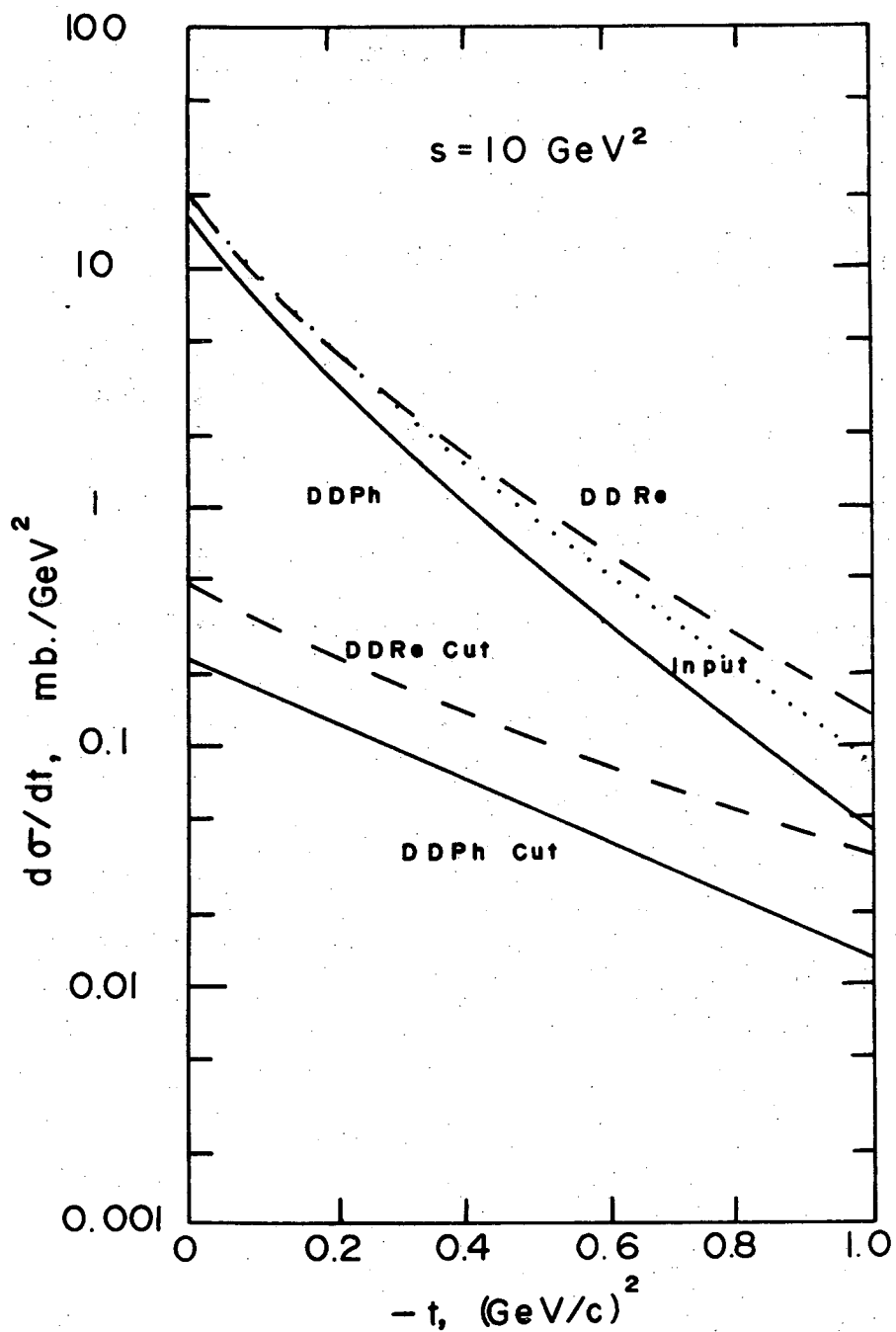
XBL707-3482

Fig. VI-6.



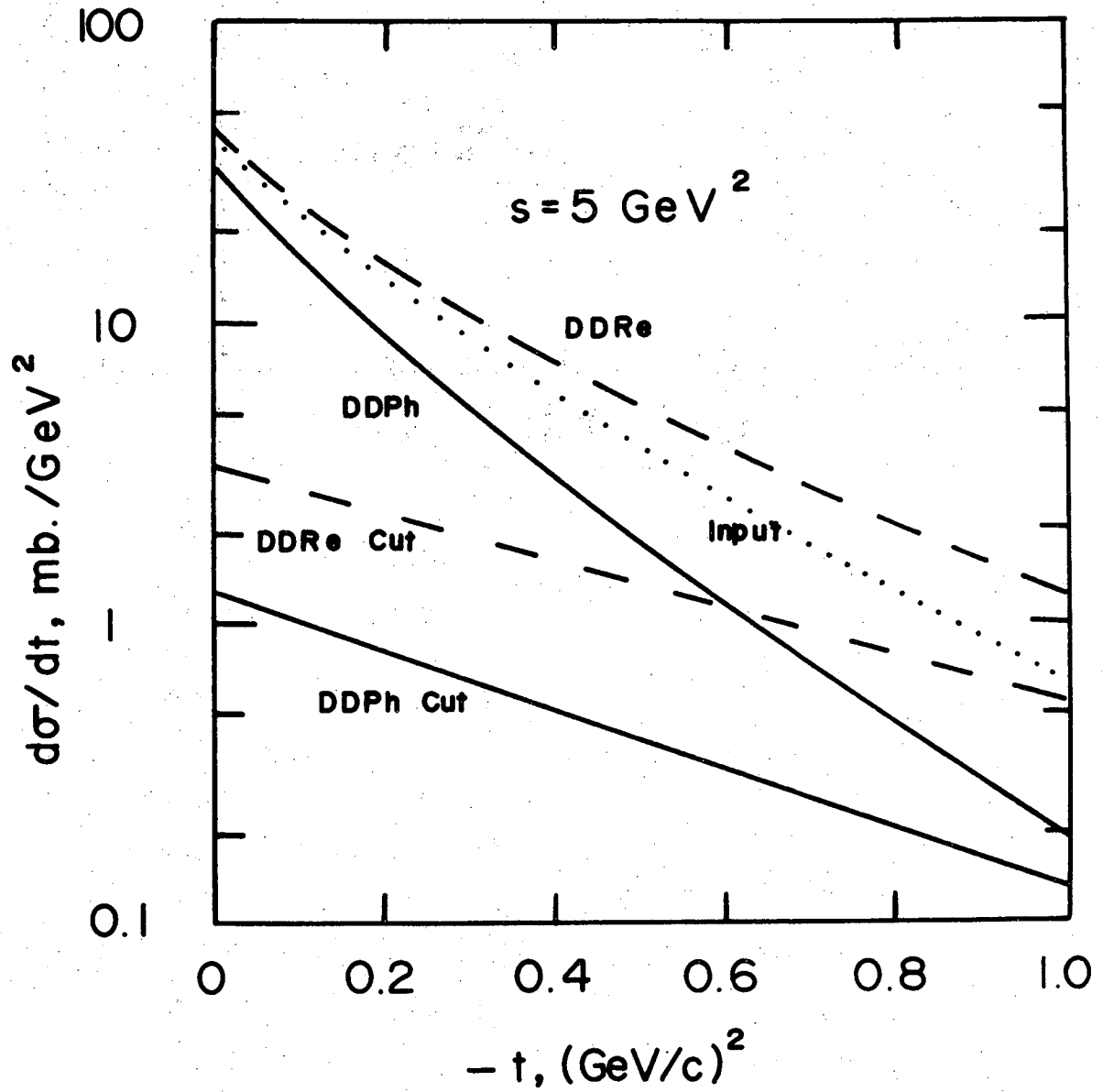
YBL 700-0461

Fig. VI-7.



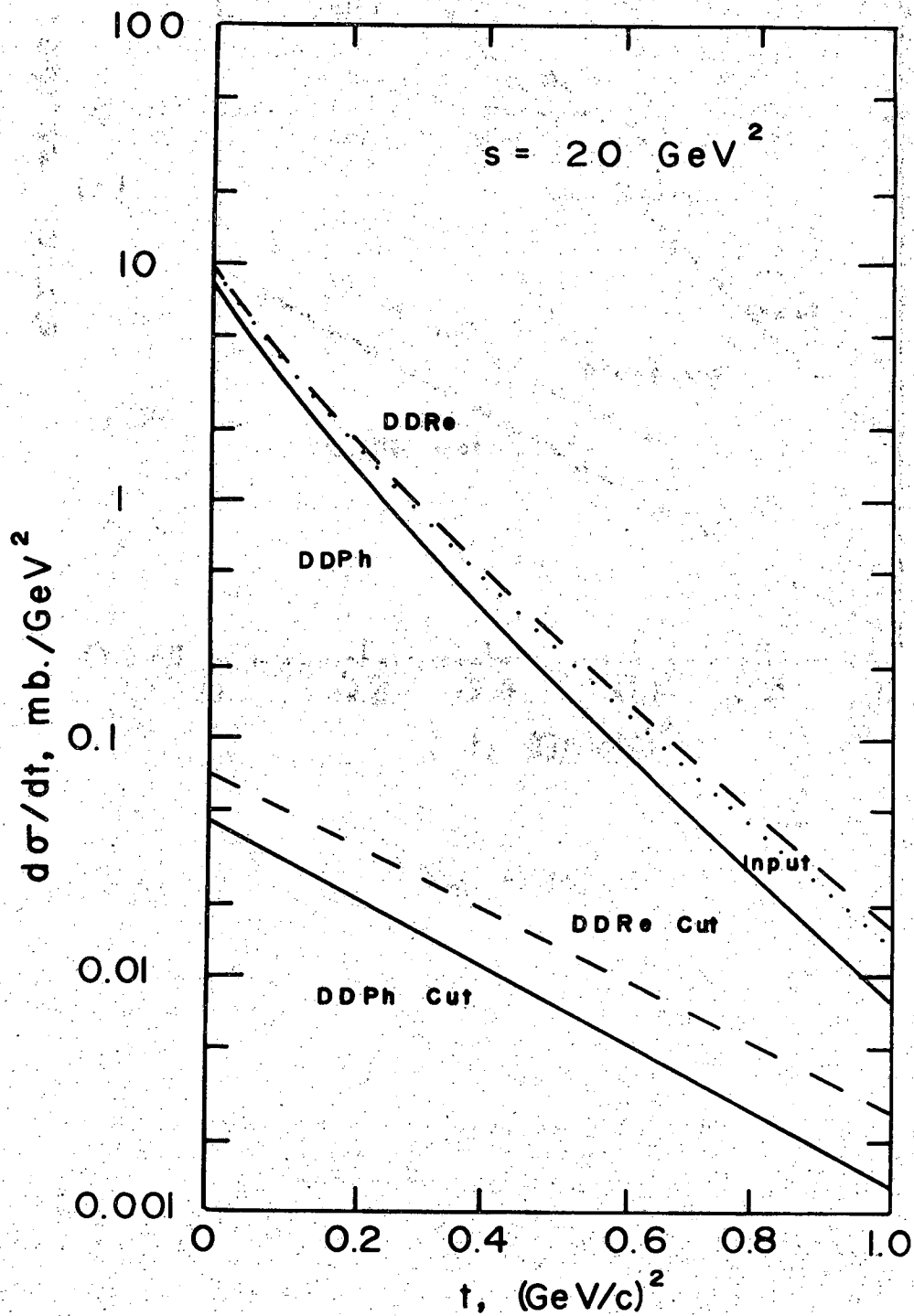
XBL 709-6460

Fig. VI-8.



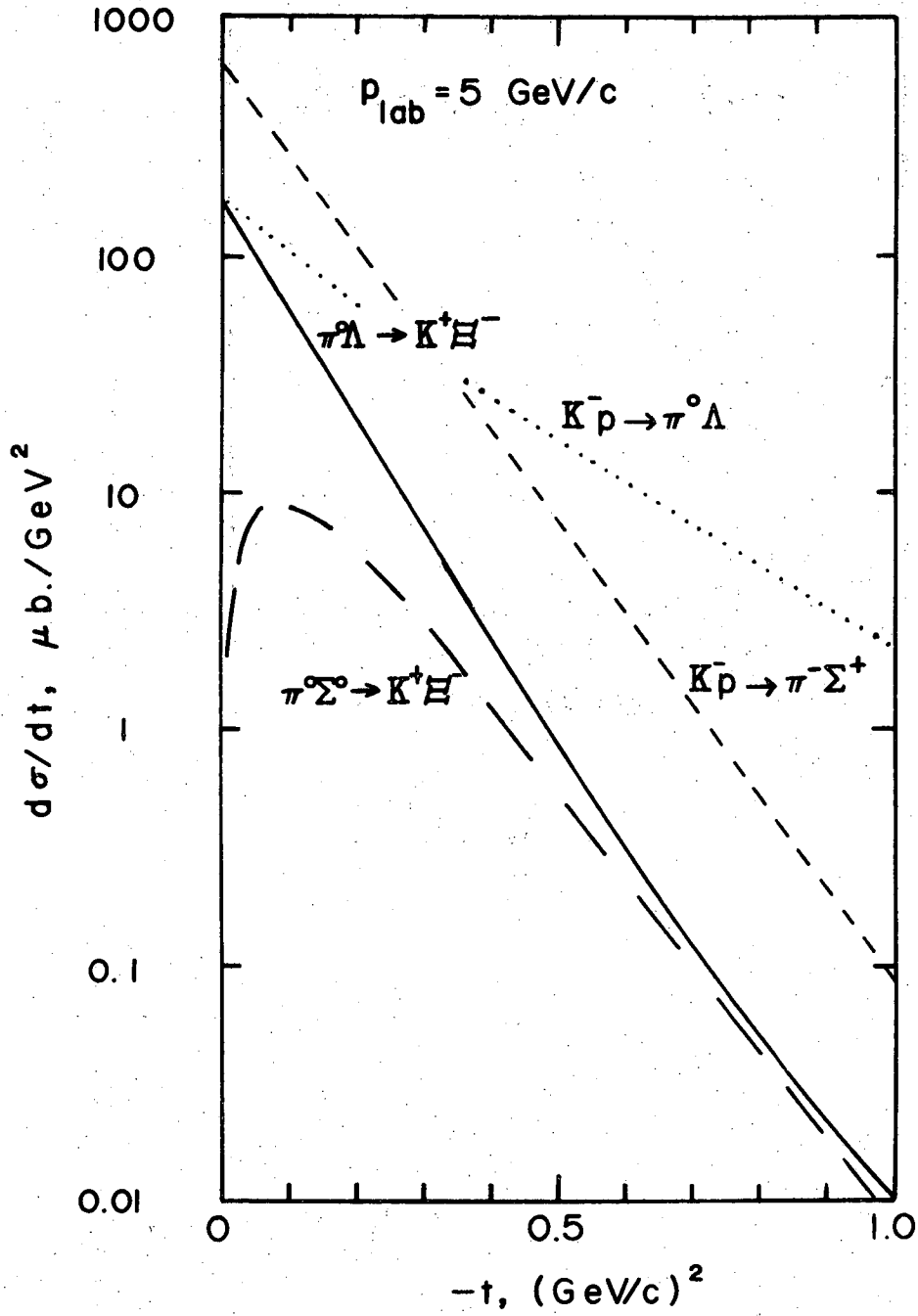
XBL 709-6459

Fig. VI-9.



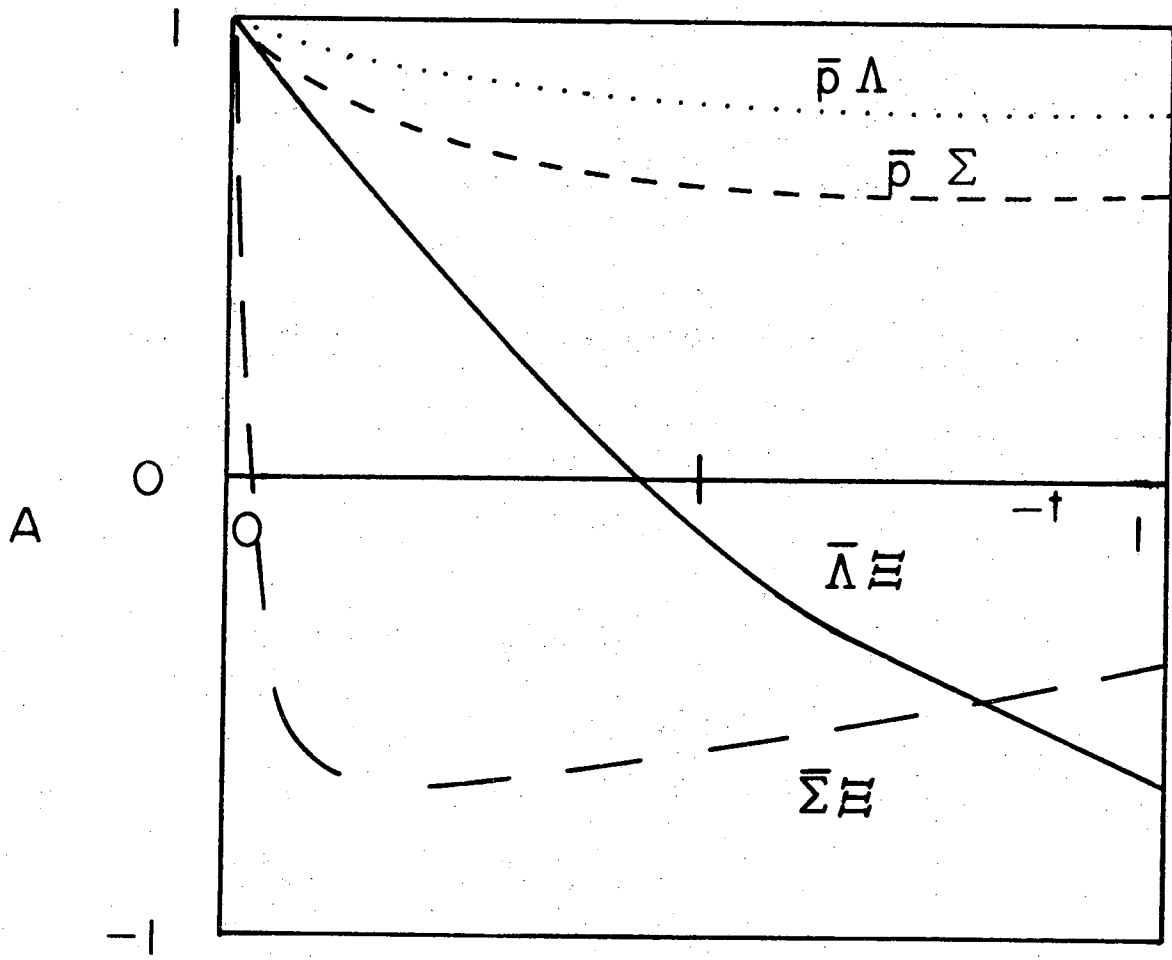
XBL 709-6458

Fig. VI-10.



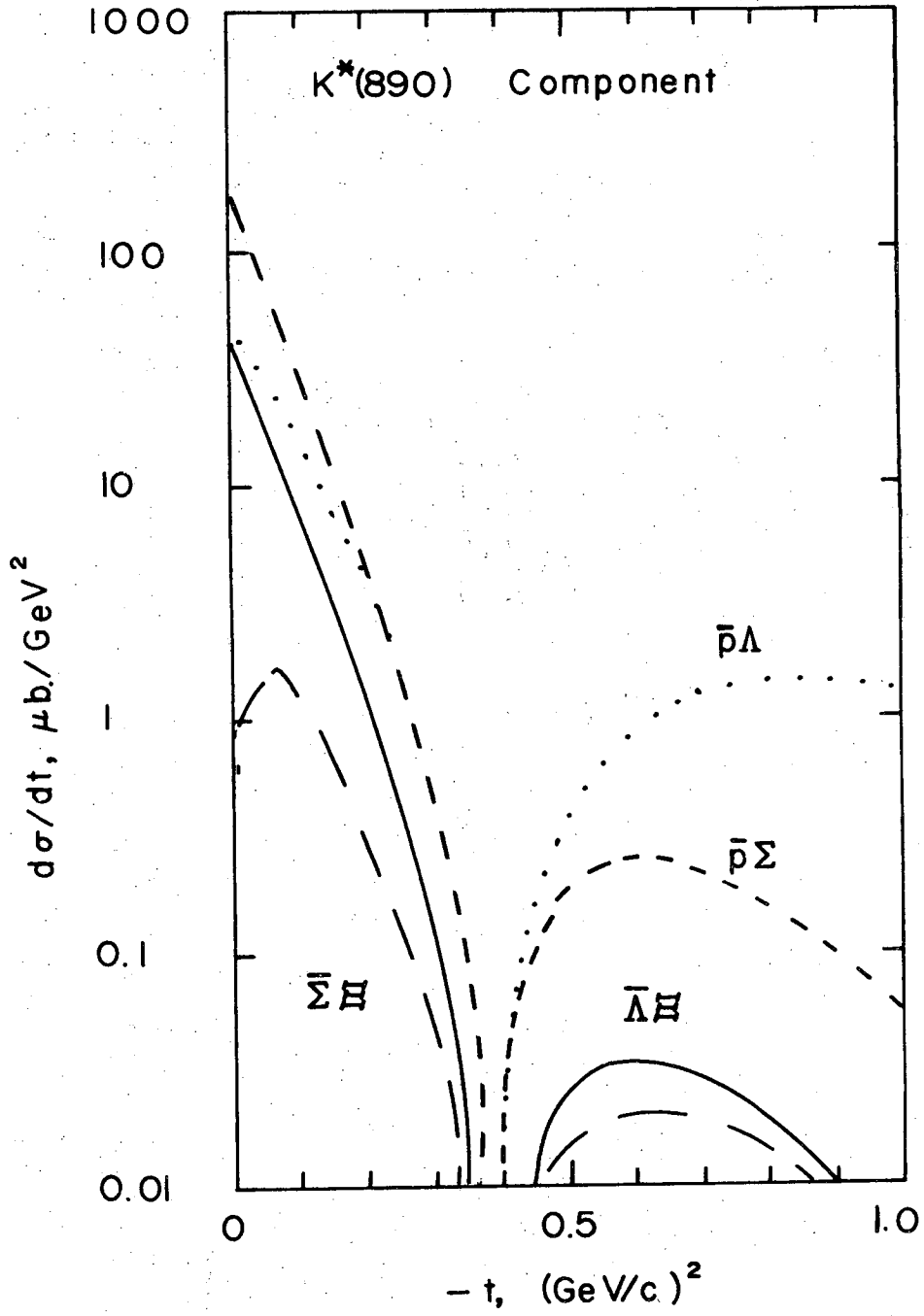
XBL 709-6466

Fig. VI-11.



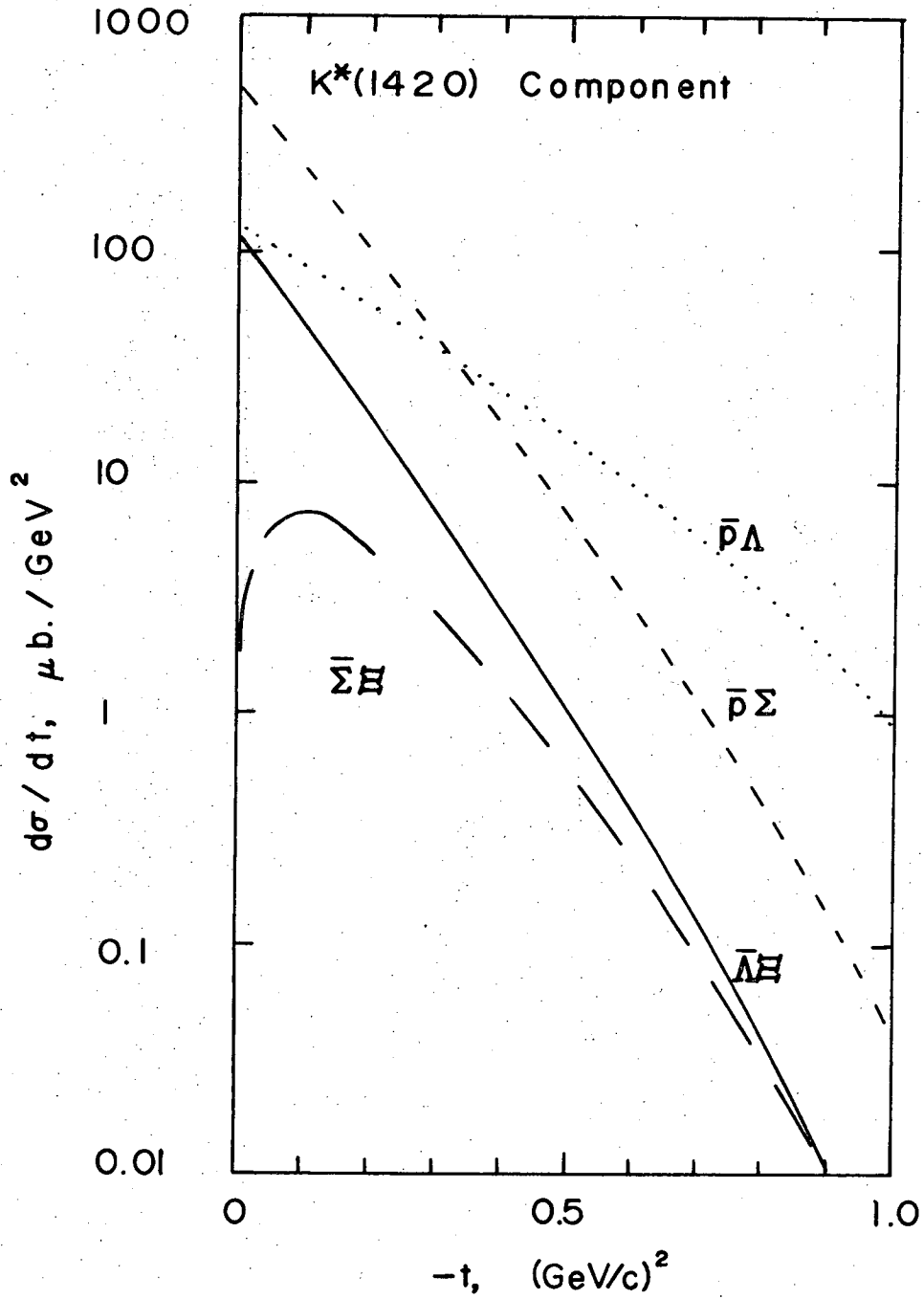
XBL 709-6467

Fig. VI-12.



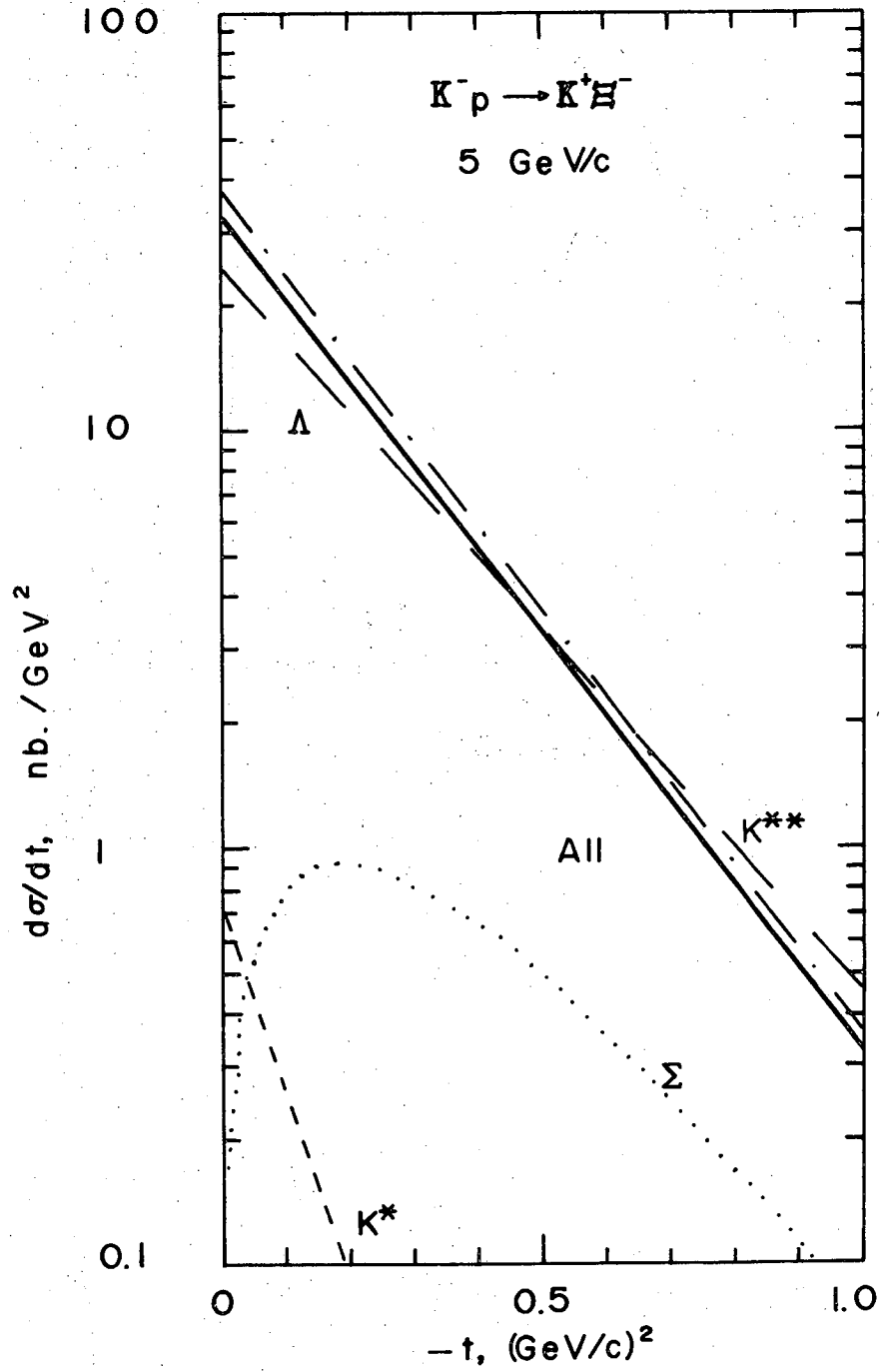
XBL 709-6468

Fig. VI-13.



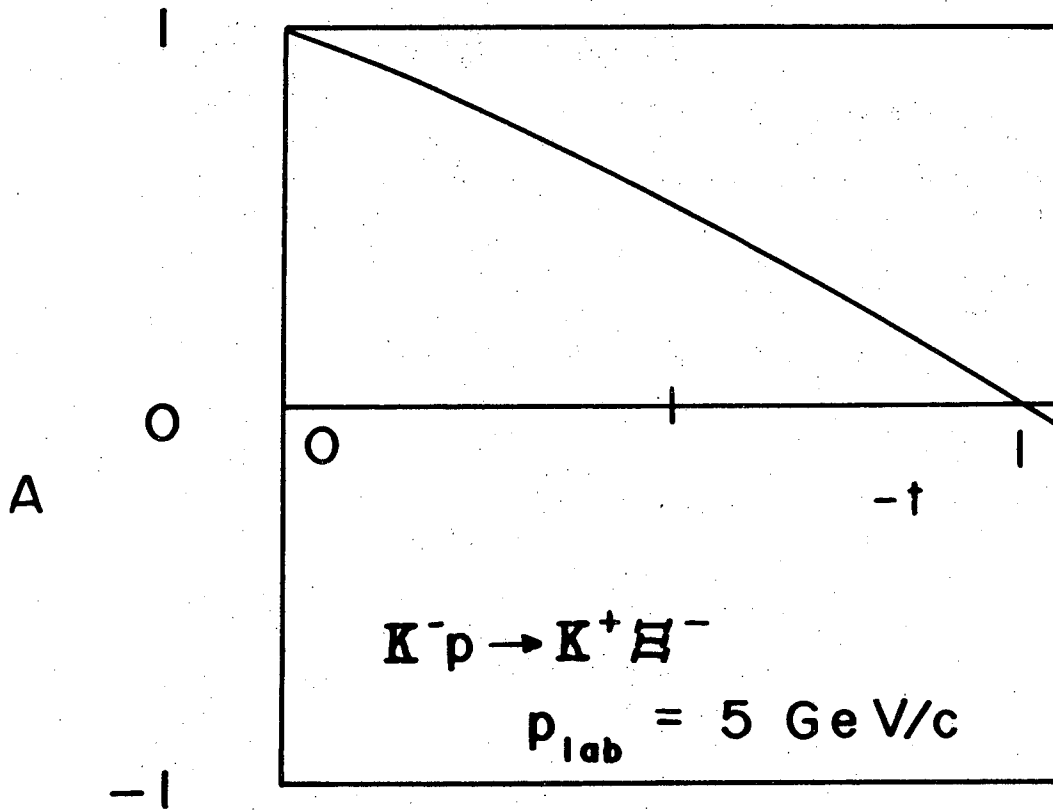
XBL 709-6469

Fig. VI-14.



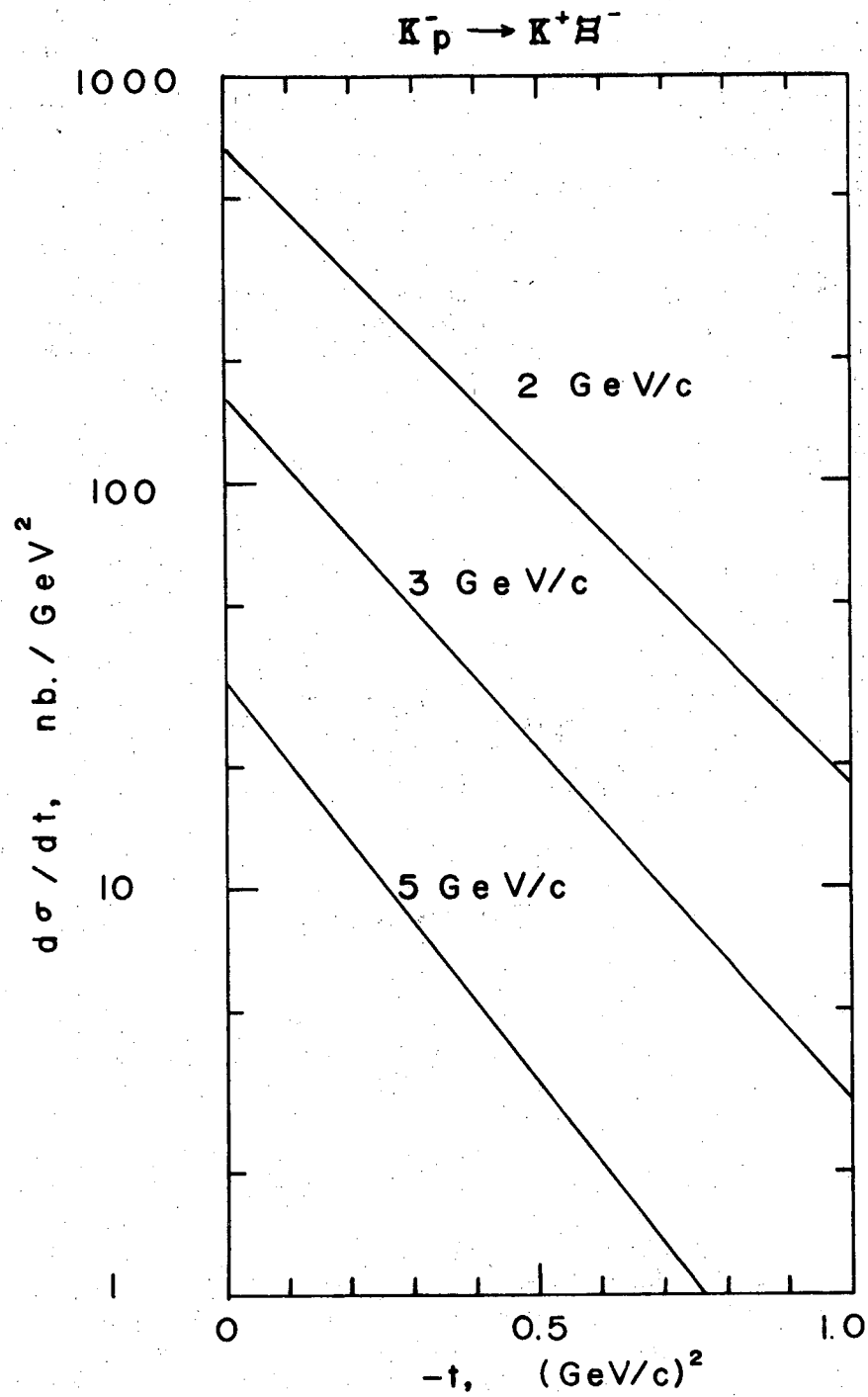
XBL 709-6470

Fig. VI-15.



XBL 709-6457

Fig. VI-16.



XBL 709-6471

Fig. VI-17.

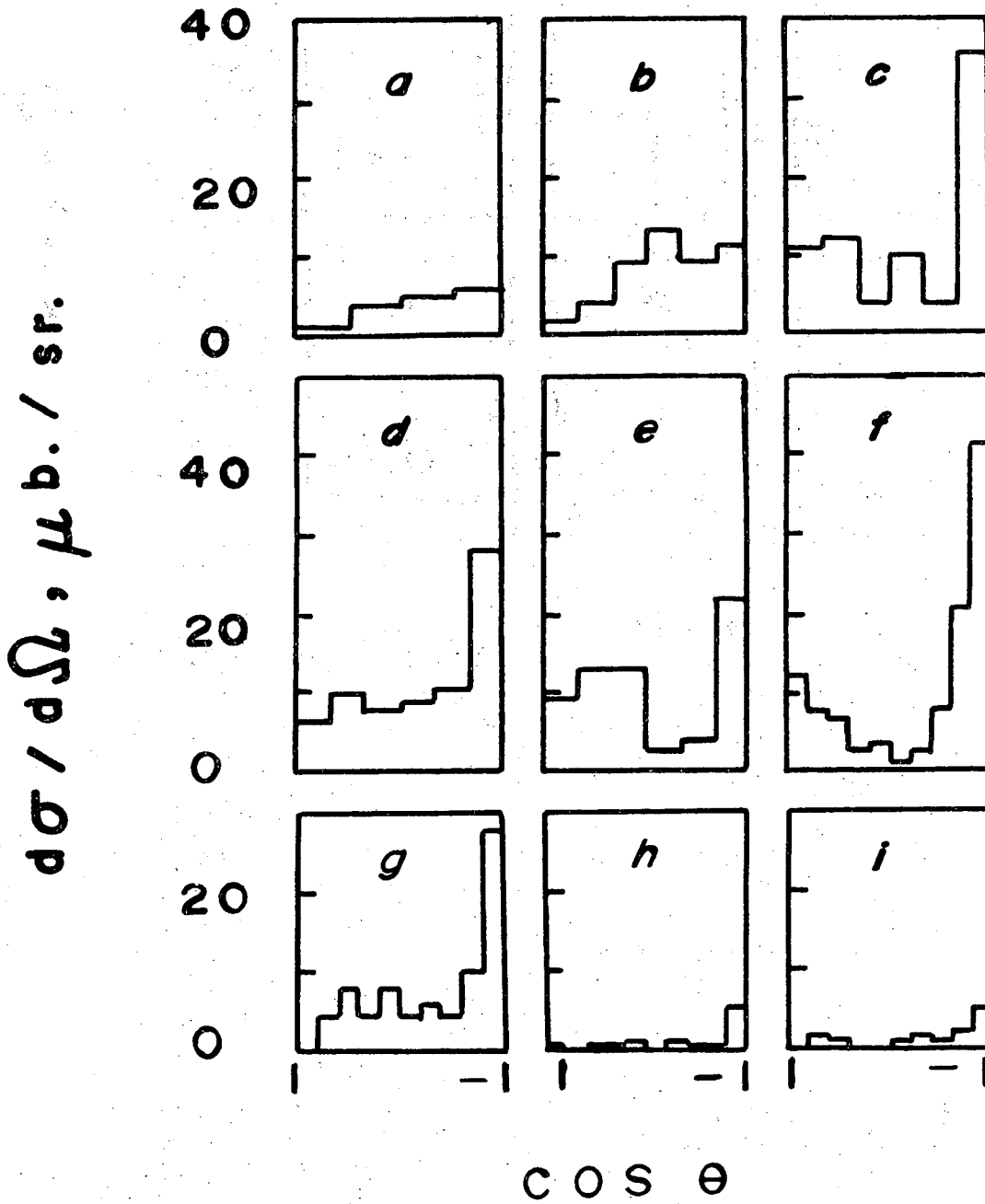
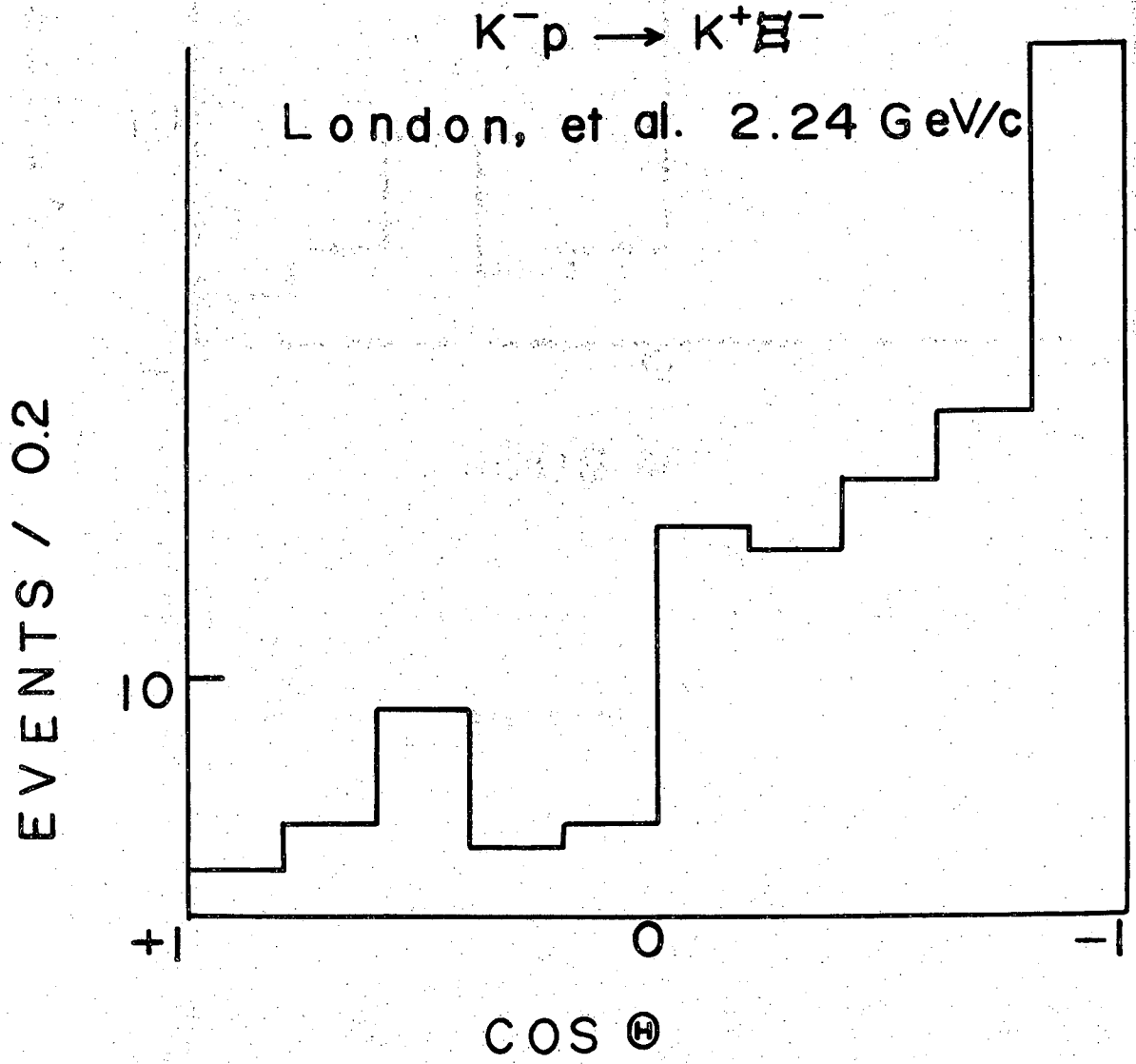


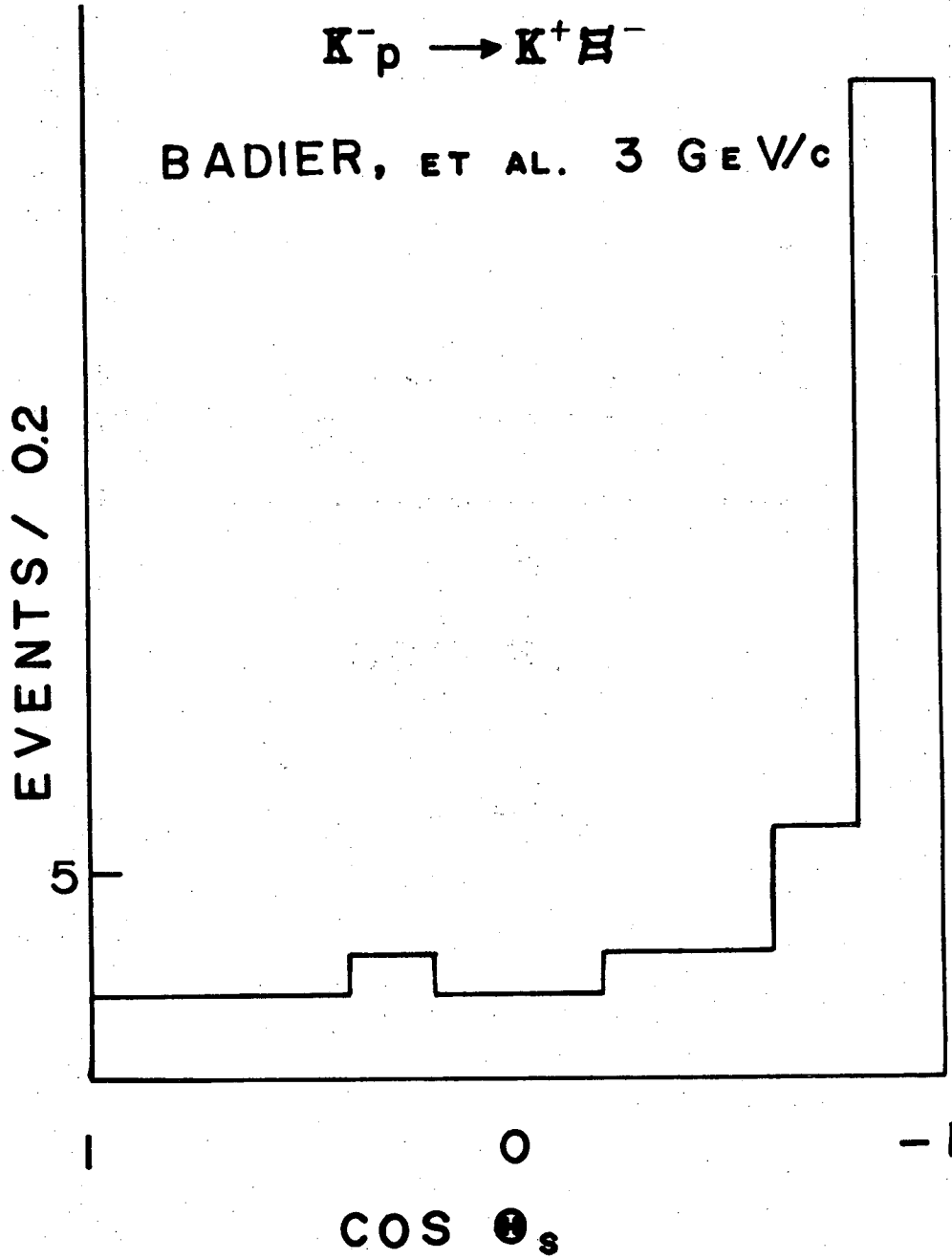
Fig. VI-18.

XBL 709-6465



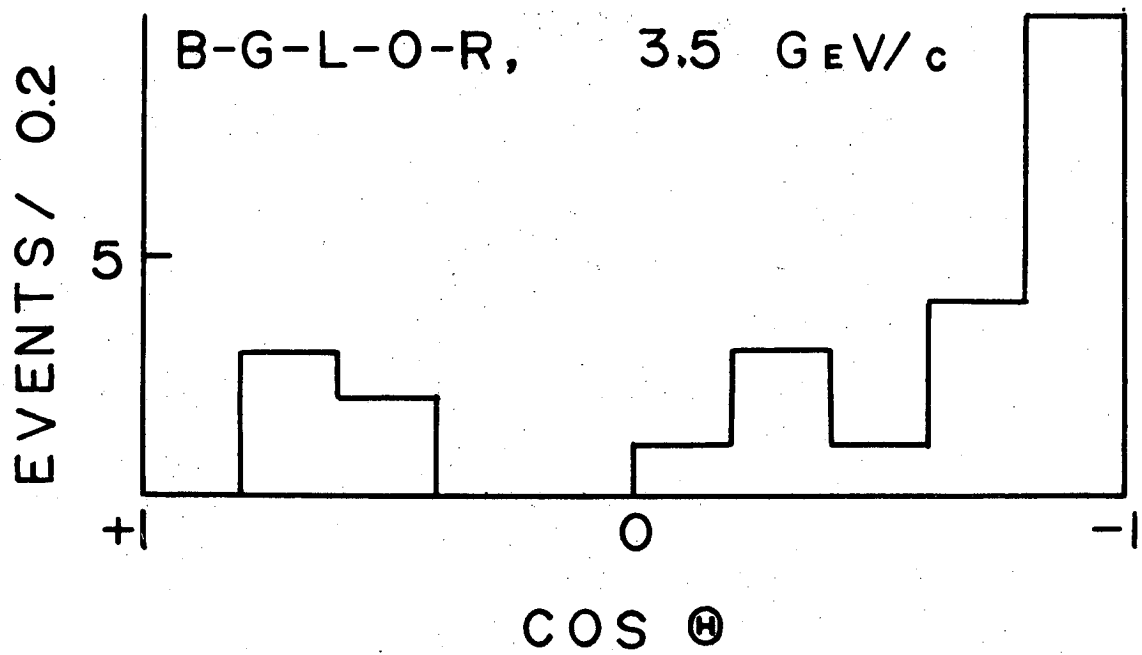
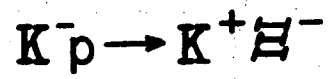
XBL 709-6464

Fig. VI-19.



XBL 709-6463

Fig. VI-20.



XBL 709-6462

Fig. VI-21.

## VII. SUMMARY AND CONCLUSION

The cause of rigorous derivations of Regge cut amplitudes certainly has not been advanced by this work. I have, however, tried to clarify some of the pitfalls one encounters in attempting to go from Feynman diagram calculations to realistic amplitudes for hadron-hadron scattering. Having gained some appreciation for the diagram approach, I formulated a phenomenological amplitude for the Regge cut arising from two-Reggeon exchange, which manifestly satisfies  $s$ - $u$  crossing. Some simple calculations were made more accessible by the recipe given for the Reggeization of  $s$ -channel helicity amplitudes. The model was formulated in terms of  $s$ -channel helicity partial-wave amplitudes, in order that detailed predictions for exotic exchange reactions might easily be made in the near future.

In the preceding chapter I reviewed the present state of affairs of Regge cuts vis à vis duality-breaking schemes. The various alternative schemes reflect an obvious need for more data. A model calculation exhibited some of the shortcomings of a theory in which exchange degeneracy is broken by Reggeon-Pomeranchuk cuts. The next step to be taken should be a quantitative study of the possibility that exchange degeneracy is broken by Reggeon-Reggeon cuts. This will require both theoretical effort to understand how to calculate cuts reliably and the accumulation of experimental data on line-reversed pairs of reactions as well. Obviously trajectories other than  $\rho$  and  $A_2$  should be the objects of study.

As an example of the exotic exchange reactions now becoming calculable, I presented predictions for the double hypercharge exchange reaction  $K^- p \rightarrow K^+ \Xi^-$ . The near-forward cross section was evaluated on the basis of a simple exchange degenerate Regge pole fit to the high-energy associated production data. There are a large number of analogous reactions which are amenable to analysis in terms of two Reggeon exchange graphs. If Regge cuts are dominant in exotic reactions, we should be able to confront cut models with experiments directly, and thereby learn about the nature of Regge cut amplitudes.

#### ACKNOWLEDGMENTS

I am grateful to Professor Robert Beringer, Professor Itzhak Kelson, and Professor Henry Margenau, who exhorted me as a callow undergraduate at Yale to pursue theoretical physics. My early discoveries of the fascination of physics were made in the company of Mssrs. George W. Cole and John G. Zornig, to whom I am indebted for comradeship and comic relief.

Professor Arthur H. Rosenfeld supplied helpful advice during my first year as a graduate student. In addition I thank him and Professor Gerson Goldhaber for their interest and for many discussions about experimental results.

My friends and collaborators, Dr. Edmond L. Berger, Dr. Geoffrey C. Fox, Professor Alfred S. Goldhaber, and Dr. Frank von Hippel, kindly shared with me their inestimable wisdom, enthusiasm, and perspective.

I express deep appreciation to Professor J. David Jackson for his patience and generosity during countless hours I spent learning by his side, and for incisive criticism and sound advice.

My wife, Elizabeth, has provided faith, hope, and love in abundant measure.

I am grateful to my parents for their encouragement.

I thank Professor Geoffrey F. Chew for his support at the Lawrence Radiation Laboratory, and for maintaining there a stimulating research environment.

I am indebted to the Woodrow Wilson National Fellowship Foundation for a Fellowship, to the University of California for a Science Fellowship, and to the United States Atomic Energy Commission

for a Research Assistantship which supported the work reported herein. Miss Georgella Perry and Mrs. Christina Graham, secretaries to the LRL Theoretical Group, contributed valuable support of a different nature.

Finally I thank the many others: teachers, fellow students, and colleagues, who have so often enlightened me.

APPENDIX A. DEFINITIONS AND CONVENTIONS

1. Kinematical Quantities

For two body to two body collisions, I order the particles as in Fig. A-1. The direct (s-) channel reaction is  $12 \rightarrow 34$ ; the crossed (t-) channel reaction is  $1\bar{3} \rightarrow \bar{2}4$ . The Mandelstam invariants are

$$\left. \begin{aligned} s &= -(p_1 + p_2)^2 = -(p_3 + p_4)^2 \\ t &= -(p_1 - p_3)^2 = -(p_2 - p_4)^2 \\ u &= -(p_1 - p_4)^2 = -(p_2 - p_3)^2 \end{aligned} \right\} \quad (\text{A.1.1})$$

where I specify a four-vector by  $v = (\underline{v}, v_0)$ , and  $v \cdot w = \underline{v} \cdot \underline{w} - v_0 w_0$ .

The Mandelstam variables satisfy

$$s + t + u = \sum_{i=1}^4 m_i^2 \equiv \Sigma. \quad (\text{A.1.2})$$

It is convenient to define threshold and pseudothreshold factors

$$\left. \begin{aligned} \phi_{ij}^{[x]} &= [x - (m_i + m_j)^2]^{\frac{1}{2}} \\ \psi_{ij}^{[x]} &= [x - (m_i - m_j)^2]^{\frac{1}{2}} \end{aligned} \right\} \quad (\text{A.1.3})$$

where (ij) specifies the incoming or outgoing pair of particles in the x-channel. For my choice of particle labels x,(ij) occur in the combinations  $x(ij) = s(12), s(34), t(13), t(24), u(14), u(23)$ . Now let

$\chi_{ij} = \phi_{ij}^{[x]} \psi_{ij}^{[x]}$  be a generic symbol for  $\phi_{ij}, \psi_{ij}, \chi_{ij}$ . The

energy of particle "i" in the x-channel center of mass (c.m.) system

is

$$\omega_i = (x + m_i^2 - m_j^2)/2x^{\frac{1}{2}}. \quad (\text{A.1.4})$$

The magnitude of the corresponding three-momentum is

$$p_{ij} = \chi_{ij}/2x^{\frac{1}{2}}. \quad (\text{A.1.5})$$

The Kibble function (Kibble, 1959)  $\Phi(s,t,u)$  is positive within the physical region, and vanishes on the boundary of the physical region.

$$\begin{aligned} \Phi(s,t,u) = & \text{stu} - s(m_1^2 m_2^2 + m_3^2 m_4^2) - t(m_1^2 m_3^2 + m_2^2 m_4^2) \\ & - u(m_1^2 m_4^2 + m_2^2 m_3^2) + 2m_1^2 m_2^2 m_3^2 m_4^2 \left( \sum_{i=1}^4 m_i^{-2} \right). \end{aligned} \quad (\text{A.1.6})$$

It is also related to the x-channel c.m. scattering angle by

$$\sin^2 \theta_x = 4x \Phi(s,t,u) / [\chi_{ij} \chi_{i+j}]^2. \quad (\text{A.1.7})$$

The c.m. scattering angle is given more compactly by

$$\begin{aligned} s_{12} s_{34} \cos \theta_s &= s(t - u) + (m_1^2 - m_2^2)(m_3^2 - m_4^2), \\ t_{12} t_{34} \cos \theta_t &= t(s - u) + (m_1^2 - m_3^2)(m_2^2 - m_4^2). \end{aligned} \quad (\text{A.1.8})$$

For the reaction  $ab \rightarrow cd$  I choose the positive z-axis along  $\hat{p}_a$ , and the positive y-axis along  $\hat{p}_a \times \hat{p}_c$  (in conformity with the Basel convention). Thus the reaction takes place in the x-z plane. The coordinate system is illustrated in Fig. A-2.

## 2. Single Particle States

Following Jacob and Wick (1959) and Wick (1962) let  $|p^0; \lambda\rangle$  be an invariantly normed state with four-momentum  $p^0 = (0, m)$  and spin component  $\lambda$  along the z-direction.\* (I suppress a label for the total spin, s.) These rest states are assumed to transform in the usual way† under rotations r:

$$R|p^0; \lambda\rangle = \sum_{\mu} \mathcal{D}_{\mu\lambda}^s(r) |p^0; \mu\rangle. \quad (\text{A.2.1})$$

Now define

$$|p; \lambda\rangle = R_{\phi, \theta, -\phi} Z |p^0; \lambda\rangle \quad (\text{A.2.2})$$

---

\* By invariant normalization I mean  $\langle p'; \lambda' | p; \lambda \rangle = (2\pi)^3 \delta_{\lambda', \lambda} \tilde{\delta}(p', p)$  where  $\delta_{\lambda', \lambda}$  is a Kronecker delta and  $\tilde{\delta}(p, p') = 2(p^2 + m^2)^{\frac{1}{2}} \delta^{(3)}(\underline{p} - \underline{p}')$  is the invariant  $\delta$ -function on the mass shell. This corresponds to using the invariant volume element on the mass shell,  $\tilde{d}p = [2(p^2 + m^2)^{\frac{1}{2}}]^{-1} d^3\underline{p} = \delta^+(p^2 + m^2) d^4p$ , in place of the normal volume element.

† I specify a rotation by the Euler angles  $(\alpha\beta\gamma)$ ; thus  $R_{\alpha\beta\gamma} = e^{-i\alpha J_z} e^{-i\beta J_y} e^{-i\gamma J_z}$ . This follows the convention of Brink and Satchler (1968), Rose (1957), and Messiah (1960) that  $\mathcal{D}(\alpha\beta\gamma)$  rotates the system through Euler angles  $(\alpha\beta\gamma)$ . Others (e.g. Wigner, 1959, and Edmonds, 1957) use the opposite convention, that  $\mathcal{D}(\alpha\beta\gamma)$  rotates the system through angles  $(-\alpha, -\beta, -\gamma)$ . Explicit representations of rotation matrices are given in Appendix B.

for  $\{0 < \theta < \pi; -\pi < \phi < \pi\}$ , where  $Z$  is a "boost" in the  $z$ -direction, which imparts to the particle the desired momentum. The rotation  $R$  takes care of the direction. The helicity  $\lambda$  is the projection of spin on the direction of motion.

Let us now use  $h(p)$  to denote the Lorentz transformation (A.2.2) and  $H(p)$  to indicate the corresponding operator,

$$H(p) = R_{\phi, \theta, -\phi} Z, \quad (\text{A.2.3})$$

which generates the state of four-momentum  $p$ . The particular form (A.2.3) is the Jacob-Wick helicity convention, but I will note some other possibilities below. Now apply  $\ell[L]$ , an arbitrary Lorentz transformation such that  $\ell p = p'$ . The resulting state will be  $|p'; \lambda\rangle = H(p')|p^0; \lambda\rangle$ . Furthermore,  $\ell p \equiv \ell h(p)p^0 = p' = h(p')p^0$ , so that  $h^{-1}(p') \ell h(p)p^0 = p^0$ . In other words, the transformation  $h^{-1}(p') \ell h(p)$  is an element of the little group (isotropy group) of  $p^0$ , and is therefore a rotation  $r$ . Thus

$$\left. \begin{aligned} L|p; \lambda\rangle &= LH(p)|p^0; \lambda\rangle = H(p')R|p^0; \lambda\rangle = \\ &= H(p') \sum_{\mu} \mathcal{D}_{\mu\lambda}^s(r) |p^0; \mu\rangle = \sum_{\mu} U_{\mu\lambda}(\ell, p) |p'; \mu\rangle, \end{aligned} \right\} \quad (\text{A.2.4})$$

where  $U(\ell, p) = \mathcal{D}^s(r) = \mathcal{D}^s(h^{-1}(p') \ell h(p))$ . (This shows that  $U$  is unitary.) Consequently the transformation law for helicity states is

$$L|p; \lambda\rangle = \sum_{\mu} \mathcal{D}_{\mu\lambda}^s(h^{-1}(\ell p) \ell h(p)) |p'; \mu\rangle. \quad (\text{A.2.5})$$

Among the other kinds of single particle states which can be defined by their transformation properties I mention in particular Wigner spin states (Wigner, 1939, 1957; Blatt and Biedenharn, 1952), for which the projection of spin on the z-axis is specified:

$$L|p, m\rangle = \sum_{m'} \mathcal{D}_{m', m}^s(b^{-1}(\ell p) \ell b(p)) | \ell p; m' \rangle, \quad (\text{A.2.6})$$

where  $b(p)$  is a pure boost along the direction  $p$ . I also define transversity states (Kotanski, 1966a,b), for which the projection of spin on the negative normal to the reaction plane is specified:

$$L|p, \tau\rangle = \sum_{\tau'} \mathcal{D}_{\tau', \tau}^s \left[ R_{\frac{\pi}{2}, \frac{\pi}{2}, \frac{\pi}{2}} h^{-1}(\ell p) \ell h(p) \left( R_{\frac{\pi}{2}, \frac{\pi}{2}, \frac{\pi}{2}} \right)^{-1} \right] | \ell p, \tau' \rangle. \quad (\text{A.2.7})$$

Figure A-3 shows the axes of quantization for these three kinds of states.

Lastly I mention spinor states (Joos, 1962), which are defined by extending the operator  $\mathcal{D}$  to be a representation of the homogeneous Lorentz group, instead of the rotation group as before. Spinor states transform as

$$L|p; a\rangle = \sum_b \mathcal{D}_{ba}^s[\ell] | \ell p; b \rangle. \quad (\text{A.2.8})$$

### 3. Scattering Amplitudes\*

The S-matrix element connecting an initial state  $a$  of total four-momentum  $p_a$  with a final state  $b$  of total four-momentum  $p_b$  is related to the scattering amplitude  $T_{ba}$  by

$$S_{ba} = \delta_{ba} + i(2\pi)^4 \delta^{(4)}(p_b - p_a) T_{ba}. \quad (\text{A.3.1})$$

The transition probability per unit time is given by

$$P_{ba} = (2\pi)^4 \delta^{(4)}(p_b - p_a) |T_{ba}|^2. \quad (\text{A.3.2})$$

It is straightforward to derive the following useful relations between the scattering amplitude and observables.

(i) General decay process  $\alpha \rightarrow (1, 2, \dots, n) \equiv \beta$ . The decay rate is

$$dW_{\beta\alpha} = \frac{(2\pi)^4 \delta^{(4)}(p_\beta - p_\alpha)}{2\omega_\alpha} |T_{\beta\alpha}|^2 \prod_{i=1}^n \frac{\tilde{d}p_i}{(2\pi)^3}. \quad (\text{A.3.3})$$

(ii) Two body decay  $\alpha \rightarrow (1, 2) \equiv \beta$ .

$$dW_{\beta\alpha} = \frac{1}{64\pi^2} |T_{\beta\alpha}|^2 \frac{d\Omega}{m_\alpha^3} d\Omega_{\text{c.m.}}. \quad (\text{A.3.4})$$

(iii) General two body collision cross section

$\alpha \equiv (1, 2) \rightarrow (3, 4, \dots, n) \equiv \beta$

$$d\sigma = \frac{(2\pi)^4}{2s^{1/2}} \delta^{(4)}(p_\beta - p_\alpha) |T_{\beta\alpha}|^2 \prod_{i=3}^n \frac{\tilde{d}p_i}{(2\pi)^3}. \quad (\text{A.3.5})$$

\* See Collins and Squires (1968), and Taylor (1965).

(iv) Two body to two body cross section  $\alpha \equiv (1,2) \rightarrow (3,4) \equiv \beta$

$$\frac{d\sigma}{d\Omega_{c.m.}} = \frac{\mathcal{S}_{34}}{64\pi^2 s \mathcal{S}_{12}} |T_{\beta\alpha}|^2. \quad (\text{A.3.6})$$

Since

$$d\Omega_{c.m.} = \frac{2sdt}{\mathcal{S}_{12} \mathcal{S}_{34}} d\phi, \quad (\text{A.3.7})$$

$$\frac{d\sigma}{dt} = \frac{1}{16\pi \mathcal{S}_{12}^2} |T_{\beta\alpha}|^2. \quad (\text{A.3.8})$$

The unitarity of the S-matrix implies

$$(SS^\dagger)_{ba} = \sum_c S_{bc} S_{ca}^\dagger = \delta_{ba}. \quad (\text{A.3.9})$$

Substituting (A.3.1) we find

$$i[T_{ba} - T_{ba}^*] = -(2\pi)^4 \sum_c \delta^{(4)}(p_a - p_c) T_{bc} T_{ac}^*, \quad (\text{A.3.10})$$

where the channels  $a$  and  $b$  now satisfy the four-momentum conservation relation,  $p_b = p_a$ , and  $\sum_c$  means integration over  $\tilde{dp}/(2\pi)^3$  for each particle in channel  $c$  and summation over all channels  $c$ . If channels  $a$  and  $b$  are the same, Eqs. (A.3.5) and (A.3.10) give the optical theorem relation between total cross section and imaginary part of the forward scattering amplitude,

$$\sigma_{\text{total}}(a \rightarrow \text{all}) = \frac{1}{\mathcal{J}_{12}} \text{Im}[T_{aa}(s, t=0)]. \quad (\text{A.3.11})$$

With  $T_{aa} = 8\pi s^{\frac{1}{2}} f_{\text{c.m.}}(0^\circ)$ , Eq. (A.3.11) takes a more familiar form

$$\frac{4\pi}{p_{\text{c.m.}}} \text{Im}[f_{\text{c.m.}}(0^\circ)] = \sigma_{\text{total}}, \quad (\text{A.3.12})$$

where  $p_{\text{c.m.}}$  is the initial c.m. momentum and  $f_{\text{c.m.}}(0^\circ)$  is the forward spin nonflip scattering amplitude. [Thus  $f_{\text{c.m.}}$  corresponds to the normalization adopted by Jacob and Wick (1959) in which  $d\sigma/d\Omega_{\text{c.m.}} = |f(\theta)|^2$ .]

Different kinds of amplitudes may be obtained by taking matrix elements of  $T$  between the several kinds of states described in Sec. A.2. The most useful amplitudes are helicity amplitudes. For these it is customary to insert an additional phase factor  $(-1)^{s_2+s_4-(\lambda_2+\lambda_4)}$  so that, for example,

$$H_s^{\lambda_3\lambda_4; \lambda_1\lambda_2} = (-1)^{s_2+s_4-(\lambda_2+\lambda_4)} \langle \lambda_3\lambda_4 | T | \lambda_1\lambda_2 \rangle \quad (\text{A.3.13})$$

defines the s-channel helicity amplitude. With the normalization exhibited in Eq. (A.3.6), the differential cross section averaged over initial helicities and summed over final helicities is given by

$$\frac{d\sigma}{d\Omega_{\text{c.m.}}} = \frac{1}{64\pi^2 s} \cdot \frac{\mathcal{J}_{34}}{\mathcal{J}_{12}} \cdot \frac{1}{(2s_1+1)(2s_2+1)} \times \sum_{\lambda_1\lambda_2\lambda_3\lambda_4} \left| H_s^{\lambda_3\lambda_4; \lambda_1\lambda_2} \right|^2, \quad (\text{A.3.14})$$

where  $s_i$  is the spin of particle  $i$ . A minor subtlety arises here, namely that the number of helicity states of a massless particle is only 2, not  $2s + 1$ . For a massless particle incident an obvious modification of the statistical factor is therefore required.

The helicity partial wave expansion can be written in the form

$$H_s^{\lambda_3\lambda_4:\lambda_1\lambda_2}(s,t) = \sum_{J=m}^{\infty} (J + \frac{1}{2}) \langle \lambda_3\lambda_4 | h_s^J(s) | \lambda_1\lambda_2 \rangle d_{\lambda\mu}^J(\theta_s) e^{i(\lambda-\mu)\phi}, \quad (\text{A.3.15})$$

where  $\lambda = \lambda_1 - \lambda_2$ ,  $\mu = \lambda_3 - \lambda_4$ , and  $m = \text{Max}(|\lambda|, |\mu|)$ . The properties of the rotation matrix  $d^J$  are reviewed in Appendix B. Hereafter I choose  $\phi = 0$ ; this reflects my convention for the reaction plane. The orthogonality property of  $d^J$  [cf. Eq. (B.1.8)] permits the inversion of (A.3.15) for  $J \geq m$ :

$$\langle \lambda_3\lambda_4 | h_s^J(s) | \lambda_1\lambda_2 \rangle = \int_{-1}^1 d(\cos \theta_s) H_s^{\lambda_3\lambda_4:\lambda_1\lambda_2}(s, \cos \theta_s) d_{\lambda\mu}^J(\theta_s). \quad (\text{A.3.16})$$

Relations among the helicity amplitudes may be obtained from the discrete symmetries. From parity we find

$$\left. \begin{aligned} \langle -\lambda_3, -\lambda_4 | h_s^J(s) | -\lambda_1, -\lambda_2 \rangle &= \eta_g \langle \lambda_3\lambda_4 | h_s^J(s) | \lambda_1\lambda_2 \rangle, \\ \eta_g &= (\eta_3\eta_4/\eta_1\eta_2)(-1)^{s_3+s_4-(s_1+s_2)}, \end{aligned} \right\} (\text{A.3.17})$$

with  $\eta_i$  the intrinsic parity of the  $i$ th particle. Translated into a condition on the helicity amplitudes themselves, this is

$$\left. \begin{aligned}
 H_s^{-\lambda_3, -\lambda_4; -\lambda_1, -\lambda_2}(\theta_s, \phi) &= \eta_g H_s^{\lambda_3 \lambda_4; \lambda_1 \lambda_2}(\theta_s, \pi - \phi) \\
 &= \eta_g (-1)^{\lambda - \mu} H_s^{\lambda_3 \lambda_4; \lambda_1 \lambda_2}(\theta_s, -\phi) .
 \end{aligned} \right\} \quad (A.3.18)$$

From time reversal we obtain

$$\langle \lambda_1 \lambda_2 | h_s^J(s) | \lambda_3 \lambda_4 \rangle = \langle \lambda_3 \lambda_4 | h_s^J(s) | \lambda_1 \lambda_2 \rangle, \quad (A.3.19)$$

whence

$$H_s^{\lambda_1 \lambda_2; \lambda_3 \lambda_4} = (-1)^{\lambda - \mu} H_s^{\lambda_3 \lambda_4; \lambda_1 \lambda_2}. \quad (A.3.20)$$

To close this section I briefly note the relations between helicity amplitudes and some other amplitudes.

(i) Wigner amplitudes. With particle 1 (2) along the plus (minus) z-axis, the relation to helicity amplitudes is

$$W_{s[1,2]}^{\mu_3 \mu_4; \mu_1 \mu_2} = d_{\mu_4, -\lambda_4}^{s_4}(\theta_s) d_{\mu_3, \lambda_3}^{s_3}(\theta_s) H_s^{\lambda_4 \lambda_3; \mu_1, -\mu_2}. \quad (A.3.21)$$

The Wigner (spin) amplitudes are usually expanded in terms of angular momentum states (Blatt and Biedenharn, 1952) as

$$\begin{aligned}
 W_{s[1,2]}^{\mu_3 \mu_4; \mu_1 \mu_2} &= \sum_{\substack{s_i, s_f \\ (\mu_i, \mu_f)}} \langle s_1 s_2 \mu_1 \mu_2 | s_i \mu_i \rangle \langle s_3 s_4 \mu_3 \mu_4 | s_f \mu_f \rangle \\
 &\times \sum_{l_i, l_f, J} (2l_i + 1)^{\frac{1}{2}} (2l_f + 1)^{\frac{1}{2}} \langle l_f s_f \mu_i - \mu_f, \mu_f | J \mu_i \rangle \langle l_i s_i 0 \mu_i | J \mu_i \rangle \\
 &\times T[J, l_i, s_i, l_f, s_f] d_{\mu_i - \mu_f, 0}^{l_f}(\theta_s). \quad (A.3.22)
 \end{aligned}$$

The versatility of the helicity amplitudes invented by Jacob and Wick (1959) has rendered these amplitudes somewhat archaic.

(ii) Transversity amplitudes. These amplitudes, introduced by Kotanski (1966a,b) are occasionally useful in the study of kinematic constraints at thresholds and pseudothresholds. They are related to the helicity amplitudes by

$$\begin{aligned}
 K_s^{\tau_3 \tau_4 : \tau_1 \tau_2} &= D_{\tau_3 \lambda_3}^{s_3} \left( \frac{\pi}{2}, \frac{\pi}{2}, \frac{\pi}{2} \right) D_{\tau_4, -\lambda_4}^{s_4} \left( \frac{\pi}{2}, \frac{\pi}{2}, \frac{\pi}{2} \right) \\
 &\times H_s^{\lambda_3 \lambda_4 : \lambda_1 \lambda_2} D_{\lambda_1 \tau_1}^{s_1} \left( \frac{\pi}{2}, -\frac{\pi}{2}, \frac{\pi}{2} \right) D_{-\lambda_2 \tau_2}^{s_2} \left( \frac{\pi}{2}, -\frac{\pi}{2}, \frac{\pi}{2} \right). \quad (A.3.23)
 \end{aligned}$$

This corresponds to taking the negative normal to the reaction plane as the axis of quantization for the transversities  $\tau$ . The utility of these amplitudes at thresholds results from the fact that the crossing matrix becomes diagonal in the transversity basis.

Being unconcerned in this thesis with rigorous analyticity properties of scattering amplitudes, I forego listing the properties of spinor amplitudes (Joos, 1962) and M-functions (Williams, 1963).

#### 4. Crossing Relations for Helicity Amplitudes\*

Trueman and Wick (1964)--hereafter TW--have given an elegant geometrical derivation of the crossing matrix for helicity amplitudes. Fox (1967) determined the overall phase in the TW relation and it is his result which I quote here.

---

\* See Trueman and Wick (1964), Muzinich (1964), Fox (1967), Cohen-Tannoudji, Morel, and Navelet (1968).

$$H_s^{\lambda_3 \lambda_4 : \lambda_1 \lambda_2} = \epsilon_{23} \epsilon_{34} \epsilon_{42} \Lambda_3^* \Lambda_2 e^{-i\pi[s_2 - s_3 + \mu_1 + \mu_2 + \mu_3 + \mu_4]} \times d_{\lambda_1 \mu_1}^{s_1}(\chi_1) d_{\lambda_2 \mu_2}^{s_2}(\chi_2) d_{\lambda_3 \mu_3}^{s_3}(\chi_3) d_{\lambda_4 \mu_4}^{s_4}(\chi_4) H_t^{\mu_2 \mu_4 : \mu_1 \mu_3}. \quad (\text{A.4.1})$$

The crossing angles  $\chi_i$  all satisfy  $0 \leq \chi_i \leq \pi$ ; they are defined by

$$\begin{aligned} S_{12} T_{13} \cos \chi_1 &= (s + m_1^2 - m_2^2)(t + m_1^2 - m_3^2) + 2m_1^2 \Delta, \\ S_{12} T_{24} \cos \chi_2 &= -(s + m_2^2 - m_1^2)(t + m_2^2 - m_4^2) + 2m_2^2 \Delta, \\ S_{34} T_{13} \cos \chi_3 &= -(s + m_3^2 - m_4^2)(t + m_3^2 - m_1^2) + 2m_3^2 \Delta, \\ S_{34} T_{24} \cos \chi_4 &= (s + m_4^2 - m_3^2)(t + m_4^2 - m_2^2) + 2m_4^2 \Delta, \end{aligned} \quad (\text{A.4.2})$$

where  $\Delta = m_3^2 + m_2^2 - m_1^2 - m_4^2$ . The phase  $\epsilon_{ij}$  is +1 unless  $i$  and  $j$  are both fermions in which case  $\epsilon_{ij} = -1$ . The crossing phase  $\Lambda_a$  corresponds to the relative phase between the particle annihilation operator  $a_\alpha$  and the antiparticle creation operator  $\bar{a}_\alpha^\dagger$  in the field theory approach of Weinberg (1964a,b) and of Carruthers and Krisch (1965). For example they define the spinor

$$\chi_\alpha = (2\pi)^{-3/2} \int \tilde{d}p [a_\alpha e^{ip \cdot x} + \Lambda_a^* \bar{a}_\alpha^\dagger e^{-ip \cdot x}]. \quad (\text{A.4.3})$$

The crossing phase is included to make contact with the isospin crossing phase of Carruthers and Krisch. If  $\eta_p, \eta_c, \eta_T$  are the phase factors which appear in the transformations of the single particle states under the discrete operators parity, charge conjugation, and time reversal, then

$$\Lambda_a = \Lambda_a^- = \begin{cases} \eta_p \eta_c \eta_T, & \text{for bosons,} \\ +i\eta_p \eta_c \eta_T, & \text{for fermions.} \end{cases} \quad (\text{A.4.4})$$

See also the general discussion of Feinberg and Weinberg (1959).

A velocity space diagram as popularized by Wick (1962) is helpful for visualizing the meaning of the crossing angles. Indeed one can actually calculate the angles from such a picture by means of non-Euclidean geometry.\* The rules are given by Wick (1962). In Fig. A-4 is shown the velocity space diagram for the final (s-channel) configuration. The lines leaving a vertex represent the directions of the corresponding particles as seen from the rest frame associated with that vertex. Thus  $\chi_1$  is the angle between the direction of particle 3 and the direction of particle 2, measured in the rest frame  $O_1$  of particle 1. Likewise  $\theta_s$  is the angle between particle 1 and particle 3, measured in the s-channel c.m. frame,  $O_s$ .

### 5. Perturbation Theory Conventions

Spinor notation. The  $\gamma$ -matrices are Hermitian, and  $\gamma_4$  is diagonal. Explicitly,

$$\tilde{\gamma} = \begin{pmatrix} 0 & -i\tilde{\sigma} \\ i\tilde{\sigma} & 0 \end{pmatrix}, \quad \gamma_4 = \begin{pmatrix} 1 & 0 \\ 0 & -1 \end{pmatrix}, \quad \gamma_5 = \begin{pmatrix} 0 & -1 \\ -1 & 0 \end{pmatrix}. \quad (\text{A.5.1})$$

The Pauli matrices  $\tilde{\sigma}$  are as usual

\*

For an elementary discussion see Sommerfeld (1952).

$$\sigma_x = \begin{pmatrix} 0 & 1 \\ 1 & 0 \end{pmatrix}, \quad \sigma_y = \begin{pmatrix} 0 & -i \\ i & 0 \end{pmatrix}, \quad \sigma_z = \begin{pmatrix} 1 & 0 \\ 0 & -1 \end{pmatrix}. \quad (\text{A.5.2})$$

The spin tensor is

$$\sigma_{\mu\nu} = (1/2i)[r_\mu, r_\nu] = (1/2i)(r_\mu r_\nu - r_\nu r_\mu). \quad (\text{A.5.3})$$

Spinors are normalized according to  $\bar{u}u = -\bar{v}v = 2m$ , and satisfy the free-particle Dirac equations

$$(m + i\mathbf{r}\cdot\mathbf{p}) u(\mathbf{p}) = 0, \quad (m - i\mathbf{r}\cdot\mathbf{p}) v(\mathbf{p}) = 0. \quad (\text{A.5.4})$$

For an antiparticle of momentum  $\mathbf{p}$  and helicity  $\lambda$  it is sometimes useful to replace

$$v_\lambda(\mathbf{p}) = (-1)^{\lambda - \frac{1}{2}} \gamma_5 u_{-\lambda}(\mathbf{p}). \quad (\text{A.5.5})$$

The Dirac conjugate spinor is  $\bar{u}_\lambda(\mathbf{p}) = [u_\lambda(\mathbf{p})]^\dagger \gamma_4$ .

Explicit representation in the helicity basis. The positive energy spinor with momentum  $\mathbf{p} = |\mathbf{p}|\hat{\mathbf{z}}$  and helicity  $\lambda$  is

$$u_\lambda(\mathbf{p}\hat{\mathbf{z}}) = (E + m)^{\frac{1}{2}} \begin{pmatrix} \chi_\lambda \\ \frac{2\lambda p}{E + m} \chi_\lambda \end{pmatrix}, \quad (\text{A.5.6})$$

where  $m$  is the particle mass,  $E = (p^2 + m^2)^{\frac{1}{2}}$ , and

$$\chi_{\frac{1}{2}} = \begin{pmatrix} 1 \\ 0 \end{pmatrix}, \quad \chi_{-\frac{1}{2}} = \begin{pmatrix} 0 \\ 1 \end{pmatrix}. \quad (\text{A.5.7})$$

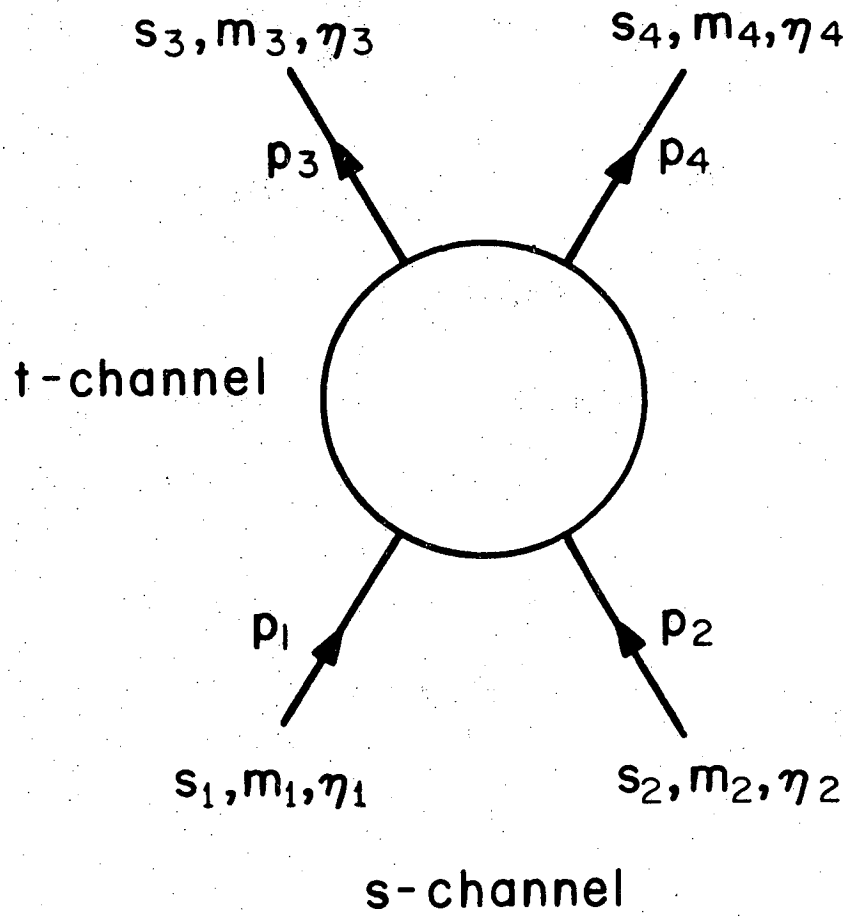
The spinor corresponding to a particle with momentum  $\underline{p}'$  such that  $\hat{p}' \cdot \hat{z} = \cos \theta$  is obtained by a rotation about the y-axis. Thus

$$\begin{aligned}
 u_{\lambda}(\underline{p}') &= e^{-i\sigma_y \theta/2} u_{\lambda}(\underline{p}\hat{z}) \\
 &= (E + m)^{\frac{1}{2}} \begin{bmatrix} \alpha \cos \frac{\theta}{2} - (1 - \alpha) \sin \frac{\theta}{2} \\ \alpha \sin \frac{\theta}{2} + (1 - \alpha) \cos \frac{\theta}{2} \\ [\alpha \cos \frac{\theta}{2} - (1 - \alpha) \sin \frac{\theta}{2}] 2\lambda p' / (E + m) \\ [\alpha \sin \frac{\theta}{2} + (1 - \alpha) \cos \frac{\theta}{2}] 2\lambda p' / (E + m) \end{bmatrix} \quad (\text{A.5.8})
 \end{aligned}$$

where  $\alpha = \frac{1}{2} + \lambda$ . I do not incorporate the Jacob and Wick (1959) particle 2 phase into my spinor. This is instead explicit in (A.3.13) which defines helicity amplitudes.

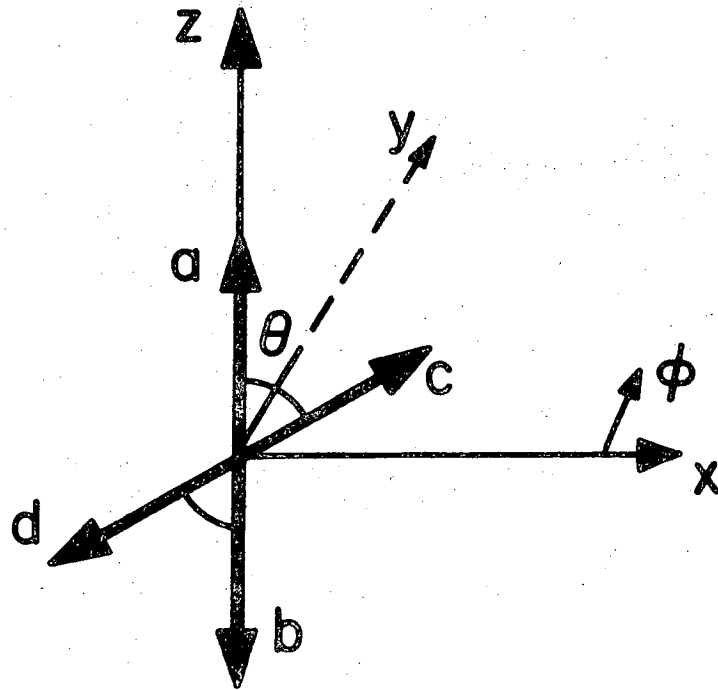
FIGURE CAPTIONS

- Fig. A-1. Labeling of particles for a two body to two body collision. The momenta are labeled  $p_i$ , masses  $m_i$ , particle spins  $s_i$ , and intrinsic parities of the particles  $\eta_i$ .
- Fig. A-2. Coordinate system for two body scattering. The scattering angle is  $\theta$ . The azimuthal angle  $\phi$  is equal to zero for scattering in the  $x$ - $z$  plane.
- Fig. A-3. Coordinate systems for the definition of single particle states. The axes  $x$ - $y$ - $z$  are fixed in space. The particle momentum is  $p$ ; the quantization axis is in each case along  $z_0$ .
- Fig. A-4. Velocity space diagram for the  $s$ -channel configuration. The meaning of the angles is explained in the text.



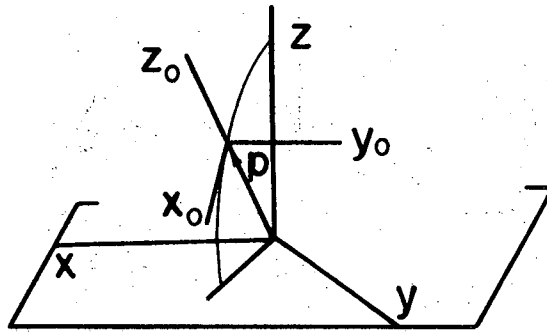
XBL707-3483

Fig. A-1.

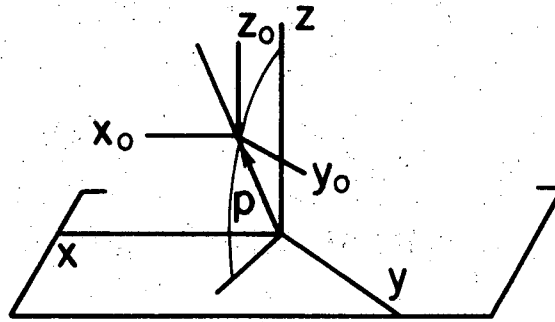


XBL707-3472

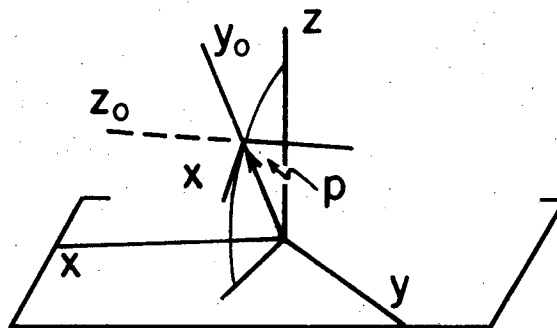
Fig. A-2.



(a) helicity



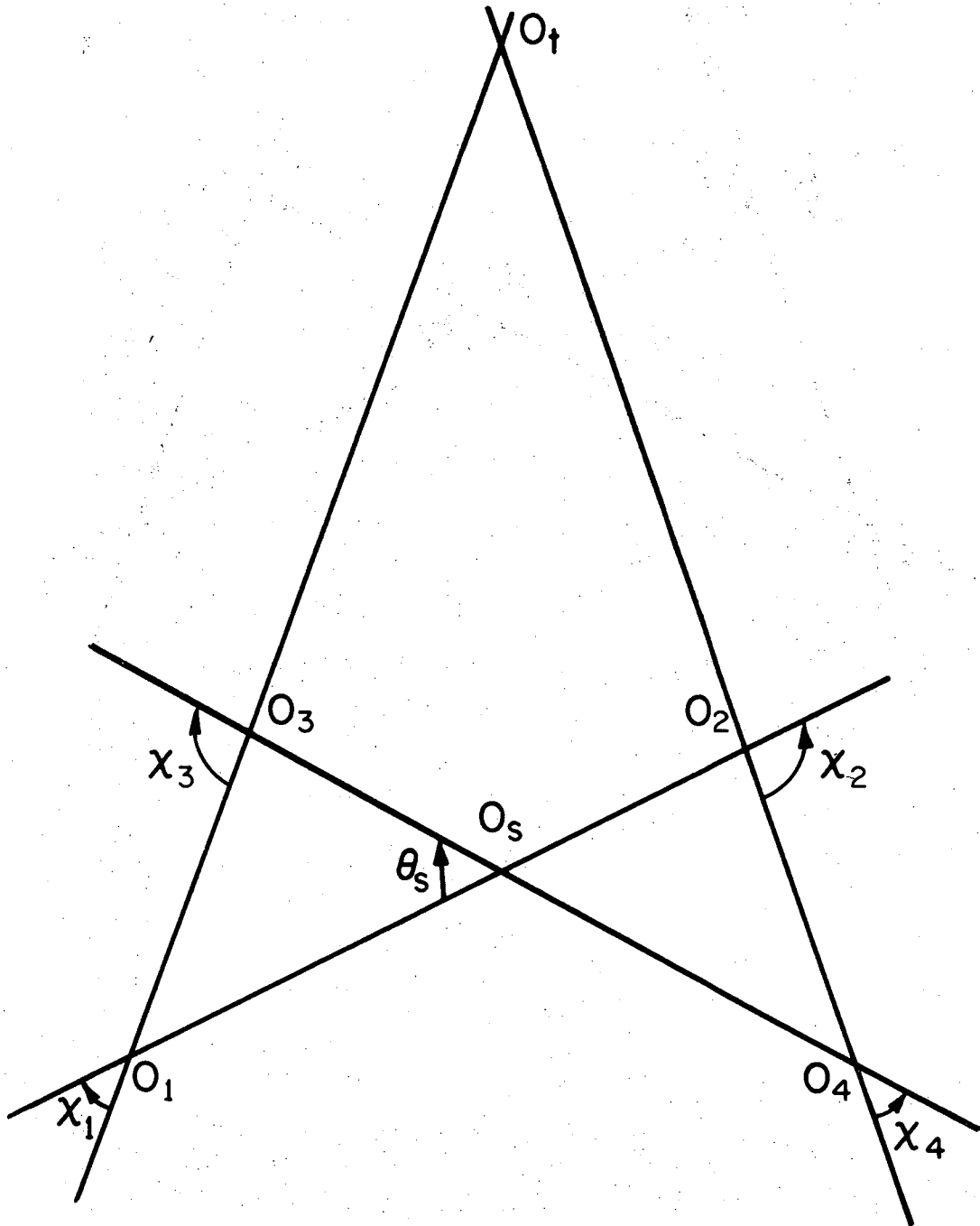
(b) spin



(c) transversity

XBL707-3480

Fig. A-3.



XBL707-3479

Fig. A-4.

APPENDIX B. PROPERTIES OF ROTATION MATRICES

1. Definition and Properties

In an irreducible representation of the rotation group of dimension  $(2J + 1)$  corresponding to an angular momentum  $J$  the rotation  $(\alpha\beta\gamma)$  is represented by the matrix

$$\mathcal{D}_{M'M}^J(\alpha\beta\gamma) = \langle JM' | R_{\alpha\beta\gamma} | JM \rangle. \quad (\text{B.1.1})$$

As the operator  $R^\dagger$  is the adjoint of  $R$ , its matrix elements are related to those of  $R$  by

$$\langle JM | R^\dagger | JM' \rangle = \langle JM' | R | JM \rangle^* = (\mathcal{D}_{M'M}^J)^*. \quad (\text{B.1.2})$$

The operator  $R$  is unitary:

$$(R_{\alpha\beta\gamma}^\dagger)^{-1} = (R_{\alpha\beta\gamma})^{-1} = R_{-\gamma, -\beta, -\alpha};$$

hence

$$(\mathcal{D}_{MM'}^J(\alpha\beta\gamma))^* = \mathcal{D}_{M'M}^J(-\gamma, -\beta, -\alpha). \quad (\text{B.1.3})$$

Furthermore, the property  $RR^\dagger = R^\dagger R = 1$  implies

$$\sum_{M'} (\mathcal{D}_{M'N}^J(r))^* \mathcal{D}_{M'M}^J(r) = \delta_{MN}, \quad (\text{B.1.4})$$

$$\sum_{M'} \mathcal{D}_{MM'}^J(r) (\mathcal{D}_{NM'}^J(r))^* = \delta_{MN}. \quad (\text{B.1.5})$$

---

\* See Brink and Satchler (1968), Andrews and Gunson (1964), Collins and Squires (1968).

Because the basis states of the representation are chosen as eigenfunctions of  $J_z$ , and  $R$  has the form specified in the footnote to Eq. (A.2.1), the matrices simplify to

$$\begin{aligned}
 D_{MN}^J(\alpha\beta\gamma) &= \langle JM | e^{-i\alpha J_z} e^{-i\beta J_y} e^{-i\gamma J_z} | JN \rangle \\
 &= \exp[-i(\alpha M + \gamma N)] \langle JM | e^{-i\beta J_y} | JN \rangle \\
 &= \exp[-i(\alpha M + \gamma N)] d_{MN}^J(\beta).
 \end{aligned}
 \tag{B.1.6}$$

The phases of the rotation matrices depend upon the convention adopted for the Euler angles and upon the choice of phases of the matrix elements of  $\tilde{J}$ . With the Condon and Shortley (1935) choice of phases,  $\langle jm | J_z | jm \rangle = m$ ;  $\langle j_m \pm 1 | J_{\pm} | jm \rangle = [(j \pm m + 1)(j \mp m)]^{\frac{1}{2}}$ , the reduced rotation matrices  $d^j$  are real. They satisfy the symmetry properties

$$d_{\lambda\mu}^j(\theta) = d_{-\mu, -\lambda}^j(\theta) = (-1)^{\lambda-\mu} d_{\mu\lambda}^j(\theta) = d_{\mu\lambda}^j(-\theta) = (-1)^{j+\lambda} d_{\lambda, -\mu}^j(\pi-\theta).
 \tag{B.1.7}$$

The orthogonality relations are

$$\int_0^\pi d_{\lambda\mu}^j(\theta) d_{\lambda\mu}^{j'}(\theta) \sin \theta \, d\theta = \delta_{jj'} \frac{2}{2j+1},
 \tag{B.1.8}$$

$$\sum_{\lambda} d_{\lambda\mu}^j(\theta) d_{\lambda\mu'}^j(\theta) = \delta_{\mu\mu'},
 \tag{B.1.9}$$

$$\frac{1}{2} \sum_j (2j+1) d_{\lambda\mu}^j(\theta) d_{\lambda\mu}^j(\theta') = \delta(\cos \theta - \cos \theta').
 \tag{B.1.10}$$

## 2. Expansions in Terms of Other Functions

It is fruitful to obtain expansions for the reduced matrices in terms of well-studied functions, for this allows the deduction of analytic properties. First note the expansion in terms of Jacobi polynomials  $P_n^{ab}(z)$ ,

$$d_{\lambda\mu}^j(\theta) = (-1)^{n-\mu} \left[ \frac{(j+m)!(j-m)!}{(j+n)!(j-n)!} \right]^{\frac{1}{2}} [\sin(\theta/2)]^{|\lambda-\mu|} [\cos(\theta/2)]^{|\lambda+\mu|} \\ \times P_{j-m}^{|\lambda-\mu|, \lambda+\mu}(\cos \theta), \quad (\text{B.2.1})$$

where  $m = \text{Max}(\lambda, \mu)$ ,  $n = \text{Min}(\lambda, \mu)$ , and the expansion only holds for  $m \geq 0$ . For  $(j-m)$  a nonnegative integer, the function  $P_{j-m}^{ab}(z)$  is a polynomial in  $z$ . As a consequence the expansion (B.2.1) is useful for establishing analytic properties of  $d^j$  in  $z$ .

To exhibit the analytic structure of  $d^j$  in the  $j$  plane it is convenient to express the reduced matrices in terms of the hypergeometric function, by

$$d_{\lambda\mu}^j(\theta) = \frac{(-1)^{n-\lambda}}{|\lambda-\mu|!} [\sin(\theta/2)]^{|\lambda-\mu|} [\cos(\theta/2)]^{\lambda+\mu} \\ \times \left[ \frac{(j+m)!(j-n)!}{(j+n)!(j-m)!} \right]^{\frac{1}{2}} F(-j+m, j+m+1, m-n+1; \sin^2(\theta/2)). \quad (\text{B.2.2})$$

The hypergeometric function is analytic in  $j$ , so all the  $j$ -plane singularities are explicit in the square root factor. The singularities occur at integral values of  $(j-m)$  for which either

$$n \ll j < m \quad (B.2.3a)$$

or

$$-m \ll j < n. \quad (B.2.3b)$$

Taking the asymptotic form of  $F(a, b, c; (1 - z)/2)$  for large  $z = \cos \theta$ , one obtains the asymptotic expression

$$d_{\lambda\mu}^j(\theta) \sim \frac{(-1)^{n-\mu} i^{m-n}}{2j+1} \left[ \frac{(j+m)!(j-n)!}{(j+n)!(j-m)!} \right]^{\frac{1}{2}} \\ \times \left\{ \frac{(2j+1)!(z/2)^j}{(j+m)!(j-n)!} \left[ 1 + \mathcal{O}(z^{-2}) \right] - \frac{(-2j-1)!(z/2)^{-j-1}}{(-j-1+m)!(-j-1-n)!} \right. \\ \left. \times \left[ 1 + \mathcal{O}(z^{-1}) \right] \right\}, \quad (B.2.4)$$

again for  $m \geq 0$ .

Next consider the functions  $e_{\lambda\mu}^j(\theta)$ , the relation of which to the  $d_{\lambda\mu}^j(\theta)$  is analogous to the relation of the  $Q_\ell(z)$  [Legendre functions of the second kind] to the  $P_\ell(z)$  [Legendre functions of the first kind]. These functions were introduced by Andrews and Gunson (1964), who also provided a valuable discussion of the properties of the  $e^j$  for nonintegral  $j$ .<sup>\*</sup> The expansion of the reduced rotation functions of the second kind in terms of Jacobi Polynomials is

---

\* Note that the functions  $e_j^{\lambda\mu}(\theta)$  of Andrews and Gunson (1964) are  $(-1)^{\lambda-\mu}$  times my  $e_{\lambda\mu}^j(\theta)$ .

$$e_{\lambda\mu}^j(\theta) = (-1)^{n-\lambda} \left[ \frac{(j+m)!(j-n)!}{(j-m)!(j+n)!} \right]^{\frac{1}{2}} [\sin(\theta/2)]^{|\lambda-\mu|} [\cos(\theta/2)]^{\lambda+\mu}$$

$$\times Q_{j-m}^{|\lambda-\mu|, \lambda+\mu}(\cos \theta), \quad (\text{B.2.5})$$

for  $m \geq 0$ . The e-function have the symmetry properties

$$e_{\lambda\mu}^j(\theta) = (-1)^{\lambda-\mu} e_{-\lambda, -\mu}^j(\theta) = (-1)^{\lambda-\mu} e_{\mu\lambda}^j(\theta). \quad (\text{B.2.6})$$

The Jacobi functions of the second kind are related to those of the first kind by

$$Q_n^{ab}(z) = \left(\frac{1}{2}\right)(z-1)^{-a}(z+1)^{-b} \int_{-1}^1 \frac{dz'}{z-z'} (1-z')^a (1+z')^b$$

$$\times P_n^{ab}(z'), \quad (\text{B.2.7})$$

for  $n$  a nonnegative integer.

A useful relation between the  $d^j$  and the  $e^j$  is

$$\frac{\pi d_{\lambda\mu}^j(\theta)}{\sin \pi(j-\lambda)} = \frac{e_{\lambda\mu}^j(\theta)}{\cos \pi(j-\lambda)} - \frac{e_{-\lambda, -\mu}^{-j-1}(\theta)}{\cos \pi(j-\lambda)}. \quad (\text{B.2.8})$$

Finally, the asymptotic behavior of  $e^j$  for large  $z$  is given by

$$e_{\lambda\mu}^j(\theta) = \frac{(-1)^{n-\lambda}}{2(2j+1)!} [(j+\lambda)!(j-\lambda)!(j+\mu)!(j-\mu)!]^{\frac{1}{2}}$$

$$\times \exp[\pm i\pi(\lambda-\mu)/2] (z/2)^{-j-1} [1 + \mathcal{O}(z^{-1})], \quad (\text{B.2.9})$$

where the  $\pm$  occurs as  $\text{Im } z \gtrless 0$ .

Let us also mention two special cases for which the  $\mathcal{D}$ -functions are particularly simple:

$$\mathcal{D}_{m0}^j(\alpha\beta\gamma) = \left(\frac{2j+1}{4\pi}\right) [Y_j^m(\beta,\alpha)]^*, \quad (\text{B.2.10})$$

and

$$d_{m0}^j(\beta) = (-1)^m \left[\frac{(j-m)!}{(j+m)!}\right]^{\frac{1}{2}} P_j^m(\beta), \quad m > 0. \quad (\text{B.2.11})$$

Here  $Y_j^m$  is a spherical harmonic and  $P_j^m$  is an associated Legendre function. In Table B-1 I have listed some explicit forms of the d-functions for low spins.

### 3. Computational Details

The d-functions required in the calculations described in Chapter VI were evaluated numerically by forward recursion of the Legendre functions, using the formulae (Jacob and Wick, 1959)

$$d_{00}^j(\theta) = P_j(\cos \theta), \quad (\text{B.3.1})$$

$$d_{\frac{1}{2},\frac{1}{2}}^{j+\frac{1}{2}}(\theta) = (j+1)^{-1} \cos(\theta/2)(P'_{j+1} - P'_j), \quad (\text{B.3.2})$$

$$d_{\frac{1}{2},-\frac{1}{2}}^{j+\frac{1}{2}}(\theta) = (j+1)^{-1} \sin(\theta/2)(P'_{j+1} + P'_j), \quad (\text{B.3.3})$$

where  $P'_j$  means  $dP_j(\cos \theta)/d \cos \theta$ . The Legendre functions were computed from the recurrence relations

$$(v+1)P_{v+1}(z) = (2v+1)zP_v(z) - vP_{v-1}(z), \quad (\text{B.3.4})$$

$$(z^2 - 1) \frac{dP_\nu(z)}{dz} = \nu z P_\nu(z) - \nu P_{\nu-1}(z), \quad (\text{B.3.5})$$

stated by Abramowitz and Stegun (1964).

Table B-1. Explicit forms of the reduced rotation matrices for low spins.

$$d_{00}^0(\theta) = 1$$

$$d_{\frac{1}{2}\frac{1}{2}}^{\frac{1}{2}}(\theta) = d_{-\frac{1}{2},-\frac{1}{2}}^{\frac{1}{2}}(\theta) = \cos(\theta/2)$$

$$d_{-\frac{1}{2},\frac{1}{2}}^{\frac{1}{2}}(\theta) = -d_{\frac{1}{2},-\frac{1}{2}}^{\frac{1}{2}}(\theta) = \sin(\theta/2)$$

$$d_{11}^1(\theta) = d_{-1,-1}^1(\theta) = \frac{1}{2}(1 + \cos \theta)$$

$$d_{10}^1(\theta) = d_{-1,0}^1(\theta) = -d_{01}^1(\theta) = -d_{0,-1}^1(\theta) = -\sin \theta/\sqrt{2}$$

$$d_{00}^1(\theta) = \cos \theta$$

$$d_{1,-1}^1(\theta) = d_{-1,1}^1(\theta) = \frac{1}{2}(1 - \cos \theta)$$

APPENDIX C. REGGEIZATION OF S-CHANNEL HELICITY AMPLITUDES

The model formulated in Chapter V is rather cumbersome, requiring several applications of the helicity crossing matrix to complete a calculation. For detailed fits this would present little obstacle to the computer but for the illustrative calculations we wish to examine in this thesis these complications merely obscure the physics. For these model calculations it suffices to Reggeize the s-channel helicity amplitudes, to leading order in  $s$ .

a) The General Result, Following from Crossing

The formulation of high-energy exchange models in terms of direct-channel amplitudes has been studied by Fox (1967) and by Cohen-Tannoudji, Salin, and Morel (1968). To leading order in  $s$ , Regge theory is as easily expressed in the s-channel as in the t-channel. A simple solution to the problem is possible because the helicity crossing matrix factorizes (to leading order in  $s$ ), as noticed by Fox and Leader (1967). The leading order contribution of a boson Regge pole at  $j = \alpha(t)$  may be written as

$$H_t^{\lambda_2 \lambda_4 : \lambda_1 \lambda_3} = -e^{-i\pi(\lambda_1 - \lambda_3 - \lambda_2 + \lambda_4)/2} \frac{(\tau + e^{-i\pi\alpha(t)})}{2 \sin \pi\alpha(t)} \cdot \gamma'_{\lambda_3 \lambda_1} \gamma'_{\lambda_4 \lambda_2} (s/s_0)^{\alpha(t)}, \quad (C.1.1)$$

where the Regge pole has signature  $\tau$  and scale factor  $s_0$ . The Trueman and Wick (1964) helicity crossing matrix is given in Appendix A.4, so we only restate the basic formula here

$$H_s^{\mu_3\mu_4:\mu_1\mu_2} = \epsilon_{23}\epsilon_{34}\epsilon_{42}\Lambda_2\Lambda_3^* e^{-i\pi[\sigma_2-\sigma_3+\mu_1+\mu_2+\mu_3+\mu_4]} \cdot d_{\mu_1\lambda_1}^{\sigma_1}(\chi_1) d_{\mu_2\lambda_2}^{\sigma_2}(\chi_2) d_{\mu_3\lambda_3}^{\sigma_3}(\chi_3) d_{\mu_4\lambda_4}^{\sigma_4}(\chi_4) H_t^{\lambda_2\lambda_4:\lambda_1\lambda_3} \quad (A.4.1)$$

Applied to (C.1.1), the helicity crossing matrix gives an expression for  $H_s$  which I rewrite in a more symmetrical form as

$$H_s^{\mu_3\mu_4:\mu_1\mu_2} = -\epsilon_{23}\epsilon_{34}\epsilon_{42}\Lambda_2\Lambda_3^* \frac{(\tau + e^{-i\pi\alpha(t)})}{2 \sin \pi\alpha(t)} g_{\mu_3\mu_1} g_{\mu_4\mu_2} \left(\frac{s}{s_0}\right)^{\alpha(t)} \cdot (-1)^{\sigma_2+\mu_2} (-1)^{\sigma_4-\mu_4} \eta_2^P \eta_4^P \tau^P, \quad (C.1.2)$$

where the Regge pole has parity  $P$  and the (s-channel) external particles 2 and 4 have intrinsic parities  $\eta_2^P, \eta_4^P$ . The s-channel Regge residue functions are

$$g_{\mu_a\mu_b} = \sum_{\lambda_a, \lambda_b} e^{i\pi(\lambda_a+\lambda_b)} (-1)^{\sigma_a+\lambda_a} \gamma_{\lambda_a\lambda_b}^{\sigma_a, \sigma_b} \cdot d_{\lambda_a\mu_a}^{\sigma_a}(-\chi_a^\infty) d_{\lambda_b\mu_b}^{\sigma_b}(-\chi_b^\infty), \quad (C.1.3)$$

where

$$\left. \begin{aligned} \cos \chi_a^\infty &= -\frac{(t + m_a^2 - m_b^2)}{\mathcal{J}_{ab}} \\ \cos \chi_b^\infty &= \frac{(t + m_b^2 - m_a^2)}{\mathcal{J}_{ab}} \end{aligned} \right\} \quad (C.1.4)$$

are Trueman-Wick crossing angles in the limit  $s \rightarrow \infty$ . [The "extra phases" in (C.1.2), not present in (A.4.1) are the result of a parity operation at the 2-4 vertex the purpose of which was to define the functions  $g_{\mu_3\mu_1}$  and  $g_{\mu_4\mu_2}$  in the same way. This is accomplished by undoing the asymmetry in the definitions of  $\chi_1$  compared with  $\chi_3$  and of  $\chi_2$  compared with  $\chi_4$  in (A.4.2).] The practical advantages of attention to the crossing phases become apparent only when comparing several reactions and indeed such care is superfluous for some of the more basic features I wish to study below.

b) Effects of Discrete Symmetries on the Residue Functions

Parity conservation at each vertex for the exchange of a particle of spin  $J$  and parity  $P$  implies a relation among the t-channel helicity partial-wave amplitudes,

$$H_{t,J}^{\lambda_2\lambda_4:\lambda_1\lambda_3} = \eta_2^P \eta_4^P P(-1)^{J+\sigma_2+\sigma_4} H_{t,J}^{-\lambda_2-\lambda_4:\lambda_1\lambda_3}. \quad (C.1.5)$$

For Reggeon exchange, the quantity  $(-1)^J$  is replaced by  $\tau$ . This may be translated into a condition on the t-channel residue functions,

$$r'_{\lambda_4\lambda_2} = \eta_2^P \eta_4^P \tau P(-1)^{\sigma_2+\sigma_4} r'_{-\lambda_4,-\lambda_2}, \quad (C.1.6)$$

thence into a condition on the s-channel residue functions,

$$g_{\mu_4\mu_2} = \eta_2^P \eta_4^P \tau P(-1)^{\sigma_2+\sigma_4} (-1)^{\mu_2+\mu_4} g_{-\mu_4,-\mu_2}. \quad (C.1.7)$$

If particle  $\bar{2}$  equals particle 4, then

$$r'_{\lambda_4\lambda_2} = \tau r'_{\lambda_2\lambda_4}, \quad (C.1.8)$$

but if a state of definite t-channel isospin (I) has been formed there is in addition an isospin swapping phase  $(-1)^{2I_4 - I}$ . The condition is equally simple in the s-channel, namely

$$g_{\mu_4 \mu_2} = \tau g_{\mu_2 \mu_4}. \quad (\text{C.1.9})$$

Similarly if particle 2 equals particle 4, then we may form states of definite G-parity in the t-channel, for which

$$r'_{\lambda_4 \lambda_2} = \tau G (-1)^I r'_{\lambda_2 \lambda_4} = \tau C_n r'_{\lambda_2 \lambda_4} \quad (\text{C.1.10})$$

where G is the G-parity of the exchanged Reggeon and  $C_n$  is the charge conjugation eigenvalue for the neutral member of the Reggeon isomultiplet. Again the condition is equally simple in the s-channel,

$$g_{\mu_4 \mu_2} = \tau C_n g_{\mu_2 \mu_4}. \quad (\text{C.1.11})$$

Evidently it is possible to form combinations of s-channel amplitudes which have definite t-channel properties, e.g. s-channel combinations with definite t-channel parity.

### c) Consequences of Factorization

Asymptotically the physical region boundary lies at  $t = 0$ . Thus the half-angle factors that ensure angular momentum conservation [compare Eq. (A.3.15)] appear as powers of  $t^{\frac{1}{2}}$  in the residue functions. In particular amplitudes must vanish at  $t = 0$  at least as rapidly as the half-angle factors prescribe. For example, the s-channel residues must have the minimal behavior\*

---

\* In this context,  $t$  is to be understood as  $t/s_0$ .

$$g_{\mu_3\mu_1} g_{\mu_4\mu_2} \propto (-t)^{\frac{1}{2}|\mu_1 - \mu_2 - \mu_3 + \mu_4|}, \quad (C.1.12)$$

as  $t \rightarrow 0^-$ . However  $g_{\mu_3\mu_1} g_{\mu_4\mu_2}$  is related by parity [and with no powers of  $(-t)^{\frac{1}{2}}$ ] to  $g_{\mu_3\mu_1} g_{-\mu_4, -\mu_2}$  through (C.1.7), so the residues must also satisfy

$$g_{\mu_3\mu_1} g_{\mu_4\mu_2} \propto (-t)^{\frac{1}{2}|\mu_1 + \mu_2 - \mu_3 - \mu_4|}, \quad (C.1.13)$$

as  $t \rightarrow 0^-$ , which contradicts (C.1.12) unless  $(\mu_1 - \mu_3) = 0$ , or  $(\mu_2 - \mu_4) = 0$ , or both are equal to zero. The only way to make (C.1.12) and (C.1.13) consistent with each other is to make both  $H_s^{\mu_3\mu_4; \mu_1\mu_2}$  and  $H_s^{\mu_3, -\mu_4; \mu_1, -\mu_2}$  vanish at the faster rate by taking

$$g_{\mu_3\mu_1} g_{\mu_4\mu_2} \underset{t \rightarrow 0}{\propto} (-t)^{\frac{1}{2}(|\mu_3 - \mu_1| + |\mu_4 - \mu_2|)}. \quad (C.1.14)$$

In order to satisfy factorization and parity we must therefore have

$$g_{\mu_a\mu_b} \propto (-t)^{\frac{1}{2}|\mu_a - \mu_b|}. \quad (C.1.15)$$

Apart from this behavior at  $t = 0$   $g_{\mu_a\mu_b}$  is free of all kinematical singularities.

The stringent constraints implied by (C.1.15) are responsible for some quite definite predictions which are in fact in conflict with experiment. In charged pion photoproduction the s-channel nonflip amplitude (written as  $H_s^{\lambda_\pi \lambda_{N'}; \lambda_\gamma \lambda_N}$ )

$$H_s^{0, \frac{1}{2}; -1, -\frac{1}{2}}$$

may be finite at  $t = 0$  and satisfy angular momentum conservation. If, however  $H_s^{0, \frac{1}{2}; -1, -\frac{1}{2}}$  receives contributions from a single Regge pole the factorization argument given above implies that

$$H_s^{0, \frac{1}{2}; -1, -\frac{1}{2}} \underset{t \rightarrow 0}{\propto} [(-t)^{\frac{1}{2}}]^2 \sim t. \quad (C.1.16)$$

This prediction is dramatically contradicted by the data (Boyarski et al., 1968a,b) on  $\gamma N \rightarrow \pi^{\pm} N'$  which display sharp forward peaks. The argument leading to (C.1.16) first was stated by Drell and Sullivan (1967).

Another classic example occurs in  $np \rightarrow pn$ , i.e. neutron-proton charge exchange for which the amplitude

$$H_s^{-\frac{1}{2}, -\frac{1}{2}; \frac{1}{2}, \frac{1}{2}} \left\{ \begin{array}{l} \propto \text{constant, by angular momentum conservation,} \\ \propto t, \text{ in a one-pole model.} \end{array} \right. \quad (C.1.17)$$

The latter prediction is again contradicted by data (Manning et al., 1966) which display a sharp forward peak. Further references for photoproduction may be found in Jackson and Quigg (1969, 1970). An enlightening discussion of the behavior at  $t = 0$  is given in Appendix B(e) of Jackson (1970).

#### d) Conspiracy

The result (C.1.15) which followed from factorization and parity indicates that no matter how many different Regge poles contribute to the scattering amplitude,  $H_s \propto (-t)^{\frac{1}{2}} \{ |^{\mu_1 - \mu_3}|^+ |^{\mu_2 - \mu_4}| \}$  rather than  $(-t)^{\frac{1}{2}} |^{\mu_1 - \mu_2 - \mu_3 + \mu_4}|$  as expected from rotational invariance. Such a prediction is not however inevitable and in view of the experimental situation one may try to thwart the factorization argument by considering two poles which differ only in

their values of  $\tau P$  and which collide in the  $j$  plane for  $t = 0$ . Before giving the result I note that such a conspiracy of poles is not the only way around the argument. All that is required is to add a contribution which does not factorize, for example the absorptive corrections discussed in Sec. V.1. Factorization holds for pole residues, so Regge cuts are exempt from its restrictions. An understandable and didactic treatment of conspiracy in terms of poles is given by Leader (1969), and a more detailed discussion than the one I give here appears in Cohen-Tannoudji, Salin, and Morel (1968). I reproduce the crude results of Fox (1967) which are sufficient for practical purposes.

Thus the s-channel residue functions  $g$  corresponding to the original Regge pole and  $h$  corresponding to the conspirator Regge pole must satisfy

$$g_{\mu_3\mu_1} g_{\mu_4\mu_2} - h_{\mu_3\mu_1} h_{\mu_4\mu_2} \propto (-t)^{\frac{1}{2}|\mu_1 - \mu_2 - \mu_3 + \mu_4|}, \quad (C.1.18)$$

and by parity

$$g_{\mu_3\mu_1} g_{\mu_4\mu_2} + h_{\mu_3\mu_1} h_{\mu_4\mu_2} \propto (-t)^{\frac{1}{2}|\mu_1 + \mu_2 - \mu_3 - \mu_4|}. \quad (C.1.19)$$

A consistent solution is to take

$$h_{\mu_a\mu_b}, g_{\mu_a\mu_b} \begin{cases} \propto (-t)^{\frac{1}{2}|\mu_a - \mu_b| - \frac{1}{2}}, & \text{for } |\mu_a - \mu_b| \neq 0 \\ \propto (-t)^{\frac{1}{2}}, & \text{for } |\mu_a - \mu_b| = 0 \end{cases} \quad (C.1.20)$$

and

$$g_{\mu_a\mu_b} = +ih_{\mu_a\mu_b} (1 + \mathcal{O}(t)) \quad \text{for } \mu_a - \mu_b > 0 \quad (C.1.21)$$

whereas the coefficients of  $(-t)^{\frac{1}{2}}$  for  $\mu_a - \mu_b = 0$  are arbitrary. This is the prescription of Fox (1967).

It is worthwhile to illustrate it with a simple example. Consider the s-channel nonflip amplitude for photoproduction mentioned above. Before conspiracy we have

$$H_s^{0, \frac{1}{2}; -1, -\frac{1}{2}} \propto g_{0, -1} g_{\frac{1}{2}, -\frac{1}{2}} \propto [(-t)^{\frac{1}{2}}]^1 [(-t)^{\frac{1}{2}}]^1 \propto t \quad (\text{C.1.21})$$

but after conspiracy,

$$\begin{aligned} H_s^{0, \frac{1}{2}; -1, -\frac{1}{2}} &\propto g_{0, -1} g_{\frac{1}{2}, -\frac{1}{2}} - h_{0, -1} h_{\frac{1}{2}, -\frac{1}{2}} \\ &\propto ih_{0, -1} [1 + \mathcal{O}(t)] ih_{\frac{1}{2}, -\frac{1}{2}} [1 + \mathcal{O}(t)] \\ &\quad - h_{0, -1} h_{\frac{1}{2}, -\frac{1}{2}} \\ &\propto h_{0, -1} h_{\frac{1}{2}, -\frac{1}{2}} + \mathcal{O}(t) \\ &\propto 1 + \mathcal{O}(t) \end{aligned} \quad (\text{C.1.22})$$

is finite at  $t = 0$ . The amplitude related by parity to  $H_s^{0, \frac{1}{2}; -1, -\frac{1}{2}}$ , which is a double-flip amplitude in the s-channel, continues to vanish as  $t$ , as required by rotational invariance. Thus

$$H_s^{0, -\frac{1}{2}; -1, \frac{1}{2}} \propto g_{0, -1} g_{\frac{1}{2}, -\frac{1}{2}} + h_{0, -1} h_{\frac{1}{2}, -\frac{1}{2}} \propto t. \quad (\text{C.1.23})$$

e) Putting in the Physical Region Boundary

Nonasymptotically

I adopt the same prescription as was used by Fox (1967) and by Cohen-Tannoudji, Salin, and Morel (1968), which is to multiply Eq. (C.1.2) by the factor

$$\frac{\left\{ \left( \frac{s}{s_0} \right)^{\frac{1}{2}} \sin \frac{\theta_s}{2} \right\}^{|\mu_1 - \mu_2 - \mu_3 + \mu_4|} \left\{ \cos \frac{\theta_s}{2} \right\}^{|\mu_1 - \mu_2 + \mu_3 - \mu_4|}}{\left\{ \left( \frac{-t}{s_0} \right)^{\frac{1}{2}} \right\}^{|\mu_1 - \mu_2 - \mu_3 + \mu_4|}}$$

$$= \left\{ (-s/t)^{\frac{1}{2}} \sin \frac{\theta_s}{2} \right\}^{|\mu_1 - \mu_2 - \mu_3 + \mu_4|} \left\{ \cos \frac{\theta_s}{2} \right\}^{|\mu_1 - \mu_2 + \mu_3 - \mu_4|} \quad . \quad (C.1.24)$$

Two objections may be raised against this form. The first is that upon crossing to the t-channel we should find in addition to the Regge pole at  $\alpha(t)$  a sequence of parallel trajectories, integrally spaced for all t. This reflects the fact that our recipe is not a proper one for moderate values of s. The second flaw, noticed by Fox, is the lack of proper analyticity in s. Thus if the Regge pole makes a particle of spin j at  $t = M^2$  our recipe does not force the pole residue in  $H_t$  to have an s-dependence  $\propto d^j(\theta_t)$ . One expects this shortcoming to be more important, the nearer the particle is to the physical region.

For the pion Regge pole Fox (1967) reports 50% nonasymptotic corrections at  $s = 5(\text{GeV}/c)^2$ . This reinforces my claim, made at the beginning of this section that the Reggeized s-channel amplitudes are more useful for model calculations than for detailed fits.

Finally let us state our phenomenological prescription in detail.

$$\begin{aligned}
 H_s^{\mu_3 \mu_4; \mu_1 \mu_2} &= -\epsilon_{23} \epsilon_{34} \epsilon_{42} \Lambda_2 \Lambda_3^* (-1)^{\sigma_2 + \mu_2} (-1)^{\sigma_4 - \mu_4} \eta_2^P \eta_4^P \tau^P \\
 &\cdot \left\{ \left( -\frac{s}{t} \right)^{\frac{1}{2}} \sin \frac{\theta_s}{2} \right\}^{|\mu_1 - \mu_2 - \mu_3 + \mu_4|} \left\{ \cos \frac{\theta_s}{2} \right\}^{|\mu_1 - \mu_2 + \mu_3 - \mu_4|} \frac{(\tau + e^{-i\pi\alpha(t)})}{2 \sin \pi\alpha(t)} \\
 &\cdot g_{\mu_3 \mu_1}(t) g_{\mu_4 \mu_2}(t) \left( \frac{s}{s_0} \right)^{\alpha(t)}, \tag{C.1.25}
 \end{aligned}$$

where  $g_{\mu_a \mu_b}(t) = \hat{g}_{\mu_a \mu_b}(t) \left( \frac{-t}{s_0} \right)^{\frac{1}{2} |\mu_a - \mu_b|}$ , and  $\hat{g}$  is regular in  $t$ .

REFERENCES

- Abramowitz, M., and I. Stegun, 1964, Handbook of Mathematical Functions (National Bureau of Standards, Washington, D.C.).
- Alvarez, L. W., et al., 1962, Proceedings XI International Conference on High Energy Physics, CERN, p. 433.
- Amati, D., S. Fubini, and A. Stanghellini, 1962a, Phys. Letters 1, 29.
- Amati, D., S. Fubini, and A. Stanghellini, 1962b, Nuovo Cimento 26, 896.
- Andrews, M., and J. Gunson, 1964, J. Math. Phys. 5, 1391.
- Arnold, R. C., 1965, Phys. Rev. Letters 14, 657.
- Arnold, R. C., 1967, Phys. Rev. 153, 1523.
- Astbury, P., et al., 1966, Phys. Letters 23, 396.
- Auvil, P. R., F. Halzen, C. Michael, and J. Weyers, 1970, Phys. Letters 31B, 303.
- Badier, J., et al., 1964, XII International Conference on High Energy Physics, Dubna.
- Badier, J., et al., 1966, Preprint CEA-R 3037 (unpublished).
- Barger, V., 1969, Proceedings Regge Pole Conference, University of California, Irvine.
- Barger, V., and D. B. Cline, 1969, Phenomenological Theories of High Energy Scattering (W. A. Benjamin, Inc., New York).
- Bertanza, L., et al., 1962, Proceedings XI International Conference on High Energy Physics, CERN, p. 284.
- Birmingham-Glasgow-London (I.C.)-Oxford-Rutherford Laboratory Collaboration, 1965, Oxford Conference.
- Birmingham-Glasgow-London (I.C.)-Oxford-Rutherford Laboratory Collaboration, 1966, Phys. Rev. 152, 1148.

- Birnbaum, D., et al., 1970, Phys. Letters 31B, 484.
- Bjorken, J. D., and T. T. Wu, 1963, Phys. Rev. 130, 2566.
- Blatt, J. M., and L. C. Biedenharn, 1952, Rev. Mod. Phys. 24, 258.
- Boyarski, A. M., et al., 1968a, Phys. Rev. Letters 20, 300.
- Boyarski, A. M., et al., 1968b, Phys. Rev. Letters 21, 1767.
- Brink, D. M., and G. R. Satchler, 1968, Angular Momentum (Oxford University Press, Oxford), second edition.
- Carruthers, P., and J. P. Krisch, 1965, Ann. Phys. (N.Y.) 33, 1.
- Chew, G. F., and S. C. Frautschi, 1961, Phys. Rev. Letters 7, 394.
- Chew, G. F., and S. C. Frautschi, 1962, Phys. Rev. Letters 8, 41.
- Chiu, C. B., 1969, Rev. Mod. Phys. 41, 640.
- Chiu, C. B., and J. Finkelstein, 1969, Nuovo Cimento 59A, 92.
- Cline, D., J. Matos, and D. D. Reeder, 1969, Phys. Rev. Letters 23, 1318.
- Cohen-Tannoudji, G., A. Morel, and H. Navelet, 1967, Nuovo Cimento 48A, 1075.
- Cohen-Tannoudji, G., A. Morel, and H. Navelet, 1968, Ann. Phys. (N.Y.) 46, 239.
- Cohen-Tannoudji, G., Ph. Salin, and A. Morel, 1968, Nuovo Cimento 60A, 412.
- Collins, P. D. B., and E. J. Squires, 1968, Regge Poles in Particle Physics, Springer Tracts in Modern Physics No. 45 (Springer-Verlag, Berlin).
- Condon, E. U., and G. H. Shortley, 1935, Theory of Atomic Spectra (Cambridge University Press, Cambridge).
- Courant, R., and D. Hilbert, 1953, Methods of Mathematical Physics (Interscience Publishers, New York), vol. I.

- Dauber, P. M., et al., 1969, Phys. Rev. 179, 1262.
- Dean, N. W., 1968, Nucl. Phys. B7, 311.
- Dolen, R., D. Horn, and C. Schmid, 1967, Phys. Rev. Letters 19, 402.
- Dolen, R., D. Horn, and C. Schmid, 1968, Phys. Rev. 166, 1678.
- Drell, S. D., and J. D. Sullivan, 1967, Phys. Rev. Letters 19, 268.
- Durand, L., III, and Y. T. Chiu, 1964, Phys. Rev. Letters 12, 399; 13,  
45(E).
- Edmonds, A. R., 1957, Angular Momentum in Quantum Mechanics (Princeton  
University Press, Princeton).
- Eden, R. J., 1952, Proc. Roy. Soc. A, 210, 388.
- Eden, R. J., P. V. Landshoff, D. I. Olive, and J. C. Polkinghorne, 1966,  
The Analytic S-Matrix (Cambridge University Press, Cambridge).
- Erdelyi, A. (ed.), 1953, The Bateman Manuscript Project, Higher  
Transcendental Functions, 3 volumes; Tables of Integral Transforms,  
2 volumes (McGraw-Hill, New York).
- Feinberg, G., and S. Weinberg, 1959, Nuovo Cimento 14, 571.
- Firestone, A., et al., 1970,  $K^+n$  Charge Exchange at 12 GeV/c, Lawrence  
Radiation Laboratory Report UCRL-19880.
- Fox, G. C., 1967, University of Cambridge Thesis, unpublished.
- Fox, G. C., 1970, in High Energy Collisions, ed. C. N. Yang, et al.  
(Gordon and Breach, Science Publishers, Inc., New York), p. 367.
- Fox, G. C., and E. Leader, 1967, Phys. Rev. Letters 18, 628.
- Fox, G. C., and C. Quigg, 1970, in preparation.
- Froissart, M., 1961, Report to the LaJolla Conference (unpublished).
- Gilman, F. J., 1969, Phys. Letters 29B, 673.
- Gottfried, K., and J. C. Jackson, 1964, Nuovo Cimento 34, 735.

- Gribov, V. N., 1961, Zh. Eksp. Teor. Fiz. 41, 1962 [Eng. trans., Sov. Phys.-JETP 14, 1395 (1962)].
- Gribov, V. N., 1967, Zh. Eksp. Teor. Fiz. 53, 654 [Eng. trans., Sov. Phys.-JETP 26, 414 (1968)].
- Gribov, V. N., and A. A. Migdal, 1968, Yad. Fiz. 8, 1002, 1213 [Eng. trans., Sov. Phys.-SJNP 8, 583, 703 (1969)].
- Harari, H., 1969, Phys. Rev. Letters 22, 562.
- Harrington, D. R., 1969, Phys. Rev. 184, 1745.
- Henry, F., G. L. Kane, J. Pumplin, and M. Ross, 1969, Phys. Rev. 182, 1579.
- Jackson, J. D., 1965, Rev. Mod. Phys. 37, 484.
- Jackson, J. D., 1970, Rev. Mod. Phys. 42, 12.
- Jackson, J. D., J. T. Donohue, K. Gottfried, R. Keyser, and B. E. Y. Svensson, 1965, Phys. Rev. 139, B428.
- Jackson, J. D., and C. Quigg, 1969, Phys. Letters 29B, 236.
- Jackson, J. D., and C. Quigg, 1970, Remarks on Pion Photoproduction, Lawrence Radiation Laboratory Report UCRL-19410, and Nucl. Phys. B22, (to be published).
- Jacob, M., and G. C. Wick, 1959, Ann. Phys. (N.Y.) 7, 404.
- Joachain, C. J., and C. Quigg, 1970, High-Energy Hadron-Deuteron Scattering, Lawrence Radiation Laboratory Report UCRL-19851 (unpublished).
- Joos, H., 1962, Fortschritte der Physik 10, 65.
- Kaidalov, A. B., and B. M. Karnakov, 1969a, Phys. Letters 29B, 372.
- Kaidalov, A. B., and B. M. Karnakov, 1969b, Phys. Letters 29B, 376.
- Kibble, T. W. B., 1959, Phys. Rev. 117, 1159.
- Kikkawa, K., B. Sakita, and M. Virasoro, 1969, Phys. Rev. 184, 1701.

- Kirz, J., 1970, in High Energy Collisions, ed. C. N. Yang, et al.  
(Gordon and Breach, Science Publishers, Inc., New York), p. 59.
- Kotanski, A., 1966a, Acta Phys. Polon. 29, 699.
- Kotanski, A., 1966b, Acta Phys. Polon. 30, 629.
- Krzywicki, A., 1970, Orsay preprint LPTHE 70/18.
- Krzywicki, A., and J. Tran Thanh Van, 1969, Phys. Letters 30B, 185.
- Lai, K. W., and J. Louie, 1970, Nucl Phys. B19, 205.
- Landshoff, P. V., 1969, "Regge Cuts: A Review of the Theory," DAMTP  
69/30.
- Leader, E., 1969, "Daughters, Conspiracies, Toller Poles: Some Problems  
in the Reggeization of Relativistic Processes," Lectures given at  
the Boulder Summer Institute for Theoretical Physics, and Caltech  
preprint.
- London, G. W., et al., 1966, Phys. Rev. 143, 1034.
- Lovelace, C., 1969, Nucl. Phys. B12, 253.
- Lyons, L., 1966, Nuovo Cimento 43A, 888.
- Mandelstam, S., 1958, Phys. Rev. 112, 1344.
- Mandelstam, S., 1962, Ann. Phys. (N.Y.) 19, 254.
- Mandelstam, S., 1963, Nuovo Cimento 30, 1127, 1148.
- Manning, G., et al., 1966, Nuovo Cimento 41A, 167.
- Mathews, R. D., 1969, Nucl. Phys. B11, 339.
- Matsuda, S., 1969, Nucl. Phys. B9, 113.
- Messiah, A., 1966, Quantum Mechanics (John Wiley and Sons, Inc., New  
York, fifth printing, 1966), Chap. XIII.
- Meyers, C., and Ph. Salin, 1970, Nucl. Phys. B19, 237.
- Michael, C., 1969a, Phys. Letters 29B, 230.

- Michael, C., 1969b, Nucl. Phys. B13, 644.
- Muzinich, I., 1964, J. Math. Phys. 5, 1481.
- O'Donovan, P. J., 1970, Arizona State Preprint ASU-HEP-13.
- Polkinghorne, J. C., 1963, J. Math. Phys. 4, 1396.
- Polkinghorne, J. C., 1970, Nucl. Phys. B16, 321.
- Quigg, C., 1970, Decay Distributions in  $K_2p \rightarrow (K^*, \bar{K}^*)p$  as Tests of Exchange Degeneracy, Lawrence Radiation Laboratory Informal Note UCID-3418 (unpublished).
- Regge, T., 1959, Nuovo Cimento 14, 951.
- Regge, T., 1960, Nuovo Cimento 18, 947.
- Risk, C., 1970, The Derivation of the Absorptive Model from Feynman Diagrams, Lawrence Radiation Laboratory Report UCRL-19453 (unpublished).
- Rivers, R. J., 1968, Nuovo Cimento 57A, 174.
- Rose, M. E., 1957, Elementary Theory of Angular Momentum (John Wiley and Sons, Inc., New York).
- Rosner, J. L., 1969, Phys. Rev. Letters 22, 689.
- Rosner, J. L., 1970, Caltech Preprint 68-254.
- Ross, M. H., and G. L. Shaw, 1964, Phys. Rev. Letters 12, 627.
- Ross, M., F. S. Henyey, and G. L. Kane, 1970, Michigan preprint HE-70-5.
- Rothe, H. J., 1967, Phys. Rev. 159, 1471.
- Schmid, C., 1969, Lettere al Nuovo Cimento 1, 165.
- Sommerfeld, A., 1949, Partial Differential Equations in Physics (Academic Press, New York).
- Sommerfeld, A., 1952, Lectures in Theoretical Physics, vol. III, "Electrodynamics" (Academic Press, New York), pp. 229-235.

- Sonderegger, P., 1970, in High Energy Collisions, ed. C. N. Yang, et al  
(Gordon and Breach, Science Publishers, Inc. New York) p. 259.
- Sopkovich, N. J., 1962, Nuovo Cimento 26, 186.
- Sudakov, V. V., 1956, Zh. Eksp. Teor. Fiz. 30, 87 (English trans.,  
Sov. Phys.-JETP 3, 65).
- Taylor, J. R., 1965, J. Math. Phys. 7, 181.
- Ticho, H., 1962, Proceedings XI International Conference on High Energy  
Physics, CERN, p. 436.
- Titchmarsh, E. C., 1939, Theory of Functions (Oxford University Press,  
Oxford; second ed.).
- Trueman, T. L., and G. C. Wick, 1964, Ann. Phys. (N.Y.) 26, 322.
- Veneziano, G., 1968, Nuovo Cimento 57A, 190.
- Watson, G. N., 1918, Proc. Roy. Soc. 95, 83.
- Weinberg, S., 1964a, Phys. Rev. 133, B1318.
- Weinberg, S., 1964b, Phys. Rev. 134, B882.
- Wick, G. C., 1962, Ann. Phys. (N.Y.) 18, 65.
- Wigner, E. P., 1939, Ann. Math. 40, 194.
- Wigner, E. P., 1957, Rev. Mod. Phys. 29, 255.
- Wigner, E. P., 1959, Group Theory and Its Application to the Quantum  
Mechanics of Atomic Spectra (Academic Press, New York).
- Wilkin, C., 1964, Nuovo Cimento 31, 377.
- Williams, D., 1963, Construction of Invariant Scalar Amplitudes Without  
Kinematical Singularities for Arbitrary-Spin Nonzero-Mass Two-Body  
Scattering Processes, Lawrence Radiation Laboratory Report UCRL-  
11113 (unpublished).
- Winbow, G. A., 1969, Phys. Rev. 177, 2533.

## LEGAL NOTICE

*This report was prepared as an account of Government sponsored work. Neither the United States, nor the Commission, nor any person acting on behalf of the Commission:*

- A. Makes any warranty or representation, expressed or implied, with respect to the accuracy, completeness, or usefulness of the information contained in this report, or that the use of any information, apparatus, method, or process disclosed in this report may not infringe privately owned rights; or*
- B. Assumes any liabilities with respect to the use of, or for damages resulting from the use of any information, apparatus, method, or process disclosed in this report.*

*As used in the above, "person acting on behalf of the Commission" includes any employee or contractor of the Commission, or employee of such contractor, to the extent that such employee or contractor of the Commission, or employee of such contractor prepares, disseminates, or provides access to, any information pursuant to his employment or contract with the Commission, or his employment with such contractor.*

TECHNICAL INFORMATION DIVISION  
LAWRENCE RADIATION LABORATORY  
UNIVERSITY OF CALIFORNIA  
BERKELEY, CALIFORNIA 94720